

Development of 3D cancer cell models for pre-clinical research

**- Evaluation of the tumour
microenvironment in 3D stirred-systems**



UNIVERSIDADE DE COIMBRA

Development of 3D cancer cell models for pre-clinical research - Evaluation of the tumour microenvironment in 3D stirred-systems

Copyright Susana Caçador Veloso, FFUC

A Faculdade de Farmácia e a Universidade de Coimbra têm o direito, perpétuo e sem limites geográficos, de arquivar e publicar esta dissertação através de exemplares impressos reproduzidos em papel ou de forma digital, ou por qualquer outro meio conhecido ou que venha a ser inventado, e de a divulgar através de repositórios científicos e de admitir a sua cópia e distribuição com objetivos educacionais ou de investigação, não comerciais, desde que seja dado crédito ao autor e editor.

The Faculty of Pharmacy and the University of Coimbra are entitled, perpetual and without geographical boundaries, to archive and publish this dissertation through copies imprinted on paper or in digital form, or by any other known or to be invented medium, and to disseminate through scientific repositories and admit the copy and distribution for educational or research purposes, not commercial, as long as credit is given to the author and publisher.

“É isso que nos faz viver. Não de insatisfação. Mas de busca por mais e mais. Pela manutenção do sonho. Pelo não nos darmos por satisfeitos nem por acomodados.”

Carolina Tendon

Preface

This work was performed in the Animal Cell Technology Unit of IBET and ITQB-UNL, within the scope of the project “New models for preclinical evaluation of drug efficacy in common solid tumours” - PREDECT (www.predect.eu), funded by Inovative Medicine Initiative (<http://www.imi.europa.eu/content/home>). The main aim of this project is to create more appropriate *in vitro* platforms for target validation and drug discovery.

Part of the work herein described contributed for poster presentations in international conferences:

(1) Santo VE, Estrada M, Veloso SC, Sousa MQF, van der Kuip H, Oren M, Boghaert ER, Alves PM, Brito C “Novel robust 3D models of non-small-cell lung carcinoma for target validation and tumor-stroma cross-talk elucidation through fully-controlled bioreactor cultures”, 3D Cell Culture 2014 – Advanced Model Systems, Applications & Enabling Technologies, Freiburg, Germany, to be held 25th-27th June 2014;

(2) Santo VE, Estrada M, Veloso SC, Sousa MQF, van der Kuip H, Oren M, Boghaert ER, Alves PM, Brito C “Recapitulation of non-small-cell-lung carcinoma microenvironment in perfusion bioreactor cultures: the impact of hypoxia on tumor-stroma crosstalk”, 23rd Biennial Congress of the European Association for Cancer Research, Munich, Germany, to be held 5th-8th July 2014.

Acknowledgements

This master thesis was only possible due to the collaboration, contribution and encouragement, directly or indirectly, from different persons, to whom I would like to express a few words of gratitude and recognition.

To Prof. Dr. Paula Alves, for give me the opportunity to do my master thesis at Animal Cell Technology Unit at IBET, ITQB-UNL, for the high-quality working conditions offered and for being a strong example of leadership.

To Dr. Catarina Brito, it's a privilege and a pleasure to work with her, for her guidance, knowledge, support and patience to teach me. For being always available to scientific discussions and for being an example in science. For being always there to motivate me and give me precious advices that allowed me to growth as scientist and as a person.

To Dr. Vítor Espírito Santo, for accepting to be my co-supervisor. A deep thanks for the confidence, support, scientific knowledge, wise comments, explanations, opinions and suggestions throughout the all work.

To Prof. Dr. João Nuno Moreira, for accepting to be my internal supervisor.

To Dr. Margarida Serra, Dr. Marcos Sousa and Dr. Ana Teixeira for the scientific advices and for always being available to help in anything.

To all the TCA colleagues for the good working environment and the help during this year, specially to Catarina Pinto, Ana Paula Terrasso, Sofia Rebelo, Daniel Simão, Marta Silva, Carina Silva and Rita Costa. Special and deep thanks to Marta Estrada for all the good scientific explanations, for all the time and patience to teach me and willingness for help and support in all moments.

To Carolina Pinto Ricardo, Nuno Espinha, Tiago Aguiar, , Anis Hamdi, Daniel Pais, João Sá, Raquel Cunha and Lorena Ortiz for the friendship and advices during this year in and outside the workplace.

À Liliana, ao Canel, ao Zé, à Vanessa e a toda a malta do HIIT. Sem vocês, este ano não teria sido a mesma coisa.

A todos os amigos que fiz durante os meus anos académicos na Universidade de Coimbra, por todos os bons momentos dentro e fora da instituição, especialmente ao Rúben Oliveira, à Micky, ao Telmo, ao Crispim, ao Ricardo, à Daniela, à Paula, ao Paulo, ao Caramelo, ao Tiago, ao Mário, à Tânia, ao Teixo, ao Sales, à Sara e ao Santos.

Aos amigos de longa data, dos quais nunca me esqueço. Obrigada pela amizade e apoio.

Ao Rúben, por todo o apoio, carinho, incentivo, motivação, paciência e força que sempre me deste. Obrigada por me fazeres sempre rir e por todos os momentos partilhados. És um grande exemplo para mim.

À minha família, sem vocês nada disto teria sido possível. São para mim um exemplo de coragem e perseverança. Obrigado por todo o amor e por todo o apoio e incentivo para seguir em frente. Obrigado por estarem sempre presentes, em todos os momentos.

Abstract

Lung cancer is the leading cause of cancer-related death worldwide. Non-small cell lung cancer (NSCLC) is the most frequent type of lung cancer, constituting approximately 85% off all lung cancer cases. Despite intensive research for the development of anti-NSCLC drugs, the majority fail in clinical trials. The reasons could be due to absence of therapeutic action and/or due to side effects, which could not be predicted *in vitro* or in animal studies because they lack the human physiological characteristics. Therefore, it is urgent to develop strategies to eliminate ineffective and unsafe compounds with speed, reliability and respect for animal welfare prior to clinical stages. Preclinical models that can better recapitulate tumour microenvironment features, such as the presence of different cell types (tumour and stromal cells) and extracellular matrix (ECM) components and their 3-dimensional (3D) spatial cellular organization, including cell-cell and cell-ECM interactions, would in principle predict clinical responses with higher accuracy. Tumour stroma is a supportive tissue around the tumour, with fibroblasts being the major cell population. Tumour-stroma crosstalk promotes changes in cancer cells and tumour microenvironment, enabling tumour progression, invasion and metastasis. 3D human cellular models overcome limitations of monolayer drug tests, such as the lack of cell-cell and cell-ECM interactions and 3D spatial cellular organization, better resembling physiological complexity and drug response than 2-dimensional (2D) culture. This allows a wide range of applications in pharmacological studies and in tumour biology since tumour microenvironment can be recapitulated with co-cultures of different type of cells and components, such as the stroma.

The aim of this work was to develop scalable and reproducible 3D NSCLC human cellular models that could represent some of the above mentioned features. A 3D culture strategy was followed based on stirred culture systems. In a first approach, aggregation of NSCLC cell lines was implemented in spinner vessels. H460 and H1650 cell lines, representing large cell and bronchioalveolar carcinoma, respectively, formed cellular aggregates in suspension after 3 days of cell culture with high cell viability, cell proliferation and metabolic activity. In a second approach, 3D cell culture in stirred culture systems was combined with an alginate microencapsulation strategy for cell entrapment. H1650 cellular aggregates were encapsulated with and without immortalized normal lung fibroblasts as stromal component (mono and co-cultures, respectively). This strategy enabled to generate homogeneous microcapsules containing tumour cellular aggregates surrounded by fibroblasts, a configuration which resembles the *in vivo* situation. Moreover, this strategy

enables collagen accumulation, characteristic of tumour microenvironment, such as ECM proteins production. Microcapsule cultures were maintained in stirred culture systems for 15 days, with high cell viability within aggregates. Cell proliferation and metabolism was similar in mono and co-cultures.

Therefore, a 3D human NSCLC cellular model was accomplished, suggesting that the combination of 3D cell cultures, stirred culture systems and microencapsulation technique is a promising tool for the generation of more reliable NSCLC models that better mimic the tumour microenvironment and the possibility to study its influence in tumour progression.

Keywords: Non-small lung cancer, tumour microenvironment, stirred culture systems, 3D cellular models, cellular aggregates, microencapsulation.

Resumo:

O cancro do pulmão é a maior causa de morte por cancro no mundo inteiro. O cancro do pulmão de não-pequenas células (CPNPC) é o tipo de cancro do pulmão mais frequente, constituindo aproximadamente 85% de todos os casos de carcinoma pulmonar. Apesar da investigação intensa para desenvolver fármacos contra este tipo de cancro, a maioria deles não ultrapassa a fase de ensaios clínicos. As razões podem ser devidas à ausência de efeito terapêutico e/ou aos efeitos secundários, que não foram previstos em estudos *in vitro* nem em estudos animais, uma vez que estes não possuem as características fisiológicas do sistema humano. Deste modo, é urgente eliminar os compostos ineficazes e não seguros com a maior brevidade e eficácia, reduzindo igualmente a experimentação animal. Os modelos celulares humanos 3-dimensionais (3D) superam algumas das limitações dos testes de fármacos em monocamada de células, tais como a ausência de interações célula-célula e a organização celular espacial em 3D, o que melhor mimetiza a complexidade e resposta fisiológica a fármacos, comparando com culturas celulares em 2-dimensões (2D). Os modelos celulares em 3D têm uma vasta aplicação em estudos farmacológicos e na biologia tumoral, uma vez que o microambiente tumoral pode ser mimetizado com co-cultura de diferentes tipos celulares e componentes, como o estroma. O estroma tumoral é um tecido de suporte que existe à volta do tumor, sendo os fibroblastos a maior população celular. Interações tumor-estroma promovem alterações nas células cancerígenas e no microambiente tumoral, permitindo a progressão, invasão e metástases tumorais.

O objetivo do trabalho foi desenvolver um modelo celular 3D humano de CPNPC reprodutível e com aplicação em maior escala, com as características 3D descritas anteriormente. Foi usada uma estratégia 3D de cultura celular, baseada em sistemas de cultura agitados. Numa primeira abordagem, agregação de linhas celulares de CPCNP foi implementada. As linhas celulares H460 e H1650, representando carcinomas de grandes células e bronquioalveolar, respectivamente, formaram agregados em suspensão após 3 dias de cultura celular com alta viabilidade e proliferação celular e actividade metabólica. Numa segunda abordagem, cultura celular em 3D em sistemas de cultura agitados foi combinada com uma estratégia de encapsulação em alginato, para confinar as células no mesmo espaço físico. Agregados celulares de H1650 foram encapsulados sem e com fibroblastos do pulmão imortalizados, constituindo o componente estromal (mono- e co-cultura, respectivamente). Esta técnica possibilitou gerar cápsulas com agregados no seu interior e fibroblastos individuais à volta desses agregados, o que se aproxima da situação *in vivo*. Microcápsulas

foram mantidas em sistemas de cultura agitados até 15 dias, com alta viabilidade celular nos agregados. Proliferação e atividade metabólica foi semelhante em mono- e co-cultura. Esta estratégia permite ainda acumulação de colagénio, característica do microambiente tumoral devido à produção de proteínas da matrix extracelular,

Assim, foi possível obter um modelo celular 3D humano de CPNPC, o que sugere que a combinação de cultura celular 3D, sistemas de cultura agitados e microencapsulação é uma ferramenta promissora para alcançar modelos celulares mais eficazes que melhor mimetizam o microambiente tumoral e a possibilidade de estudar a sua influência na progressão do tumor.

Palavras-chave: Cancro do pulmão de não-pequenas células (CPNPC), microambiente tumoral, sistema de cultura agitado, modelos celulares 3D, agregados celulares, microencapsulação.

Table of contents:

Contents

| | |
|--|------|
| Index of Figures | XVII |
| Index of Tables | XIX |
| Abbreviations | XX |
| I. Introduction | 1 |
| 1.1. Lung cancer | 3 |
| 1.1.1. Risk factors | 4 |
| 1.1.2. Types of lung cancer | 4 |
| 1.1.3. Lung cancer treatment | 6 |
| 1.2. Epithelial to mesenchymal transition and metastasis | 8 |
| 1.3. Tumour microenvironment | 11 |
| 1.3.1. Stroma | 12 |
| 1.4. Cancer cell metabolism | 14 |
| 1.4.1. Tumour-stroma metabolic crosstalk | 16 |
| 1.5. Need for new cell models for pre-clinical research | 17 |
| 1.6. Cancer pre-clinical models | 19 |
| 1.6.1. The drug discovery cascade | 19 |
| 1.6.2. 2Dimensional versus 3Dimensional cell models | 21 |
| 1.6.3. 3D static cell culture methods | 23 |
| 1.6.4. 3D agitation-based cell culture methods | 28 |
| 1.6.5. Mimicking the tumour microenvironment <i>in vitro</i> | 35 |
| 1.7. Thesis aim | 37 |
| 2. Materials and Methods | 39 |
| 2.1. Cell lines and cell culture conditions | 41 |
| 2.2. Generation of NSCLC aggregates and culture conditions | 42 |
| 2.3. Development of a 3D NSCLC cellular model | 43 |
| 2.3.1. Fibroblasts membrane staining protocol | 43 |
| 2.3.2. Encapsulation of NSCLC cellular aggregates | 44 |
| 2.3.3. Mono- and co-culture of HI 650 encapsulated aggregates | 46 |
| 2.4. Analytical methods to evaluate cell culture | 47 |
| 2.4.1. Determination of cell concentration, cell viability, cell death and Apoptosis | 47 |
| 2.4.2. Aggregate size determination | 49 |
| 2.4.3. Metabolite analysis | 49 |
| 2.4.4. Phenotypic characterization of the NSCLC cellular model | 49 |
| 2.4.5. Quantification of newly synthesized ECM components | 50 |
| 2.5. Statistical analysis | 51 |

| | |
|--|----|
| 3. Results and discussion | 53 |
| 3.1. Aggregation of NSCLC cell lines in stirred culture systems | 55 |
| 3.2. Culture of encapsulated NSCLC aggregates in stirred culture systems | 64 |
| 3.3. Metabolic characterization of encapsulated NSCLC aggregates in mono- and co-culture | 72 |
| 3.4. ECM deposition and phenotypic characterization mono- and co-cultures | 76 |
| 4. Conclusion | 87 |
| 5. Future Perspectives | 91 |
| 6. References | 95 |

Index of Figures:

| | |
|---|----|
| Figure 1.1 – Respiratory system | 3 |
| Figure 1.2 – Scheme of the EGFR pathway | 8 |
| Figure 1.3 - Endothelial to mesenchymal transition and metastasis | 9 |
| Figure 1.4 – Shift between epithelial and mesenchymal morphology | 10 |
| Figure 1.5 - Tumour microenvironment | 11 |
| Figure 1.6 - Transition of a normal fibroblast to a cancer associated fibroblast (CAF) | 13 |
| Figure 1.7 - Action of activated fibroblast in the tumour microenvironment | 14 |
| Figure 1.8 – Cancer cell metabolism pathways | 15 |
| Figure 1.9 - Hallmarks of cancer | 19 |
| Figure 1.10 - Drug discovery cascade | 20 |
| Figure 1.11 - Morphological and functional cellular distribution in a tumour | 22 |
| Figure 1.12 - Forced-floating method | 23 |
| Figure 1.13 - Hanging drop method | 24 |
| Figure 1.14 - 3D cell culture method based on Matrigel | 25 |
| Figure 1.15 - Strategies to promote the release of multiple bioactive factors from a scaffold | 26 |
| Figure 1.16 - M/G residues that constitute the alginate | 27 |
| Figure 1.17 - Example of a non porous microcarrier | 28 |
| Figure 1.18 - Gyrotory shaker for Erlenmeyer | 29 |
| Figure 1.19 - Agitation-based approaches for the production of aggregates | 31 |
| Figure 1.20 – A 4-fold DASbox® Mini Bioreactor System for cell culture | 32 |
| Figure 1.21 - Design of a 3D microfluidic device | 33 |
| Figure 1.22 - Concept of cell microencapsulation | 36 |
| Figure 1.23 – Aim of the thesis and strategies performed to accomplish the objectives | 37 |
| Figure 2.1 - Stirring profile for H460 and HI650 cellular aggregation s using spinner-flasks with straight paddle impeller (Corning® Life Sciences) | 43 |
| Figure 2.2 - Schematic illustration the cell encapsulation process with alginate | 45 |
| Figure 2.3 – Strategy performed to accomplish a 3D cellular model to evaluate the effect of tumour microenvironment on tumour progression | 46 |
| Figure 3.1 - Monitoring of aggregation of NSCLC cell lines in stirred culture systems | 56 |
| Figure 3.2 – Cell death expressed by the cumulative values of LDH released during aggregation of NSCLC cell lines in stirred culture systems. | 57 |
| Figure 3.3 - Aggregate size profile along aggregation of NSCLC cell lines in stirred suspension culture systems | 58 |

| | |
|---|----|
| Figure 3.4 – Cell (a) and aggregate (b) concentration during aggregation of NSCLC cell lines in stirred culture systems. | 59 |
| Figure 3.5 – Concentration of glucose (a) and lactate (b) in the cell culture medium during aggregation of NSCLC cell lines in stirred culture systems | 61 |
| Figure 3.6 – Specific metabolic rates of glucose consumption (a) and lactate production (b) aggregation of NSCLC cell lines in stirred culture systems, from day 0 to day 1 and from day 1 to day 0 | 62 |
| Figure 3.7 – Metabolic efficiency aggregation of NSCLC cell lines in stirred culture systems | 63 |
| Figure 3.8 - Monitoring of mono and co-cultures of HI650 aggregates encapsulated with NFs in stirred culture system. | 66 |
| Figure 3.9 – Cell death expressed by cumulative values of LDH released during mono and co-cultures of HI650 aggregates encapsulated with NFs in stirred culture system | 67 |
| Figure 3.10 – Evaluation of apoptotic activity during mono and co-cultures of HI650 aggregates encapsulated with NFs in stirred culture system at days 5 and 15 of culture by fluorescence microscopy | 68 |
| Figure 3.11 - Aggregate area profile of HI650 encapsulated aggregates in mono- and co-culture with NFs using a stirred suspension culture system | 70 |
| Figure 3.12 – Cell (a) and aggregate (b) number of HI650 encapsulated aggregates in mono and co-culture with NFs using a stirred suspension culture system | 71 |
| Figure 3.13 – Concentration of glucose (a) and lactate (b) in the cell culture medium of HI650 encapsulated aggregates in mono- and co-culture with NFs using a stirred suspension culture. Specific metabolic rates of HI650 aggregates in mono and co-culture with NFs using a stirred suspension culture system for glucose consumption (c) and lactate production (d) | 73 |
| Figure 3.14 – Yield of lactate/glucose of HI650 encapsulated aggregates in mono and co-culture with NFs in stirred culture systems | 75 |
| Figure 3.15 – Collagen concentration of HI650 encapsulated aggregates in mono- and co-culture with NFs in stirred culture system throughout time | 76 |
| Figure 3.16 - Immunocharacterization of HI650 encapsulated aggregates in mono- and co-cultures with NFs in stirred culture systems at day 15 of culture | 77 |

Index of Tables

| | |
|---|----|
| Table 1.1: Main types of lung cancer and their major characteristics | 5 |
| Table 1.2: Main differences between the epithelial and mesenchymal phenotypes | 10 |
| Table 1.3: Advantages and disadvantages of different 3D cell culture techniques | 33 |
| Table 2.1: Cell lines used to generate NSCLC cellular aggregates | 41 |
| Table 2.2: List of antibodies and respective dilutions used for immunofluorescence microscopy | 50 |

Abbreviations

| | |
|--|---|
| 2D - Two dimensional | F-2,6-bisP - Fructose 2,6-bisphosphate |
| 2HG - 2-hydroxyglutarate | FAS - Fatty acid synthase |
| 3D - Three dimensional | FBS - Fetal bovine serum |
| ACL - ATP-citrate lyase | FDA - Fluorescein diacetate |
| AJ- Adherens junctions | FGF2 - Fibroblast growth factor 2 |
| α KG – Alpha ketoglutarate | FH - Fumarate hydratase |
| AKT – Protein kinase B | FSG - Fish skin gelatine |
| ALK - Anaplastic lymphoma kinase | FSP1 - Fibroblast-specific protein 1 |
| Arg–Gly–Asp or RGD - amino acid sequence arginine–glycine–aspartic acid | G – Gap junctions |
| ATP - Adenosine triphosphate | G residue - α -(1-4)-linked L-guluronic acid |
| BaCl ₂ - Barium dichloride | Glc – Glucose |
| BCL2 - B-cell lymphoma 2 | GLDC - Glycine decarboxylase |
| CAF - Cancer-associated fibroblast | GLUT1 - Glucose transporter 1 |
| Cav-1 - Caveolin-1 | Grb-2 - Growth factor receptor-bound protein 2 |
| CHO – Chinese hamster ovary | HER- Human epidermal growth factor receptor |
| CK18 – Cytokeratin 18 | hESCs - Human embryonic stem cells |
| CO ₂ – Carbon dioxide | HGF - Hepatocyte growth factor |
| Col IV – Collagen IV | HGFR - Hepatocyte growth factor receptor |
| D – Desmosomes | HIF α - Hypoxia-inducible factor, alpha subunit |
| DAPI - 4,6-diamidino-2-phenylindole | HKII - Hexokinase 2 |
| DNA - Deoxyribonucleic acid | IARC - Agency for Research on Cancer |
| DPBS – Dulbecco’s phosphate buffered saline | IDH1- Isocitrate dehydrogenase 1 |
| dsDNA - Double-stranded nucleic acids | IDH2 - Isocitrate dehydrogenase 2 |
| ECM – Extracellular matrix | IGF-I - insulin-like growth factor 1 |
| EDA-fibronectin - Fibronectin containing the extra domain A | IGF-1R - insulin-like growth factor 1 (IGF-1) receptor |
| EDTA - Ethylenediaminetetraacetic acid | IgG – Immunoglobulin G |
| EGF- Endothelial growth factor | IL1- Interleukin 1 |
| EGFR – Epidermal growth factor receptor | kDa - Kilo Daltons |
| EMT – Epithelial to mesenchymal transition | KRAS - Kirsten rat sarcoma viral oncogene homolog |
| ERBB2- v-erb-b2 avian erythroblastic leukemia viral oncogene homolog 2 | Lac – Lactate |
| | LDH - Lactate dehydrogenase |

LDHA - Lactate dehydrogenase A

LDH_{cum} – Lactate dehydrogenase cumulative

M - Molar

M residue - β -(1-4)-linked D-mannuronic acid

MAPK - Mitogen-activated protein kinase

MCLI - Induced myeloid leukemia cell differentiation protein

MCPI - Monocyte chemotactic protein I

MCT4 - Monocarboxylate transporter-4

MET – Mesenchymal to epithelial transition

MET – Mesenchymal to epithelial transition

mL - Mililiter

mM – Milimolar

MMPs- Matrix metalloproteinases

mQ water – MiliQ water

MT – Astral microtubules

mTOR – Mechanistic or mammalian target of rapamycin (serine/threonine kinase)

MTs – Longitudinal microtubules

MUC4 – Mucin 4

MYC - V-myc avian myelocytomatosis viral oncogene homolog

NaCl – Sodium chloride

NADH - Dihyronicotinamide adenine dinucleotide

NASA - National Aeronautics and Space Administration

NFs – Normal fibroblasts

NSCLC – Non-small cell lung cancer

NT2 - NTera2/ cl. D1 cell line

° C - Celsius degrees

P/S - Penicillin-streptomycin

P53 – Tumour protein p53

pAKT – Phosphorilated protein kinase B

PBS - Phosphate-buffered saline

PSC – Pancreatic stem cells

PDGF - Platelet-derived growth factor

PFA -Paraformaldehyde

PFKFB3 - Phosphofructo-2-kinase/fructose-2,6-bisphosphatase 3

PGAM1 - Phosphoglycerate mutase I

PHGDH - Phosphoglycerate dehydrogenase

PI3K - Phosphatidylinositol-4,5-bisphosphate 3-kinase

PKM2 - Pyruvate kinase M2

poly-HEMA - Poly-2-hydroxyethylmethacrylate

PTEN- Phosphatase and tensin homolog, AKT - Protein Kinase B

qGlc – Specific glucose consumption rate

qLac – Specific lactate production rate

qMet – Specific metabolic rate

qRT-PCR - Quantitative real time polymerase chain reaction

RAF- Rapidly Accelerated Fibrosarcoma

RAS – Member of the small GTPase superfamily

RGD - Arginine–glycine–aspartic acid amino acid sequence

Rpm - Rotations per minute

RT - Room temperature

RTK - Receptor tyrosine kinase

SCLC – Small cell lung cancer

SD - Standard deviation

SDFI - Stromal-cell-derived factor I

SDH - Succinate dehydrogenase

SMA – Smooth-muscle actin

SOS - Son of Sevenless

STAT 3/5 - Signal transducer and activator of transcription

TCA cycle – Tricarboxylic acid cycle

TGF α - Tumour growth factor alpha

TGF- β - Transforming growth factor-beta
THF – Tetrahydrofolate
TJ – Tight junctions
TKI - Tyrosine kinase inhibitors
TTBS - Tris-buffered saline with 0.1% (w/v) Tween
20
TX-100 - Triton X-100
Tyr-K - Tyrosine kinase
UP-MVG - Ultra Pure MVG alginate
VEGF - Vascular endothelial growth factor
w/ v - Weigh per volume
WB - Western blot
 $Y_{\text{Lac/Glc}}$ - Yield acetate/glucose
ZO-1 Zonula occludens protein 1
 α KG - α -ketoglutarate
 μm - Micrometer
 μM – Micromolar

Introduction

I.I. Introduction

I.I. Lung cancer

Lungs are the organ responsible for bringing oxygen and releasing carbon dioxide (CO₂) to and from blood circulation in order to maintain the proper function of the cells. A pair of lungs is located in the chest region on either side of the heart and each lung is composed of lobes. The left lung has two lobes and the right lung has three lobes (Warner, 2006). The bronchi are the two tubes that come from the trachea to the right and left lungs (**figure I.1**). The bronchi split into bronchioles which, in turn, divide in tiny air sacs, called alveoli.

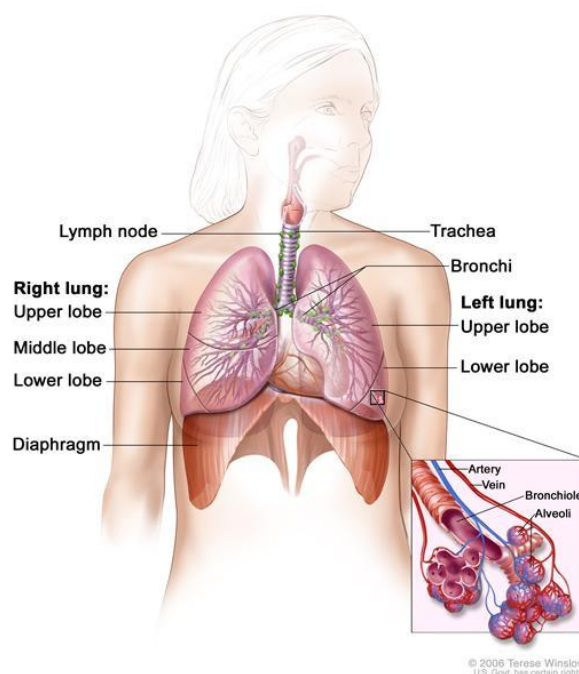


Figure I.1- Respiratory system. From: National Cancer Institute

(<http://www.cancer.gov/cancertopics/types/lung>).

Lung cancer is the leading cause of cancer-related mortality (Horn & Carbone, 2014; Malvezzi, Bertuccio, Levi, La Vecchia, & Negri, 2013). European cancer mortality for lung cancer in 2013 reported a continuing reduction in males, but a continuing increase in females (Sculier, Meert, & Berghmans, 2014). In fact, mortality from lung cancer and breast cancers are equivalent in females for the first time (Sculier *et al.*, 2014). Despite progress, the overall survival for lung cancer patients remains poor at 15%. This may be due to the fact that most of the patients only have symptoms when the disease is already in an advanced stage (Mehta,

Patel, & Sadikot, 2014). The main symptoms are coughing (including coughing blood), weight loss, chest pain and breathing difficulties (Brenner *et al.*, 2012). Therefore, it is extremely important to improve better diagnosis and treatment techniques.

1.1.1. Risk factors

Cigarette consumption remains the leading risk factor for lung cancer development and, therefore, smoking cessation is an important preventive strategy (Horn & Carbone, 2014; Miller, 2005). However, previous lung diseases such as emphysema, chronic bronchitis, tuberculosis and pneumonia can influence lung cancer risk independently of tobacco use and these diseases should be taken into consideration for assessing individual risk (Brenner *et al.*, 2012). In October 2013, the International Agency for Research on Cancer (IARC) classified outdoor air pollution as carcinogenic to humans (Raaschou-Nielsen *et al.*, 2013; Sculier *et al.*, 2014; W D Travis *et al.*, 2011). Furthermore, lung cancer can also be hereditary (Mesquita *et al.*, 1997; Miller, 2005).

1.1.2. Types of lung cancer

There are two main types of lung cancer, non-small cell lung cancer (NSCLC) and small cell lung cancer (SCLC), which arise from different epithelial cell types which accumulate different genetic mutations (Herbst, Heymach, & Lippman, 2008; Sun *et al.*, 2012). For instance, NSCLC usually has mutation mainly in epidermal growth factor receptor (EGFR) and Kirsten rat sarcoma viral oncogene homolog (KRAS) while SCLC commonly has mutation in V-myc avian myelocytomatosis viral oncogene homolog (MYC), B-cell lymphoma 2 (BCL2) and tumour protein p53 (p53) (Herbst *et al.*, 2008; Minna, 2012). All these genes are either tumour suppressor genes, such as p53, or oncogenes, such as EGFR, KRAS, MYC and BCL2 (Miller, 2005; Y. Zhong, Delgado, Gomez, Lee, & Perez-soler, 2001).

NSCLC is the most frequent type of lung cancer with almost 85% off all lung cancer cases (Read, Page, Tierney, Piccirillo, & Govindan, 2004; X. Zhong & Rescorla, 2012). Unfortunately, only 25% of all patients are diagnosed at an early stage (Hopper-Borge, 2014). NSCLC include three major histologies: adenocarcinoma, large cell carcinoma and squamous cell (epidermoid) carcinoma. Adenocarcinoma is the most common of these three. It starts on peripheral lung tissue in opposition to large cell carcinoma and squamous cell carcinoma that are more centrally located. In addition, adenocarcinoma develops from a particular type of cell that produces mucin 4 (MUC4), which is a major constituent of mucus (Singh *et al.*,

2006; Singh, Chaturvedi, & Batra, 2007). The second most common NSCLC is squamous cell carcinoma, which appears in the large airways and it is characterized by flat cells. The large cell carcinoma is characterized by large cells, presenting a higher volume of cytoplasm and large nuclei and nucleoli (Popper, 2011).

SCLC corresponds to approximately 15% of all cases (Babakooi, Fu, Yang, Linden, & Dowlati, 2013; Rathi N. Pillai and Taofeek K. Owonikoko, 2014; Read et al., 2004). This cancer type is characterized by cells that secrete neuroendocrines hormones , being more prevalent in primary and secondary bronchi (Herbst et al., 2008; Rathi N. Pillai and Taofeek K. Owonikoko, 2014).

SCLC has higher sensitivity to chemotherapy in a very early stage of disease comparing with NSCLC in its. Despite this, patients usually suffer from the disease recurrence (Rathi N. Pillai and Taofeek K. Owonikoko, 2014) since SCLC promotes metastasis in the beginning of the disease (Babakooi et al., 2013). **Table I.I** summarizes the main types of lung cancer and its pathologic features.

Table I.I: Main types of lung cancer and their major characteristics

| Lung Cancer Type | Lung Cancer Subtype | Main Characteristics | References |
|------------------|------------------------|---|--|
| NSCLC | Adeno-carcinoma | <ul style="list-style-type: none"> • Location in the organ periphery; • Originated from small airway epithelial and alveolar cells; • Most common type in patients who have never smoked; • Usually present EGFR mutations (possible targeted therapy); • Tend to form glands and secrete mucins, especially MUC4. | (Herbst et al., 2008; Llinares et al., 2004; Singh et al., 2007) |
| | Squamous cell | <ul style="list-style-type: none"> • Location in the organ centre and periphery; • Strongly associated with cigarette | (Herbst et al., 2008; |

| | | | |
|--------------|----------------------------------|--|--|
| NSCLC | carcinoma | smoking; <ul style="list-style-type: none"> • Arises from large airway epithelial cells; • Intrathoracic spread rather than distant metastasis, therefore, best prognosis. | William D Travis, 2011) |
| | Large cell carcinoma | <ul style="list-style-type: none"> • Location in the organ periphery • Strongly associated with cigarette smoking; • Grows and spreads quickly • | (Popper, 2011; Sun et al., 2012) |
| | Small-cell lung carcinoma | <ul style="list-style-type: none"> • Location in the centre; • Strongest smoking association; • Arises from pulmonary neuroendocrine cells; • Rapid growth and early distant metastasis (brain, liver, bone), leading to the disease recurrence and worst prognosis; • Chemotherapy sensitivity only in early stage | (Herbst et al., 2008; Sun et al., 2012, Rathi N. Pillai and Taofeek K. Owonikoko, 2014;) |

1.1.3. Lung cancer treatment

Lung cancer treatment is based in four approaches: surgery, radiation therapy, chemotherapy and targeted therapy. These strategies are described below and their use depends on different factors, such as the type and stage of cancer as well the possible side effects and the patient overall health (Coldren et al., 2006; Rowell & Williams, 2001; Sun et al., 2012).

- **Surgery**

Early-stage NSCLC is usually treated with a surgical resection (Myrdal, Gustafsson, Lambe, Hörte, & Ståhle, 2001; Sculier et al., 2014). However, not every patient can handle this procedure, because it is a very delicate surgery and there is a big risk of postoperative complications. In patients with advanced stage and inoperable NSCLC other treatments, such as the radiotherapy, chemotherapy and targeted therapy should be applied (Bradley et al., 2004; Myrdal et al., 2001).

- **Radiotherapy and Chemotherapy**

Radiotherapy involves the use of radiation, usually X-rays. There is a high rate of treatment failure when using radiotherapy alone, being only efficient when the tumor is local and small (less than 4 cm)(Bradley et al., 2004; Rowell & Williams, 2001; Timmerman et al., 2006). Therefore, radiotherapy has a better result on the patient outcome when combined with chemotherapy (Mehta et al., 2014; Sculier et al., 2014). If radiotherapy is applied in an early stage of the disease it may aim to eliminate the cancer entirely. When applied in an advanced stage, this treatment approach aims to decrease the size of the tumour and control it for some time (Dosoretz et al., 1993; Gauden, Ramsay and Tripcony, 1995).

Doublet chemotherapy using platinum derivatives with another cytotoxic agent, such as docetaxel is the standard first-line treatment for advanced NSCLC (Dearing, Sangal, & Weiss, 2014; Sculier et al., 2014). It is usually combined with radiotherapy (Mehta et al., 2014; Myrdal et al., 2001). However, many of the relapsing cancers gain chemotherapy resistance, which contributes to the poor survival rate related to lung cancer. Even though the cancer resistance mechanism has been extremely studied *in vitro* (Dearing et al., 2014; Ma, 2012), the reasons for this process *in vivo* are not quite understood. Therefore, more research must be done in this topic in order to improve chemotherapeutic methods already used. Another disadvantage of the use of chemotherapy/radiotherapy is their side effects, such as gastrointestinal distress, kidney and nerve damage and bone marrow suppression (Mehta et al., 2014).

- **Targeted Therapy**

Targeted therapy aims to use drugs or other substances to damage specifically the malignant cells and not the normal cells (Ladanyi & Pao, 2008; Zhuang, Zhao, Zhao, Chang, & Wang, 2014). There are different types of lung cancer which can be characterized by specific molecular receptors or genes that are usually mutated in cancer cells, such as the EGFR and anaplastic lymphoma kinase (ALK) (Ladanyi & Pao, 2008; Ma, 2012). Tyrosine kinase inhibitors (TKI) are commonly used as a molecular targeted therapy included in the second and third line of treatment regimen of NSCLC (Hopper-Borge, 2014; W D Travis et al., 2011; Vasekar, Liu, Zheng, & Belani, 2014). Erlotinib and gefitinib are examples of TKI already approved in Europe for the therapy of NSCLC (Ma, 2012; Zhuang et al., 2014). Their

target is EGFR, which regulates cell proliferation, apoptosis, angiogenesis and tumour invasion (**figure 1.2**). Crizotinib is another TKI approved in Europe that block the activity of ALK, which play a role in cancer cell growth, metastasis and angiogenesis of 2 to 7% of NSCLC (Ma, 2012; Shackelford, Vora, Mayhall, & Cotelingam, 2014). Other molecular targets are being studied for the NSCLC treatment, such as human epidermal growth factor receptor (HER) family of receptors, KRAS, Phosphatidylinositol-4,5-bisphosphate 3-kinase (PI3K)/ protein kinase B (AKT)/ mammalian target of rapamycin (mTOR), PI3K/AKT/mTOR, insulin-like growth factor I (IGF-1) receptor (IGF-1R) and hepatocyte growth factor receptor (HGFR) (Zhuang *et al.*, 2014). Consequently, it is important to perform a mutation evaluation test in order to select the appropriate targeted therapy using the compound with higher efficiency levels for that specific clinical setting.

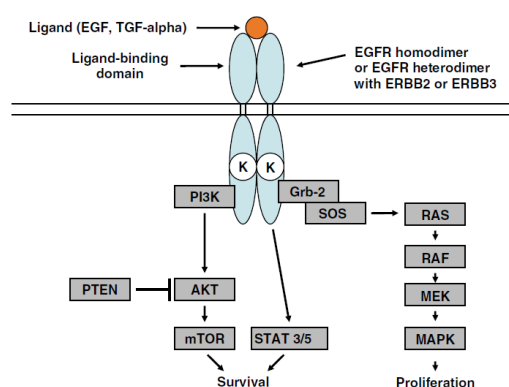


Figure 1.2 - Scheme of the EGFR pathway. Erlotinib and gefitinib block the pathway at kinase domain level (K). However, they are only effective if there is no other mutations downstream, for instance at KRAS or BRAF level. Legend: EGF- Epidermal growth factor, EGFR- Epidermal Growth Factor Receptor, TGF α - Tumour growth factor alpha, ERBB2- v-erb-b2 avian erythroblastic leukemia viral oncogene homolog 2, PIK3- Phosphatidylinositol-4,5-bisphosphate 3-kinase, PTEN- Phosphatase and tensin homolog, AKT - Protein Kinase B, mTOR- Mammalian target of rapamycin, Grb-2 - Growth factor receptor-bound protein 2, STAT 3/5 - Signal transducer and activator of transcription, SOS - Son of Sevenless is a set of genes encoding guanine nucleotide exchange factors, RAS - member of the small GTPase superfamily, RAF- Rapidly Accelerated Fibrosarcoma, MAPK - Mitogen-activated protein kinase. From (Ladanyi & Pao, 2008).

1.2. Epithelial to mesenchymal transition and metastasis

Although there has been progress in drug development and surgery in the last years, treatment for lung cancer is not highly efficient due to metastasis and disease recurrence (Xiao & He, 2010). These two events are related to cell modifications, including, function gains and losses, such as the epithelial to mesenchymal transition (EMT). EMT, an evolutionarily conserved process, is essential for the embryonic development and tumor progression and it is enrolled in the metastasis, drug resistance and growth of many tumours (Christiansen & Rajasekaran, 2006; J. M. Lee, Dedhar, Kalluri, & Thompson, 2006).

A cascade of events involving several adhesion molecules is related with the metastatic process (Hanahan & Weinberg, 2011). Cells undergo a change in their phenotype, known as EMT, which helps them to detach from the primary site and enter in the blood vessels (**figure I.3**). When in blood circulation, tumour cells can adhere to host cells or to other tumour cells, which can possibly protect them from immune detection and the mechanical force from blood flow (Xiao & He, 2010). This contributes to the progression of the tumour and metastasis (Christiansen & Rajasekaran, 2006). In these two processes, the adhesive characteristics are always changing, suggesting that they are dynamic mechanisms regarding loss and gain of cell-cell adhesion.

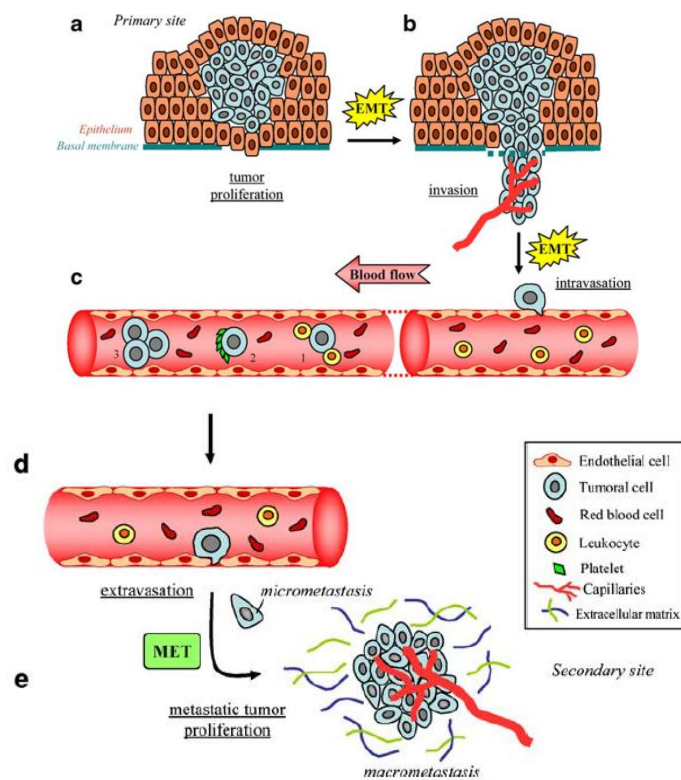


Figure I.3 – Epithelial to mesenchymal transition and metastasis. Cancer cells detach from the primary tumour and the stroma, undergoing a phenotype modification. Then, these migrating and invasive cells can invade the tissue around the primary tumour (a and b), enter the blood or lymphatic circulation by penetrating the vessels (c), reach a distant organ or tissue, extravagate the circulation (d) and might develop in a new microenvironment and generate a secondary tumour, called metastasis (e), since they undergo a mesenchymal to epithelial transition, regaining some of the cell adhesion features that they presented previously. Legend: EMT – Epithelial to mesenchymal transition; MET – Mesenchymal to epithelial transition. From (Gout & Huot, 2008).

When cancer cells undergo EMT, they lose the epithelial phenotype, by losing epithelial junction molecules such as E-cadherin or γ -catenin, while simultaneously expressing mesenchymal markers such as fibronectin and vimentin (Z. Chen et al., 2012; Hopper-Borge,

2014; Roato, 2014). This mechanism is not only related to progression, invasion and metastasis but also to drug resistance (Hopper-Borge, 2014; Roato, 2014; Xiao & He, 2010). According to Jonathan M. Lee *et al* (J. M. Lee *et al.*, 2006), decreased expression of E-cadherin and increased expression of fibronectin or vimentin is common in NSCLC. **Table I.2** present the major differences between the epithelial and mesenchymal cells (**figure I.4**).

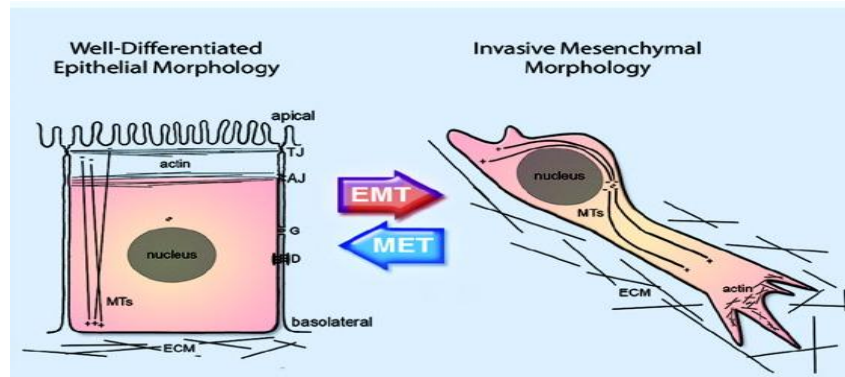


Figure I.4 - Shift between epithelial and mesenchymal morphology. Legend: AJ- Adherens junctions; TJ – Tight junctions, G – Gap junctions, D – Desmosomes, SMA – smooth-muscle actin, MMPs- Matrix metalloproteinases, MT- microtubules, , ECM – Extracellular matrix, EMT- Epithelial to mesenchymal transition, MET- Mesenchymal to epithelial transition. From (Christiansen & Rajasekaran, 2006).

Table I.2: Main differences between the epithelial and mesenchymal phenotypes

| | Epithelial Cell | Mesenchymal Cell |
|----------------------------------|---|---|
| Morphology | Apical/Basolateral Polarity | Edge Asymmetry |
| Physical Features | Cell Adhesion and Contact inhibition | Cell Motility and Invasiveness |
| Intercellular Junctions | Adherens (AJ), Tight (TJ), Gap (G) and Desmosomes (D) | Focal Adhesion and Transient Gap Junctions |
| Molecular Markers | E-cadherin, Cytokeratins | N-cadherin, Vimentin, SMA and MMPs |
| Cytoskeletal Organization | Longitudinal Microtubules (MTs) and Circumferential Actin | Astral Microtubules (MT) and Filopodial Stress Fibers |

(adapted from Christiansen and Rajasekaran, 2006)

The most common places for metastasis from lung cancer are brain, bone, opposite lung, liver and kidneys (Roato, 2014; Xiao & He, 2010). The EMT and metastasis process are

caused by alterations not only in the cancer cells, but also in the cells surrounding the tumour and in the tumour microenvironment (Fiaschi et al., 2012; Gout & Huot, 2008).

1.3. Tumour Microenvironment

Over the past decade, the reductionist view of a tumour as a group of homogeneous cancer cells has been abandoned. Nowadays, a tumour is seen as a complex organ, including a microenvironment composed by different types of cells and regions with different degrees of vascularisation, inflammation, differentiation, proliferation and invasion (**figure 1.5**) (Hanahan & Weinberg, 2011; Mueller & Fusenig, 2004). These cells change during tumour progression, generating a sequence of tumour microenvironments that enables primary, invasive, and then metastatic development. The neighbouring normal cells of the tumour also likely affect the nature of the various neoplastic microenvironments (McMillin, Negri, & Mitsiades, 2013). Cell function is influenced by multiple signals, including signals from other cells and mechanical stimuli from extracellular matrix (ECM). In addition, the phenotype modification and invasion of cancer cells are highly influenced by the surrounding environment, because some characteristics such as the rigidity, porosity and structure may probably establish concentration gradients of nutrients, growth factors, hormones and oxygen levels to the cells according to the disease stage (Velasco, Tumarkin, & Kumacheva, 2012).

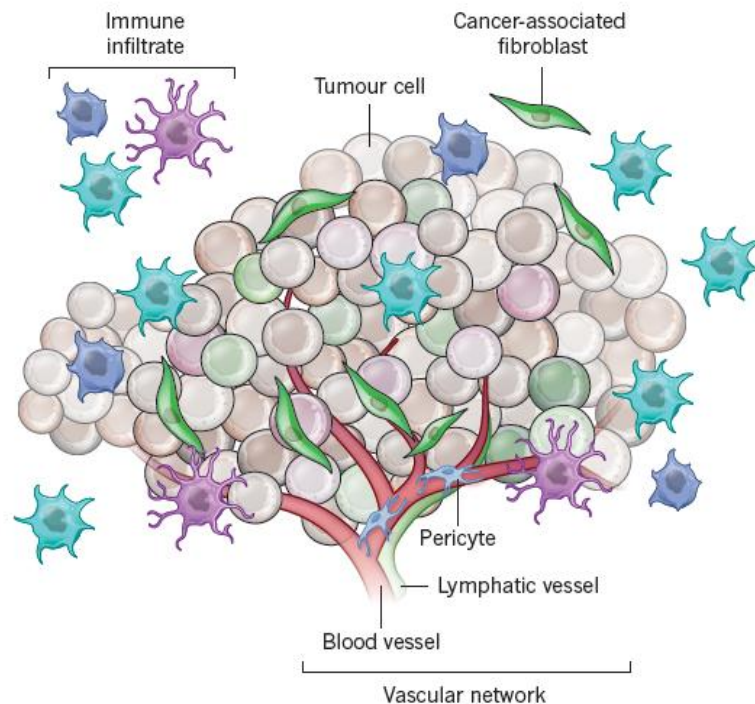


Figure 1.5 – Tumour microenvironment. Tumour heterogeneity arises from the existence of different type of cells and components, including cancer cells, extracellular matrix, vascular

endothelial, stromal and immune cells. These cells can have both pro- and anti-tumour effect and can change their activity and localization within the tumour. From (Junttila & de Sauvage, 2013).

1.3.1. Stroma

Tumour stroma is a supportive tissue around the tumour with different components, such as, ECM, mesenchymal cells, blood and lymphoid vessels, nerves and inflammatory cells (Kalluri & Zeisberg, 2006). Fibroblasts are the preponderant cell population on the tumour stroma (Green and Yamada, 2007; Rodemann, H Peter and Rennekampff, 2011; Simian *et al.*, 2001). They are non-vascular, non-epithelial and non-inflammatory cells and responsible for the fibrillar matrix synthesis of the connective tissue, once they produce type I, type III, type IV and type V collagen, fibronectin and laminin (Chang *et al.*, 2002). Fibroblasts also have a critical role in ECM homeostasis because they can produce matrix metalloproteinases (MMPs), which degrade ECM (Chang *et al.*, 2002; Green & Yamada, 2007). Moreover, fibroblasts secrete growth factors and other signals that regulate adjacent epithelia homeostasis (Kalluri & Zeisberg, 2006). There is a cross-talk between cancer cells and stroma cells during tumour progression: initial neoplasias recruit and activate stromal cell types that become preneoplastic, which in turn responds reciprocally by enhancing the neoplastic phenotypes of the neighbouring cancer cells. This stroma-tumour cross-talk leads to an increased inflammation, angiogenesis, fibroblast proliferation and proteolytic enzymes production, which contributes to tumour progression and to a pro-migratory and pro-invasive microenvironment (Gout & Huot, 2008; Mueller & Fusenig, 2004; Silzle, Randolph, Kreutz, & Kunz-Schughart, 2004). The cancer cells, again send signals back to the stroma, continuing the reprogramming of normal stromal cells in order to help the tumour progression. At last, signals from the stroma will enable cancer cells to invade normal tissues and create metastasis (Hanahan & Weinberg, 2011). When cancer cells are released into the blood stream and invade other tissue, they leave a supportive microenvironment (Christiansen & Rajasekaran, 2006). In fact, when these cancer cells invade a distant organ, they found a complete new and normal tissue microenvironment, which can possibly be a barrier to the growth of the seeded cancer cells (Hanahan & Weinberg, 2011; N. Bhowmick, 2011). Therefore, a new reciprocal interaction between cancer cells and stromal cells must be repeated. Moreover, in tumours, fibroblasts are metabolically more activated, once they secrete higher amounts of ECM and are more proliferative (Mundel, Kieran, & Kalluri, 2006). Research work with co-culture and microenvironment reconstitution assays highlights the role of fibroblasts in tumour progression (Kalluri & Zeisberg, 2006; Mueller & Fusenig, 2004;

H Peter Rodemann & Rennekampff, 2011; Silzle et al., 2004). Moreover, activated fibroblasts produce ECM rich in fibronectin and type I collagen, which contributes to tumour angiogenesis (Chang *et al.*, 2002). These activated fibroblasts existing in tumour stroma are also known as cancer-associated fibroblasts (CAF). The signals and mechanisms of transformation of a normal fibroblasts to a CAF are not completely understood (Fiaschi *et al.*, 2012; Kalluri & Zeisberg, 2006; Peng *et al.*, 2013). It is known that cancer cells secrete several molecules to the tumour stroma, such as transforming growth factor beta (TGF- β), platelet-derived growth factor (PDGF) and fibroblast growth factor 2 (FGF2), which are mediators of fibroblasts activation (**figure I.6**).

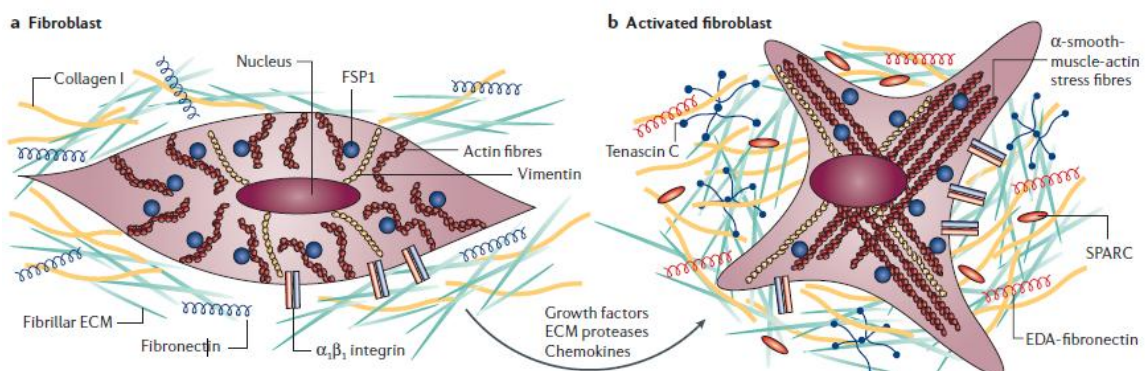


Figure I.6 – Transition of a normal fibroblast to a cancer associated fibroblast (CAF). a - The fibrillar ECM is mostly constituted by type I collagen and fibronectin. There are interactions between the fibroblasts and the microenvironment through $\alpha_1\beta_1$ integrin. Normal fibroblasts have a fusiform appearance and an actin and vimentin filaments and they also express fibroblast-specific protein I (FSP1). b- Activated fibroblasts are more proliferative and secrete more ECM proteins, such as type I collagen, tenascin C and fibronectin containing the extra domain A (EDA-fibronectin). They also express α -SMA. From (Kalluri & Zeisberg, 2006).

Fibroblasts interact with cancer, epithelial, endothelial, inflammatory cell and pericytes through the secretion of certain molecules (Mueller & Fusenig, 2004). This contributes to the modification of the microenvironment and increases oncogenic signals, which is likely to increase cancer progression (**figure I.7**) (Kalluri & Zeisberg, 2006).

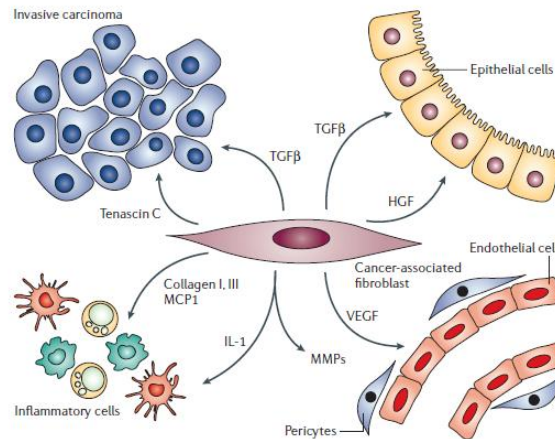


Figure 1.7- Action of activated fibroblast in the tumour microenvironment. Legend: Monocyte chemotactic protein I (MCP1); interleukin I (IL1); matrix metalloproteinases (MMPs); vascular endothelial growth factor (VEGF); transforming growth factor-beta (TGF- β); hepatocyte growth factor (HGF); stromal-cell-derived factor I (SDF1). From (Kalluri & Zeisberg, 2006).

In addition, CAFs mediate EMT of cancer cells, contributing to the progression of cancer, because many of the exogenous signals for EMT are derived from CAFs, such as MMPs, integrins and members of the TGF- β superfamily of proteins (Mueller & Fusenig, 2004; N. Bhowmick, 2011). TGF- β signalling is particularly striking for the analysis of cancer progression as at early stages it possible acts as a tumour suppressor. However, during advanced stages of cancer, TGF- β signalling promotes cancer progression and metastasis (Mueller & Fusenig, 2004). This means that the anti-proliferative effect of TGF- β is gradually lost while it facilitates EMT of cancer cells, along the progression of the disease (Siegel & Massagué, 2003). Therefore, there are evidences that support the protective action of the fibroblasts at an early stage of cancer progression. Moreover, fibroblasts produce immune-modulatory cytokines, such as interferon- γ , interleukin-6 and tumour-necrosis factor- α , which recruit cytotoxic T lymphocytes, natural killer cells and macrophages, that help to fight tumour progression at the beginning, before the tumour-stroma crosstalk (Silzle *et al.*, 2004). Additionally, the tumour-stroma crosstalk includes mutual metabolic reprogramming, responsible for the alterations on glucose uptake, for example. Therefore, it is extremely important to understand the effect of stroma cells on tumour progression and cancer cells metabolism.

1.4. Cancer cell metabolism

Glucose is one of the main nutrients to ensure cell viability, function and proliferation, since it is a carbon and energy source. In a normal epithelial cell, glucose can enter different metabolic pathways leading, for instance, to pyruvate production, CO₂

oxidation and aminoacids synthesis (Su *et al.*, 2010). However energy metabolism alteration is very characteristic of cancer cells (Daye & Wellen, 2012; Hanahan & Weinberg, 2011; Hsu & Sabatini, 2008). This aspect was first reported by Otto Warburg (1926, 1956). It is one of the main characteristics of cancer cells, known as Warburg effect (Hanahan & Weinberg, 2011). He noticed that tumour cells, unlike normal cells, reprogram their glucose metabolism, even in presence of oxygen, using aerobic glycolysis with reduced mitochondrial oxidative phosphorylation (Hsu & Sabatini, 2008; Otto Warburg, Franz Wind, 1926). The reason is that increased glycolysis enables glycolytic intermediates to enter into various biosynthetic pathways. This promotes the biosynthesis of macromolecules and organelles essentials to support the large-scale biosynthetic pathways that are required for active cell proliferation, as reviewed by Hsu (Hsu & Sabatini, 2008). Consequently, glucose is metabolized via glycolysis and produces lactate by lactate dehydrogenase (**figure 1.8**). Cancer cells are reported to be adapted to high levels of lactate (Kato *et al.*, 2013; P rtega-Gomes *et al.*, 2014).

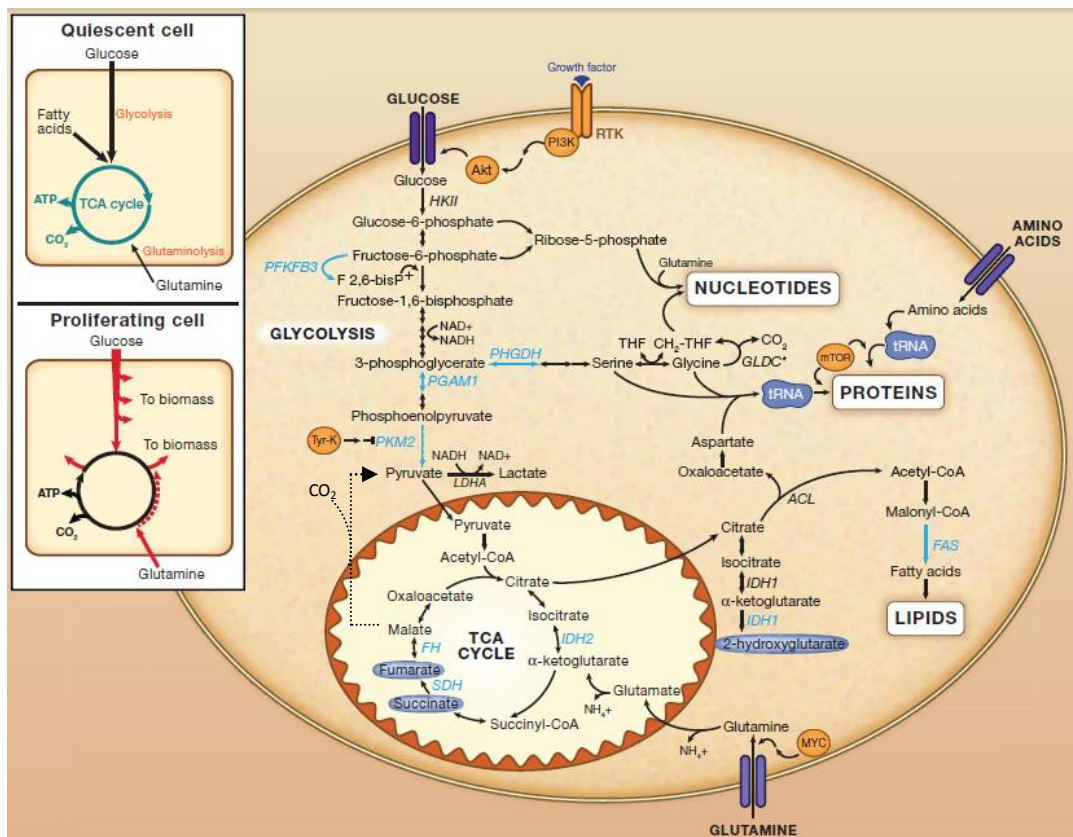


Figure 1.8 – Cancer cell metabolism pathways. Quiescent cells metabolize glucose, glutamine and fatty acids for CO₂ oxidation through tricarboxylic acid (TCA) cycle. NADH and FADH₂ are electrons carriers that will produce higher levels of energy through ATP synthesis in the mitochondrial electron transport chain. This way, quiescent cells efficiently convert the nutrients into energy to maintain cellular functions. On the other hand, rapidly proliferating cells need to generate all the proteins, lipids and nucleic acids essential to cellular division. In consequence, cancer cells have

a higher glucose and glutamine uptake, because they are the main nutrients to support cell growth. Glutamine catabolism constantly provides nutrients into the TCA cycle. This is important to preserve the TCA cycle function because there is a constant efflux of metabolites to support cell proliferation. Legend: 2HG, 2-hydroxyglutarate; α KG, alpha-ketoglutarate; ACL, ATP-citrate lyase; ATP, adenosine triphosphate; F-2,6-bisP, fructose 2,6-bisphosphate; FAS, fatty acid synthase; FH, fumarate hydratase; *GLDC, glycine decarboxylase. Note that this reaction occurs in the mitochondrion; HIF α , hypoxia-inducible factor, alpha subunit; HKII, hexokinase 2; IDH1, isocitrate dehydrogenase 1; IDH2, isocitrate dehydrogenase 2; LDHA, lactate dehydrogenase A; mTOR, mechanistic target of rapamycin; PFKFB3, phosphofructo-2-kinase/fructose-2,6-bisphosphatase3; PGAM1, phosphoglycerate mutase 1; PHGDH, phosphoglycerate dehydrogenase; PI3K, phosphatidylinositol-4,5-bisphosphate 3-kinase; PKM2, pyruvate kinase M2; RTK, receptor tyrosine kinase; SDH, succinate dehydrogenase; THF, tetrahydrofolate; Tyr-K, tyrosine kinase. Adapted from (Finley, Zhang, Ye, Ward, & Thompson, 2013)

Glutamine is the major nitrogen source of mammalian cells and an alternative energy and carbon source to glucose (H. J. Cruz, Ferreira, Freitas, Moreira, & Carrondo, 1999; Eagle, Washington, Cohen, & Levy, 1966). Therefore, glutamine is important for nitrogen metabolism, enabling the aminoacids synthesis, and acting as substrate for the TCA cycle. The cells uptake the glutamine and it is metabolized to glutamate in the cytoplasm through glutaminase activity. Glutamate is then converted into alpha-ketoglutarate (α KG) by losing the amino group, as NH_4^+ , via deamination. The α KG is incorporated directly in the TCA cycle (Newsholme *et al.*, 2003). This leads to ammonium accumulation, which can be toxic for cells and even inhibit their growth, due to intracellular pH decrease, inhibition of certain enzymes in several metabolic pathways and to cellular ionic gradients alterations (H. Cruz, Freitas, Alves, Moreira, & Carrondo, 2000; Schneider, Schütz, John, & Heinzle, 2010). There are strategies to decrease the ammonium concentration in the cell culture medium such as using dipeptides such as L-alanyl-L-glutamine in the cell culture medium, that allow a slow rate glutamine degradation and consequently a decrease in ammonium production (Christie & Butler, 1994). Lactate is mainly produced from glucose metabolism, but can also be produced in small amounts from glutamine through its conversion to glutamate which, in turn, is incorporated in TCA cycle and is converted to malate that can ultimately be metabolized to pyruvate. This one leads to lactate production though lactate dehydrogenase A (LDHA) (Zielke, Sumbilla, Sevdalian, Hawkins, & Ozand, 1980).

1.4.1. Tumour-stroma metabolic crosstalk

The reciprocal metabolic interplay between stroma and cancer cells suggests that CAFs also undergo Warburg effect and mitochondrial oxidative stress (Al, 2010; Fiaschi *et al.*, 2012). Fiaschi *et al.* observed that intercellular contact between cancer cells and stroma

cells activated the stromal fibroblasts, which increased its glucose transporter 1 (GLUT1) expression, lactate production and lactate extrusion by monocarboxylate transporter-4 (MCT4) overexpression (Fiaschi *et al.*, 2012). On the other hand, cancer cells had a higher lactate uptake to promote anabolic pathways and, consequently, cell growth. Hence, cancer cells promoted Warburg metabolism to their transformed CAFs, exploiting their byproducts, such as the lactate, in order to grow in a low glucose environment, using the lactate for TCA cycle and protein synthesis. This mechanism is an example of alternative strategies performed by plastic cancer cells, as these cells can either use Warburg metabolism in high glucose environment, but shift to reverse Warburg metabolism upon CAFs contact, if hypoxic/ischemic conditions lead to glucose starvation (Al, 2010; Pértega-Gomes *et al.*, 2014). Drugs targeting Warburg metabolism should take into consideration the multiple adaptations exploited by cancer cells, due to crosstalk with its stroma.

Therefore, developing new therapeutic strategies focusing on stromal cells such as CAFs seems to be an important step in cancer disease. The suitable therapeutic molecule should eliminate the cancer promoting characteristics but retain the tumour suppressor ones. One big advantage of targeting stroma is that these cells are not so genetically unstable as cancer cells and, consequently, do not develop drug resistance so easily (Mueller & Fusenig, 2004).

1.5. Need for new cellular models for pre-clinical research

The structure, development and functionality of a tumour is very complex because of the variety of interactions between different cell types presented in the tumour and its microenvironment (**figure 1.5**), including ECM, mesenchymal cells, blood and lymphoid vessels, nerves and inflammatory cells (Mundel *et al.*, 2006). As it was described before, there are different treatment approaches for lung cancer. However, they only provide a maximum of 5 year overall survival (Horn & Carbone, 2014; William D Travis, 2011). Consequently, the need for alternative therapies for lung cancer is urgent, as well as a better understand of the mechanisms underlying molecular pathways that can be potential therapeutic targets, such as the ones presented in **figure 1.9**. For instance, the sustaining proliferative signalling and the evasion to growth suppressor factors enable cancer cells to grow faster (Bailón-Moscoso, Romero-Benavides, & Ostrosky-Wegman, 2014). The signals behind these two mechanisms also influence cell survival and energy metabolism (Hanahan & Weinberg, 2011). Cells develop resistance to cell death by the expression of anti-apoptotic

proteins, such as the BCL2 protein family and undergo by an alteration in energy metabolism, becoming more glycolytic (Hsu & Sabatini, 2008). This means that cancer cells generate most of their ATP (adenosine triphosphate) via glycolysis, even under aerobic conditions, consuming high amounts of glucose and producing much more lactate than non-transformed cells (Hsu & Sabatini, 2008; Otto Warburg, Franz Wind, 1926). This aspect is known as the Warburg effect. Consequently, cancer cells need more nutrients to supply the high amount of energy they need. Therefore, there are signals that stimulate the formation of new vessels, such as the vascular endothelial growth factor (VEGF), which promotes angiogenesis (Alevizakos, Kaltsas, & Syrigos, 2013; Bailón-Moscoso et al., 2014; Lammers & Horn, 2013). EMT, another alteration in cancer cells mentioned above, regulates invasion and metastasis (Christiansen & Rajasekaran, 2006; J. M. Lee et al., 2006; Xiao & He, 2010). An additional factor that contributes for the tumour progression is its evasion to immune destruction, in particular by T and B lymphocytes, macrophages, and natural killer cells (Grosso & Jure-Kunkel, 2013; Hanahan & Weinberg, 2011). Genomic instability and genetic alterations are an extremely important mechanisms underlying tumour progression (Choi et al., 2010; Hanahan & Weinberg, 2011; W. Lee et al., 2010; Ma, 2012). Moreover, although inflammation occurs by innate immune cells to fight infection and heal wounds, in the microenvironment of a tumor and due to the tumor-stroma cross-talk, it has a tumour supporting effect (Landskron, De la Fuente, Thuwajit, Thuwajit, & Hermoso, 2014). So, all these mechanisms contribute for tumor progression and drug resistance, hence the need for a better comprehension of all these interacting phenomena. Nevertheless, the finding of new therapeutic targets and compounds implies their complete safety and nontoxicity for normal cells. This leads to the urgency in developing new testing strategies to identify anti-cancer agents faster, with more reliability and respect for animal welfare, in order to generate tests with higher high-throughput that can provide a more efficient treatment with the minimal side effects (Breslin & O'Driscoll, 2013). Therefore, it is extremely important to develop experimental model systems to validate putative driver lesions and to gain insight into their mechanisms of action.

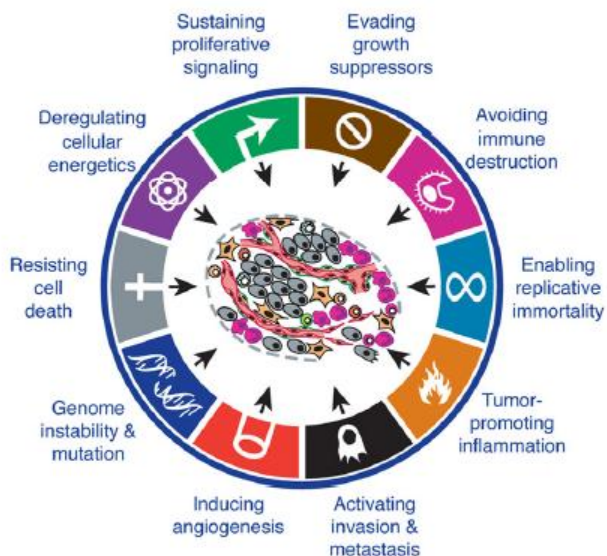


Figure 1.9 – Hallmarks of cancer. It is urgent to understand these mechanisms and to test potential drugs in the proper cellular models before its use in clinical trials. Adapted from (Hanahan & Weinberg, 2011).

1.6. Cancer preclinical models

1.6.1. The drug discovery cascade

There are several steps in order to successfully develop a new compound/drug. First, a therapeutic target needs to be found and then lead compounds are designed, developed and optimized for that specific target. After this, *in vitro* and *in vivo* tests are performed to evaluate toxicity, pharmacokinetic, absorption, distribution, metabolism and excretion properties. *In vitro* tests are performed using cell lines and *in vivo* tests using animal models, which are fundamental to determine the safety and potential usefulness of the drug. Finally, clinical trials are performed in humans to test the most effective compounds through various stages until the drug is shown to be safe and proved to have a sufficient level of efficacy to be commercialized (**figure 1.10**) (Breslin & O’Driscoll, 2013). Although a lot of compounds are being study, only 10% of them pass throughout clinical development (Hait, 2010; Hughes, Rees, Kalindjian, & Philpott, 2011).

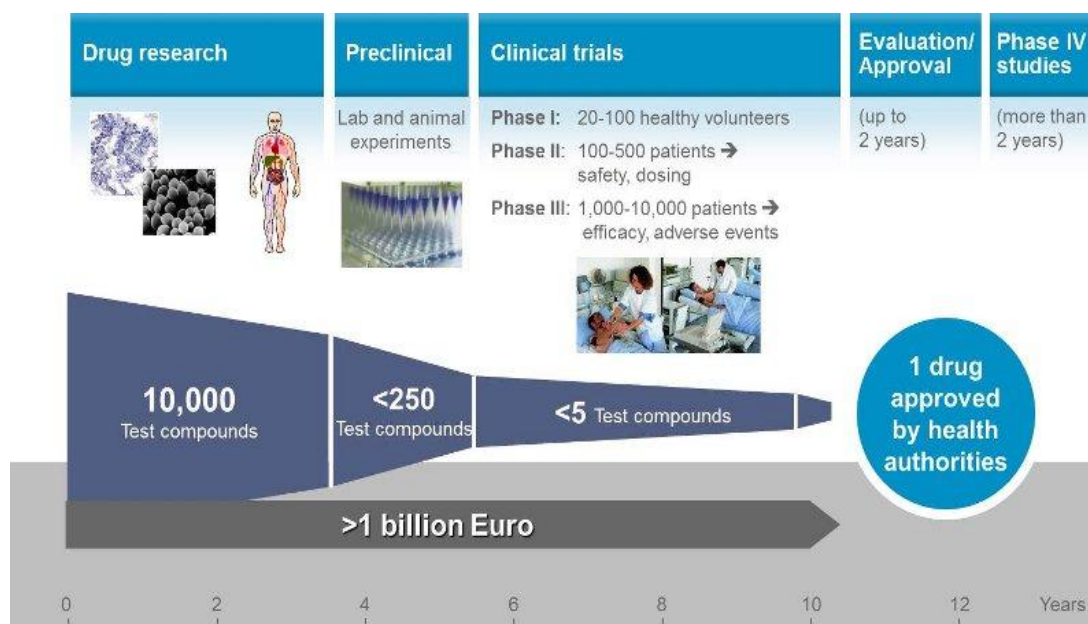


Figure I.10 – Drug discovery cascade. Developing a new medicine takes an average of 10 to 15 years. Source: based on PhRMA profile Pharmaceutical Industry 2014.

Due to the fact that the development and evaluation of a new drug is very expensive and takes several years to take place and that a lot of anti-cancer drugs fail in clinical trials (the phase of drug development with higher costs), it is urgent to eliminate the ineffective and unsafe compounds as early as possible (Hughes *et al.*, 2011). The ideal would be to do this before clinical trials, and, preferably, even before animal testing. These animal experiments cannot be dismissed during the drug development process. However, the results from the animal models should be carefully analysed in order to predict the magnitude of drug response in humans because some adverse reactions in humans do not happen during preclinical safety tests (Iwamoto, Distler, & Distler, 2011). This is due to the morphological and functional differences between animals and humans, including differences in protein expression, cell signalling pathways, responses to stimuli and affinity for ligands (Benien & Swami, 2014). All these issues support the requirement for better human cell model systems.

Consequently, it is crucial to improve *in vitro* cell models for drug testing in order to make a better choice of the right candidate drug and, as a result, to spare the cost of the development of drugs that will end to not have efficacy and safety (Breslin & O'Driscoll, 2013). Moreover, better *in vitro* cell models would also help to better understand the disease and to predict the best diagnostic, prognostic and/or treatment for each case. All of these evidence lead to the conclusion that is necessary to improve the cellular models used in cancer research in order to include the tumour three-dimensional organization,

heterogeneity and tumour-stroma crosstalk, resembling the heterogeneous expression of certain genetic markers by the different type of cells. Animal models are the most similar approaches to this theory, but there are some ethical and economical concerns related to the extrapolation from the animal studies to the human beings (Lilienblum *et al.*, 2008). Monoculture cellular models, using only one type of cell, were extensively used. However, it is already proved that the tumour associated stroma influences cancer progression. Therefore, culturing cancer cells with other types of cells, such as fibroblasts, in co-culture cellular models would better mimic the *in vivo* situation and allow a better understanding of the tumour molecular mechanisms, (Amann *et al.*, 2014; Breslin & O'Driscoll, 2013; Green & Yamada, 2007; H P Rodemann & Bamberg, 1995).

1.6.2. 2-Dimensional versus 3-Dimensional cell models

The conventional method for cell culture is to grow cells in monolayer, which is commonly used as system to analyze, for example, if a certain molecule is safe and effective as a therapeutic drug. Nevertheless solid tumours do not grow in 2-dimensions (2D), but instead in 3-dimensions (3D). ECM interactions are essential for cell differentiation, proliferation and cell survival *in vivo* and are better recapitulated in 3D cultures rather than in 2D monolayers. Furthermore, differences in cell morphology, polarity, receptor expression, oncogene expression and overall cellular architecture were noticed between cells grown as 2D monolayer and what is observed *in vivo* (Amann *et al.*, 2014; Bechyne, Szpak, Madeja, & Czyż, 2012; Carterson, Ho, Ott, Clarke, & Pierson, 2005; Yu Zhao *et al.*, 2014). Therefore, despite the easy manipulation, monitoring and characterization being advantages of the 2D culture systems, they have serious limitations related to spatial environment, structural architecture, comparability with *in vivo* systems and increased drug sensitivity because cells have a higher surface area exposure (J. Bin Kim, 2005; Pampaloni, Reynaud, & Stelzer, 2007). Consequently, 2D cellular models are not the most reliable system to select a candidate target or compound in pre-clinical research since cells in 2D structure lack many characteristics of an *in vivo* system.

Therefore, the need for cell models that mimic the environment within the target tissue, in order to produce reliable biomedical relevant results, is pushing researchers to try to develop alternative methods to 2D cell culture.

Multicellular tumour aggregates have been used as a 3D cancer cell model to investigate some aspects of tumour biology since the 1940's with the pioneer work of Holtfreter (Beetschen, 2001; Holtfreter, 1944), in which the researchers developed

aggregates of the three germ layers (mesoderm, endoderm and ectoderm) in order to study the gastrulation movements in amphibian embryos. However, multicellular spheroids only gained more attention after the research of Sutherland and co-workers (Sutherland, McCredie, & Inch, 1971) in the 1970s, in which the researchers observed a high similarity between aggregates of chinese hamster V79 lung cells and carcinoma from several patients. The authors observed an outer zone of the aggregates with many dividing cells, an intermediate area with less nutrients and oxygen that contained few dividing cells and an inner mass of necrosis (**figure I.II**). This zonal morphological and functional distribution is also observed in a carcinoma (H. Chen et al., 2014; Hashimoto et al., 2012; Moreira, Alves, Aunins, & Carrondo, 1995; Walenta et al., 2001). Therefore, aggregates started to be used because they were a useful *in vitro* cell model to evaluate aspects of tumour biology, such as the diffusion and effects of nutrients and oxygen on tumour growth.

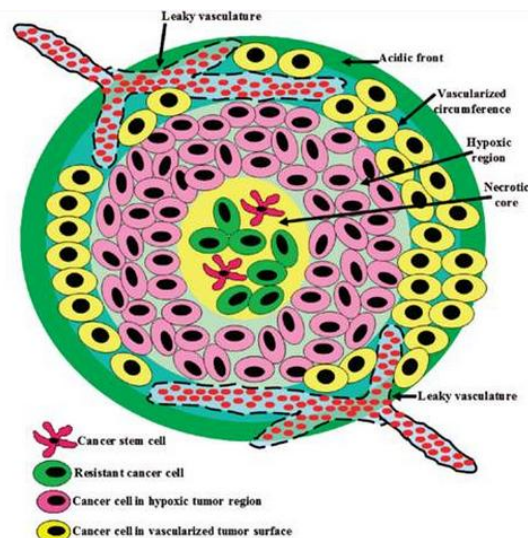


Figure I.II - Morphological and functional cellular distribution in a tumour. The scheme represents the usual structure of solid tumours representing the acidic front, the outer most vascularised surface, the hypoxic region and the necrotic core. This distribution is related with oxygen, nutrients and metabolites gradients within the solid tumour.

Adapted from <http://www.bme.umich.edu/labs/centlab/research/overview.php>.

So far, the best *in vivo* mimicking cell-based method is the 3D cell culture and it can be seen as a useful “bridge” between monolayer cultures and animal models. The co-culture of different types of cells using the 3D culture for the production of aggregates allows that the organization of heterogeneous cell populations and their growth pattern resemble the initial and avascular phase of solid tumours *in vivo*, not-yet-vascularized micrometastasis or intercapillary tumor microsites (Kelm et al., 2003). Therefore, it is urgent to develop 3D cell models and optimize the already existing methods.

There are several methods to generate a 3D cell culture. Some of them are described below.

1.6.3. 3D static cell culture methods

- **Forced-floating method**

This method consists in avoiding cell attachment to the vessel surface, by chemical modification with polymers such as 0.5% poly-2-hydroxyethylmethacrylate (poly-HEMA) (Ivascu & Kubbies, 2006) or using 1.5% agarose (Friedrich, Seidel, Ebner, & Kunz-Schughart, 2009; Ivascu & Kubbies, 2006). This surface treatment prevents cells from attaching, thus resulting in forced-floating cells and then cells are induced to aggregate through a centrifugation step (**figure I.12**). This method is advantageous because it is simple and generally reproducible, since it is usually done in multi-well plates, which also allows the seeding of the same number of cells into each well. In addition, the number of cells can easily regulate the size of the spheroids. For instance, if more cells are seeded, larger spheroids can be generated. Furthermore, forced-floating method using 96-well plates are very useful for high-throughput drug testing, because the spheroids can be easily accessible and it is possible to reproduce homogeneous spheroids in the 96-well plates. Nevertheless, there are also some drawbacks related to this method, such as the time and work spent to do the coating solutions and coating the plates before cell seeding and the difficulty to do the scale-up. The alternative is to buy low attachment plates (precoated plates) commercially accessible but this increases the cost of the method (Morizane, Doi, Kikuchi, Nishimura, & Takahashi, 2011). Moreover, medium exchange without disturbing the aggregate is difficult.

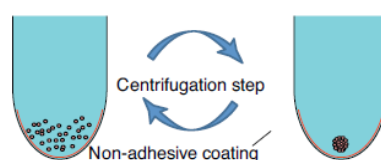


Figure I.12 – Forced-floating method. Adapted from (Breslin & O’Driscoll, 2013).

- **Hanging drop method**

Hanging drop method allows the formation of aggregates by growing a small drop of cellular suspension hanging on a glass cover slip that is inverted on a culture well (Amann et al., 2014; Fennema, Rivron, Rouwkema, van Blitterswijk, & de Boer, 2013; Kelm, Timmins,

Brown, Fussenegger, & Nielsen, 2003). The cell suspension become hanging drops and the surface tension caused by the gravitic force makes them to be kept in place while the cells accumulate at the bottom of the drop (Amann *et al.*, 2014). They stay at the air-liquid interface and can proliferate (**figure 1.13**). The size of spheroids can be regulated depending on the cell density of the seeding suspension. This is one of the advantages of this technique since it is possible to produce aggregates with well-controlled size in a fast and simple way. Another advantage is that the plates do not need to be coated with substrates as required in the technique described above (figure 1.11). However, the volume of the liquid drop is limited and that turns out to be a drawback of this technique, as the surface tension does not hold higher volumes. Another drawback is the difficulty in changing the cell culture medium without perturbing the spheroid (Tung *et al.*, 2011). In addition, this method is labour intensive, not suitable for scale-up and high-throughput drug screening because it is difficult to handle the established spheroids without damaging them (Benien & Swami, 2014).

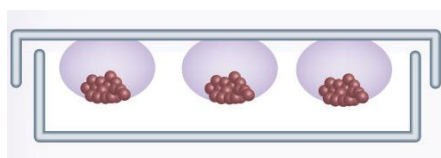


Figure 1.13 – Hanging drop method. First, the cell suspension is dispensed with a pipette and the surface with the cellular drop is inverted. The cellular suspension sticks to the hydrophilic part, forming a hanging drop. Then, single cells start to aggregate and can eventually form a single spheroid. Adapted from (Benien & Swami, 2014).

- **Matrices**

Cell-cell and cell-ECM interactions are extremely important to generate a 3D structure as they will determine cell polarization, function, differentiation and morphology (Akhtar & Streuli, 2013; Casey *et al.*, 2001; X. Zhong & Rescorla, 2012): In consequence, the use of matrices that can mimic the signals from neighbouring cells or from the basal membrane is a good strategy to develop aggregates, because it would enable cells to organize themselves as in an *in vivo* environment (Alcaraz, Nelson, & Bissell, 2004). In this method, cells can be embedded and grown within the matrice or they can be cultured in top of it (Sodunke *et al.*, 2007) (**figure 1.14**). Several materials, such as collagen, alginate and matrigel, have been used in 3D cell culture in order to mimic ECM characteristics, These materials have the advantage to maintain the 3D structure and they have been used to study intercellular interactions, cellular migration, invasion and tumour biology (J. Bin Kim, 2005).

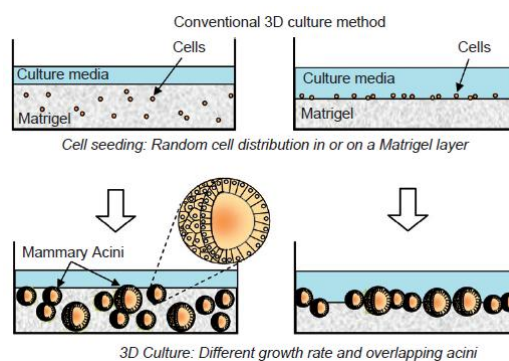


Figure 1.14 – 3D cell culture method based on Matrigel. Matrigel is one example of matrix, in which is possible to generate 3D cell structures, such as the mammary acini. Cells can be seeded within the gel or on its top. Aggregates can have different sizes due to different cell proliferation rates. From Sodunke *et al.*, 2007.

However, there are some drawbacks related to this method, because the ECM used is usually of biological origin and, therefore, there are differences in its composition according to the batch. In addition, some more complex ECM materials do not have a defined composition. Another issue to be taking into account in large-scale production of 3D spheroids is the cost of the matrix (Sodunke *et al.*, 2007). Moreover, it is difficult to control the size of the spheroids because cells are randomly seeded within or in the top of the gel and may proliferate at different rates, producing aggregates with different sizes (**figure 1.14**). In consequence, cell culture may not be homogeneous for drug testing (Vinci *et al.*, 2012). Additionally, they cannot mimic the mass transport gradient that exists in the tumour microenvironment (Benien & Swami, 2014)

- **Scaffolds**

Several types of scaffolds are already used for 3D cell culture, such as gels (Justice, Badr and Felder, 2009; Santo *et al.*, 2009). Shape, cell adhesion sites and a good diffusion of gases, nutrients and metabolites have to be considered when choosing the type of scaffold. For instance, the choice to use the scaffold with a fiber-like shape is a convenient strategy to enhance cell migration and matrix colonization, thus producing a more *in vivo*-like construct. (Justice *et al.*, 2009; Yu Zhao *et al.*, 2014). Furthermore, some of these models can have incorporated some signalling molecules, such as hormones or growth factors that contribute for the proliferation and organization of the cells in that scaffold (**figure 1.15**). To better mimic the *in vivo* microenvironment, sometimes a spatial and temporal coordination of multiple factors is demanded (Santo, *et al.*, 2009). Scaffolds can provide biomechanical and biochemical support by presenting the appropriate mediators to the surrounding tissue.

There are several strategies to control the spatial and temporal release of growth factors from the scaffold (**figure I.15**)

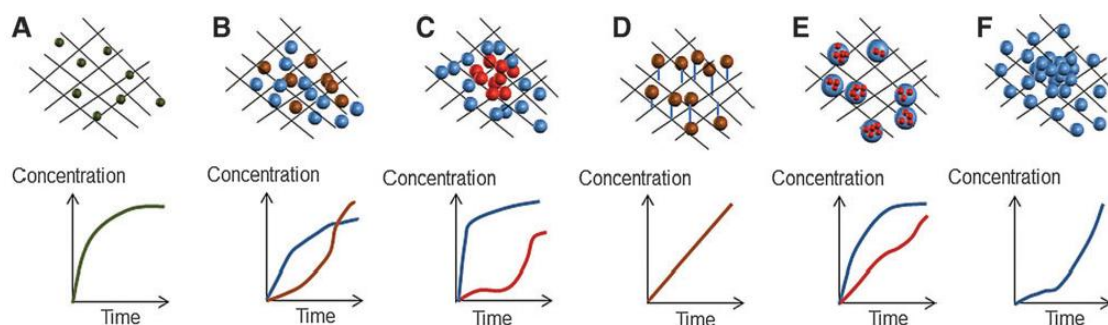


Figure I.15 - Strategies to promote the release of multiple bioactive factors from a scaffold. A) The signalling molecules are physically dispersed in the scaffold. And they are released in a fast and uncontrolled way; B) Bioactive factors are released simultaneously; C) Bioactive factors are released sequentially; D) Bioactive molecules have a spatiotemporal controlled release due to conjugation with ligands or because they are covalently bound to the scaffold. E) Nanoparticles can be incorporated inside microparticles within the scaffold promoting different release rates. F) Development of gradients of bioactive factors. From (Santo, Mano and Reis, 2013).

Employing a scaffold material is one of the strategies to create a 3D tissue structure *in vitro* because these scaffolds can provide a synthetic ECM with an appropriate template for the acquisition of a three-dimensional cellular architecture and gives essential stimuli to cell growth and tissue formation. Hydrogels, a type of highly hydrated polymer materials, such as chitosan and alginate-based hydrogels, are being used as scaffolds materials due to its biocompatibility, tissue-like properties, namely mechanical properties, nutrients and oxygen diffusion, cell motility and aqueous environment, resembling the tissue environment (Drury & Mooney, 2003; Glicklis, Shapiro, Agbaria, Merchuk, & Cohen, 2000; Yu Zhao et al., 2014). Crosslink between polymer chains by various chemical bonds and physical interactions determines the structural integrity of hydrogels. Moreover, cells cannot adhere immediately to the hydrogels because they do not have receptors to hydrogel forming polymers. To overcome this limitation of using hydrogels in cell culture, a peptide sequence capable of binding to cellular receptors, such as the amino acid sequence arginine–glycine–aspartic acid (Arg–Gly–Asp or RGD), can be covalently coupled to the polymer, (Drury & Mooney, 2003; El-sherbiny & Yacoub, 2013). This sequence is derived from numerous ECM proteins including fibronectin, laminin, vitronectin, and collagen (Drury & Mooney, 2003). Alginate is an example of a polymer used to form hydrogels. It is a natural polysaccharide extracted from the brown seaweed (Phaeophyceae) (Burey, Bhandari, Howes, & Gidley, 2008). Alginate is a linear polymer composed of β -(1-4)-linked D-mannuronic acid (M) and α -(1-4)-linked L-guluronic acid (G) residues (**figure I.16**), which gels due to the coordination of

divalent ions to the carboxylic acid groups of α - L -guluronic acid units (Velasco *et al.*, 2012). Varying the ratio of M/G monomers, modifies the crosslink density and, in consequence, the mechanical characteristics and pore size of the gel (Drury & Mooney, 2003).

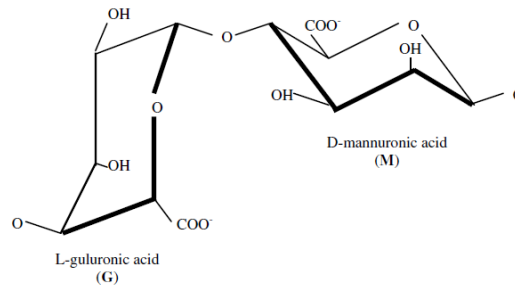


Figure I.16 – M/G residues that constitute the alginate. From (Burey *et al.*, 2008).

Alginate hydrogels are biodegradable, biosafe and high permeable to nutrients, which makes them widely used in 3D cell culture (Glicklis *et al.*, 2000; Hwang *et al.*, 2009; Miranda, 2010; Serra *et al.*, 2011). This hydrogel promotes the diffusion of oxygen, nutrients and drugs to the living cells and allows the dissipation of the waste products from the cells (Tostões *et al.*, 2011). Another advantage is the control of the pore size in order to provide the desired cell culture condition by controlling the M/G monomers ratio (Manuel & Gameiro, 2012; Wang & Wang, 2014). Furthermore, hydrogels can absorb high amounts of water or biological fluids due to its hydrophilic groups, swelling without dissolving. Hydrogels are soft and rubbery when swollen, which resembles in some extent the living tissues, giving favourable conditions for the proliferation of cells *in vitro*, maintaining its 3D structure (El-sherbiny & Yacoub, 2013).

3D organ/tissue printing is a new strategy in tissue engineering. Usually, one or more type of cells is mixed with the hydrogel and then this mixture is printed layer by layer in order to embed the cells within the hydrogel at the moment of printing. This way, a 3D scaffold with a defined shape and cellular morphology can be developed. In this technique, hydrogel scaffolds are essential because they supply the embedded cells with a support matrix and a highly hydrated microenvironment with controlled nutrient and oxygen diffusion. Moreover, the hydrogel should also provide the correct biochemical and physical signals, which are responsible for migration, proliferation and differentiation (Huh, Hamilton, & Ingber, 2011; Yu Zhao *et al.*, 2014).

Hydrogels can also be used as a base for cell-compatible microcarriers (**figure I.17**), which are spheres (generally with a diameter less than $500 \mu\text{m}^2$) that allow the culture of cells on its outer surface (non porous microcarriers) or in both sides of its surface, inside

and outside (porous microcarriers) (Benien & Swami, 2014; Schmidt, Rowley, & Kong, 2008; Serra et al., 2011). Microcarriers allow the culture of large number of cells in small volumes (Breslin & O'Driscoll, 2013; Serra et al., 2011). Collagen and laminin are used as microcarrier coatings, enhancing the cell culture on its surface (J. Bin Kim, 2005). In this case, cells grow as in 2D monolayer and physical forces from the environment and culture conditions can damage the cells (Justice et al., 2009; Kehoe, Jing, Lock, Tzanakakis, & Ph, 2010). On the contrary, porous microcarriers that allow growing cells also on inside surface, provide a protective environment from the shear forces. Another advantage of porous microcarriers is that they have higher surface area to unit volume ratio than non porous microcarriers. Moreover, microcarriers can be very advantages in specific cases: 1) to increase the total available surface of the culture substrate; 2) to grow large number of monolayers using a small container; 3) to co-culture different type of cells in close proximity; 4) to culture cells that do not aggregate spontaneously (Benien & Swami, 2014). Moreover, microcarriers deposit very easily making cell sampling, cell harvesting and downstream processing also very easy and simple. Nevertheless, microcarriers have some drawbacks concerning the adhesion to each other and the costs associated with the materials (J. Bin Kim, 2005; Serra, Brito, Correia, & Alves, 2012). Conventionally, microcarrier bead cultures involve growth in stirred tank vessels (**figure 1.19**) to assist in mixing and provision of nutrients.

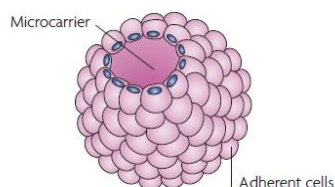


Figure 1.17 – Example of a non-porous microcarrier. Cells attach and grow on the outer surface. Adapted from (Pampaloni et al., 2007).

1.6.4. 3D agitation-based cell culture methods

Multicellular spheroids are the most common example of 3D cellular models and they can be formed by stationary, such as the examples given in **figures 1.11, 1.12, 1.13** and **1.14** or dynamic approaches (Kelm et al., 2003; Lin, Lin, & Chang, 2008). The main requisite for cells to grow as 3D aggregates is that the adhesive forces between the cells are higher than between the cells and the substrate where are cultured on (Mazzoleni, Lorenzo, & Steimberg, 2009). However, the stationary systems may have some drawbacks related to

intensive labour when preparing some specialized material in-house, control of the aggregates size, shape and number, medium exchange without damaging the aggregates, limitations on the mass transport and in some models there may be exist technical problems in retrieving the cells from the material (for example when using some type of scaffolds where the aggregates are embedded within the material) (Benien & Swami, 2014; J. Bin Kim, 2005). On the other hand, agitation-based approaches allow overcoming some of these limitations, such as a better control of the size and shape of the aggregates, homogeneity of physico-chemical parameters, for instance the pH, oxygen and nutrients, easy medium exchange and efficient diffusion of nutrients and removal of toxic byproducts (J. Bin Kim, 2005; Mazzoleni et al., 2009). Agitation-based approaches to culture cells as aggregates include gyratory rotation techniques, such as gyratory shakers, rotary culture system and stirred suspension culture systems (Brito et al., 2012; Kehoe et al., 2010; Moreira et al., 1995)..

- **Gyratory Shakers**

Gyratory rotation techniques consist in inoculating a defined concentration of cells in an erlenmeyer flask containing a specific amount of media and this flask is then rotated in a gyratory rotation (**figure I.18**) in a incubator until spheroids of required size be produced (Benien and Swami, 2014; Brito et al., 2012; Serra et al., 2011, 2012). This method is simple, cheap, produces large number of aggregates and allows a long-term cell culture. However the shear forces can damage the aggregates (J. Bin Kim, 2005).



Figure I.18 – Gyratory shaker for erlenmeyer. Cells are inoculated in the Erlenmeyer and due to agitation cells start to aggregate. From: www.wilmad-labglass.com

- **Rotary cell culture systems**

Rotary cell culture system or rotating wall vessel is a type of vessel developed by NASA (**figure I.19 a**). The container itself is rotated about a horizontal axis in order to

simulate microgravity and to expose cells to lower shear forces (Benien & Swami, 2014; Lin et al., 2008). This technique maintains cell growth in suspension and continuous medium perfusion and nutrient flow rate, assuring an efficient mass transport. Fluid turbulence and shear forces are minimized by the vessel being completely filled with medium. Cells do not attach to the walls and the speed of the rotation can be adjusted according to the type of cell and along time: slower in the beginning, when there is single cell suspension, in order to promote cell interactions and then, when cells start to adhere to each other and form larger 3D structures, the rotation needs to be higher, so that the heavier aggregates do not deposit and can continue in suspension (Hwang et al., 2009; Kelm et al., 2003). Another advantage of the rotating wall vessels is the production of long-term cultures, obtaining high yields of large spheroids. This technique also enables co-culture multiple cell types to generate a complex heterogeneous 3D *in vitro* structure and provides an efficient gas transfer through a semi-permeable membrane (J. Bin Kim, 2005; Serra et al., 2012). However, the rotary cell culture system is very expensive because specialized equipment is needed and has low scalability. In addition, it is not possible to control the number of cells that constitute each aggregate. In consequence, the suspension cell culture may have different size aggregates, which requires a manual selection of similar size aggregates to do drug screening (Friedrich et al., 2009; Ivascu & Kubbies, 2006). Another important limitation is the difficulty in sampling, which is only performed at the end of cell culture (Serra et al., 2012).

- **Stirred-tank culture vessels**

Stirred vessels are a cylindrical container with an impeller, which can be a paddle or a rod, in order to stir the cell suspension. Stirred suspension culture systems, such as stirred tank culture systems (**figure 1.19 b**)), prevent adherence of cells to the vessel allowing a suspension cell culture (Breslin & O'Driscoll, 2013; J. Bin Kim, 2005). This is achieved with constant agitation by the impeller and chemical coating of the vessel walls, for example with dimethyldichlorosilane (Breslin & O'Driscoll, 2013). As in the rotary cell culture system, the speed of agitation is adjusted during cell culture to optimize cell interactions and, in consequence, cell aggregation (Alves, 1996). The speed is then increased to control aggregates size and shape through the hydrodynamic forces and also to prevent the deposition of the bigger and heavier aggregates (Kelm et al., 2003). This culture system have several advantages, such as the production of large spheroids, long-term cultures because it enables an easy medium exchange without damaging the aggregates, the possibility to scale-

up, obtaining high yields of aggregates and easy sampling, allowing a continuous monitoring and characterization of the culture throughout time (Moreira *et al.*, 1995). In addition, the stirring dynamic allows an efficient mass transport of nutrients and cell waste products to and from the spheroids, respectively (J. Bin Kim, 2005). Despite all the advantages of the stirred tank culture systems, they still present some disadvantages, since the shear force from the paddle that create the agitation can damage physiologically the aggregates (Lin *et al.*, 2008; Serra *et al.*, 2011). However, spinner-flasks are one of the most used 3D techniques due to its simplicity, low cost and efficient production of aggregates (Benien & Swami, 2014; Breslin & O'Driscoll, 2013; J. Bin Kim, 2005).

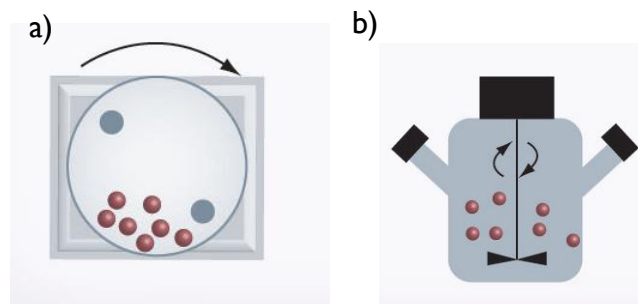


Figure 1.19 – Agitation-based approaches for the production of aggregates. a) Rotary wall vessel; b) Spinner flask with paddle impeller. Adapted from (Benien & Swami, 2014)

- **Computer-controlled stirred tank bioreactors**

Although spinners are widely used to culture cells in 3D, these systems are not fully controlled. On the other hand, computer-controlled stirred tank bioreactors (**figure 1.20**) allow an automated control of the environment, including on-line monitoring and control of specific cell culture parameters, such as temperature, pH, dissolved oxygen and nutrients (Martin, Wendt, & Heberer, 2004; Serra *et al.*, 2012; Tostões *et al.*, 2011). These variables are essential to ensure high cell viability and proliferation, contributing to high yields and long-term cultures. Additionally, this type of bioreactors have a simple design and are very flexible since they can operate in different modes, such as batch, fed batch and continuous perfusion. In the batch mode there are no medium exchanges until the end of the cell culture. In a fed batch reactor, fresh medium is continuous or periodically added to the cell culture, without any medium removal. In continuous perfusion bioreactor, fresh medium is continuously added and bioreactor medium is continuously removed, allowing an automatic and regular replacement of cell culture medium (Martin *et al.*, 2004); this enables a continuously cell feeding and waste products removal (Tostões *et al.*, 2011).

This method is very similar to the spinner, sharing some of its advantages, such as the efficient mass transport, high aggregate yields, long-term cell cultures, scalability, non-destructive sampling, aggregate size and shape control (Hutmacher & Singh, 2008; Martin et al., 2004; Miranda, 2010). However, as the spinner, computer-controlled stirred tank bioreactors have limitations regarding the shear forces due to stirring and high amounts of medium and starting cell number, which may increase the costs (Kehoe *et al.*, 2010; Mazzoleni *et al.*, 2009). Nevertheless, computer-controlled bioreactors allow a rigorous control and monitoring of environment variables and medium perfusion that are not possible in spinner-flasks (Tostões *et al.*, 2011). The control of these parameters allows for a cell behaviour more similar to what happens *in vivo* because it is possible to control, for instance, dissolved oxygen, with the aim to resemble the physiological blood flow (Kehoe *et al.*, 2010; Tostões *et al.*, 2011).



Figure 1.20 - A 4-fold DASbox® Mini Bioreactor System for cell culture. This system enables an on-line monitoring and control of specific cell culture parameters, such as temperature, pH, dissolved oxygen and nutrients. Adapted from <http://www.dasgip.com/cell-culture/>

The agitation-based approaches mentioned above have the advantage to be accommodated to different 3D culture strategies, such as cell aggregates, microcarriers, microencapsulated cells/aggregates, presenting widespread potential in cell bioengineering and, consequently, in developing new cellular models that would enable to resemble the tumour microenvironment and, thus, better understand, for instance, cancer biology and drug resistance (Jang, Cho, Cho, Park, & Jeong, 2010; Rodrigues, Diogo, da Silva, & Cabral, 2011). Moreover, stirred suspension bioreactors are commonly used in biotechnology industry; therefore, systems using this type of bioreactor may be easier to be translated to generation of products with commercial value (Kehoe *et al.*, 2010).

- **Microfluidic cell platforms**

Microfluidic devices (**figure 1.21**), or micro-bioreactors, are efficient small-scale systems that promote the formation of cellular aggregates and provide a precise control over the cell microenvironment by adjusting specific parameters such as the perfusion rate (Fennema *et al.*, 2013). This process can be easily automated and have low volume drug testing (Benien & Swami, 2014). Besides the long-term cell cultures, other advantages of using microfluidic technology are the enhanced nutrient transport, the need for small amount of reagents and cells (S.-Y. C. Chen, Hung, & Lee, 2011). However, there are some limitations such as the low scalability, high shear stress due to the perfusion and continuous removal of medium that contains factors secreted by cells that could influence cell culture (Meyvantsson & Beebe, 2008).

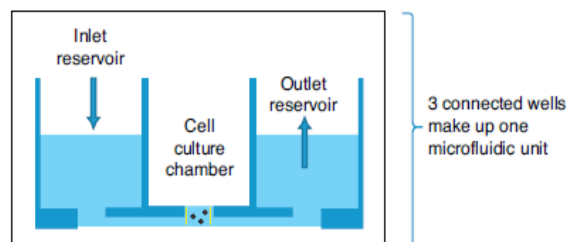


Figure 1.21 - Design of a 3D microfluidic device. It has an open-top chamber and inlet and outlet wells. There is continuous perfusion of medium from the flow inlet well, crossing the microfluidic chamber and getting out from the outlet well. Gravity and surface tension forces are the responsible for the perfusion, so this technique does not require any external pumps. This perfusion allows the cell feeding and it is due to the gravity when there is a liquid height difference between the inlet and outlet wells. The inlet well should have more liquid than the outlet well and the difference regulates the perfusion rate. Cells are dispensed directly into the open access culture chamber. Surface tension pressure prevents liquid from flowing out of the open chamber. Adapted from Breslin and O'Driscoll, 2013; Chen, S.-Y. C. *et al.*, 2011.

A summary of the advantages and disadvantages of the several 3D cell culture models is presented in **table 1.3**.

Table 1.3. Advantages and disadvantages of different 3D cell culture techniques

| Advantages | Disadvantages |
|---|--|
| <u>Forced-floating method</u> | |
| <ul style="list-style-type: none"> -Simple -Inexpensive -High-throughput testing -Spheroids easily accessible | <ul style="list-style-type: none"> -Material coating is relatively labour intensive -Produces small amounts of spheroids |
| <u>Hanging-drop method</u> | |
| <ul style="list-style-type: none"> -Homogenous spheroids -No specialized equipment required -Spheroids easily accessible | <ul style="list-style-type: none"> -Expensive when using specialised plates -Labour intensive when preparing plates in-house -Small volumes difficult medium exchange |

| | |
|--|---|
| | <ul style="list-style-type: none"> without perturbing the cells -Difficult long-term culture -Low throughput -Small number of aggregates |
| <hr/> | |
| <u>Matrices and scaffolds</u> | |
| <ul style="list-style-type: none"> -3D support that mimics <i>in vivo</i> environment -Can incorporate growth factors and other cell signalling molecules | <ul style="list-style-type: none"> -Lack of materials approved for clinical applications -Difficulties in retrieving the cells in some models -Limit mass transport -Biocompatibility and biodegradability issues |
| <hr/> | |
| <u>Rotary culture system</u> | |
| <ul style="list-style-type: none"> -Simple -Low shear stress -Efficient gas and nutrients transfer -Supports 3D cell culture, such as cell aggregates and cells immobilized on scaffolds or microcarriers -Produces large amounts of aggregates -Long-term culture -Culture several cell types | <ul style="list-style-type: none"> -Specialized equipment required -Expensive -Low scalability -Sampling only at the end of cell culture, not enabling monitoring throughout |
| <hr/> | |
| <u>Stirred tank systems</u> | |
| <ul style="list-style-type: none"> -Simple -Allows large-scale production -efficient mass transport -Spheroids easily accessible -can feed high-throughput screening - -Long-term culture - -Accurate control of physico-chemical parameters (when using computer controlled bioreactors) -Control of aggregates size and shape -Easy sampling and monitoring and characterization throughout time -Possibility to work in perfusion -Supports 3D cell culture, such as cell aggregates and cells immobilized on scaffolds or microcarriers -Culture several cell types | <ul style="list-style-type: none"> -Shear stress can be harmful for more sensitive cells -Specialized equipment required (computer-controlled bioreactors) -Expensive (computer -controlled bioreactors) -High amounts of reagents (ex: medium) |
| <hr/> | |
| <u>Microfluidic platforms</u> | |
| <ul style="list-style-type: none"> -High-throughput testing -Allows optimization of culture conditions -Accurate control of cell microenvironment through the adjust of the perfusion rate -Efficient mass transport -Allows miniaturization and the study of cell-cell interactions or single cell analysis | <ul style="list-style-type: none"> -Expensive due to required specialized equipment -Requires low amounts of reagents -Shear stress due to perfusion -Low scalability -Removal of important paracrine factors secreted by cells due to perfusion |

1.6.5. Mimicking the microenvironment *in vitro*

Cell fate, proliferation and viability are highly dependent on signals that lie in the extracellular environment, such as the ECM, soluble factors, cell–cell interactions, physical forces and physicochemical factors (Alessandri et al., 2013; Palecek, 2011; Peng et al., 2013; Santo, E. et al., 2013; Yamasaki et al., 1995). Natural ECM is composed by fibrous proteins, for instance, fibronectin, collagen and laminin (Yu Zhao et al., 2014) and some matrices and scaffolds, such as hydrogels, are widely used to mimic some ECM characteristics (Drury & Mooney, 2003; El-sherbiny & Yacoub, 2013; Wang & Wang, 2014). Soluble factors can be mimicked by medium composition allied with physiological concentration of certain supplements and with the most suitable operation mode, such as fed-batch or perfusion modes, which can be applied in stirred tank bioreactors. These culture operation modes allow a better control of physicochemical factors concerning the nutrients, metabolites, temperature, oxygen and pH and a continuous cell culture feeding and not complete removal of factors secreted by the cells, which are essential for paracrine and endocrine cell-cell interactions (Serra et al., 2012). These cell-cell interactions also depend on cellular concentration, colony size, co-culture using several cell types and cellular spatial organization. Spatial organization and 3D structure are very important to ensure a viable and functional cellular model, which can be accomplished using a microencapsulation technique, using, for instance, alginate (Alessandri et al., 2013; Serra et al., 2011). Cellular aggregates or single cells are entrapped inside the alginate capsules that allow bidirectional diffusion of nutrients, oxygen and waste products (**figure 1.22**). There are several advantages such as cells being protected against the shear forces due to the dynamic agitation when cultured in a stirred culture vessel (Serra et al., 2011; Velasco et al., 2012), which contributes to high cell viability. Additionally, cellular aggregates in alginate capsules often have apicobasal polarization (J. I. Partanen, Nieminen, & Klefstrom, 2009). This does not happen in a 2D planar cell culture where the cells are in a flat monolayer. In addition, the encapsulation method makes possible to change physical and chemically the hydrogel properties, by changing the relative amounts of gel components, for example. These changes are important to study the role the 3D microenvironment on cell fate and function and to enable an efficient mass transport, promoting a long-term cell culture (Tostões et al., 2011; Velasco et al., 2012; Wang & Wang, 2014). Moreover, cell microencapsulation using alginate has already been reported in order to enhance viability and functionality in different type of cells,

including hepatocytes, stem/progenitor cells in stirred vessels comparing to 2D cell culture, as cell monolayer, and 3D cell culture, as non encapsulated aggregates (Miranda, 2010; Serra *et al.*, 2011; Tostões *et al.*, 2011). Furthermore, the development of 3D cellular models by encapsulation allows assembling together in the same spatial environment cells with different phenotypes. In consequence, it is possible to construct a 3D *in vitro* model that simulates the heterogeneous tumour microenvironment, co-culturing, for instance, stromal fibroblasts and cancer cells aggregates within the same alginate capsule (Alessandri *et al.*, 2013). Therefore, stirred vessels combined with microencapsulation technique are a promising strategy to improve the 3D cellular models already existing in pre-clinical research.

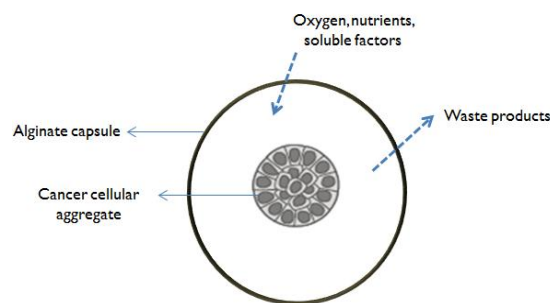


Figure 1.22 - Concept of cell microencapsulation. This technique consists of enclosing biologically active material, such as cancer cellular aggregates, within a polymeric matrix (e.g. alginate), allowing the bi-directional diffusion of nutrients, oxygen and waste.

1.7. Thesis aim

This thesis focused on the generation of a robust and scalable human cellular model of NSCLC that could better mimic the *in vivo* tumour physiology and microenvironment, with potential use for pre-clinical research and pharmacological applications. Therefore, a 3D strategy was performed to resemble: 1) the three-dimensional cellular organization of a lung tumour; 2) the tumour cellular heterogeneity, especially the tumour and fibroblast component; 3) ECM compartment.

The first aim of this thesis work was to establish a robust aggregation strategy for generation of NSCLC cellular aggregates in order to mimic cell-cell interaction between cancer cells within a tumour. To attain this, cancer cell lines representing 2 different subtypes of NSCLC derived from metastatic sites of the tumour, namely H460 (large-cell carcinoma) and H1650 (bronchioalveolar carcinoma) were cultured in stirred tank system.

The second objective was to develop a 3D NSCLC cell model that could better mimic the tumour microenvironment, including the cell-ECM interactions and the tumour cellular heterogeneity. The aggregation strategy in stirred suspension system developed in aim I was combined with a microencapsulation technique using alginate. Therefore, H1650 cancer aggregates were encapsulated with and without normal lung fibroblasts and then cultured in a stirred tank system.

All cell cultures were monitored throughout time, assessing cell viability, proliferation, metabolism, phenotype and morphology (**figure 1.23**) in order to characterize the developed 3D cell cultures.

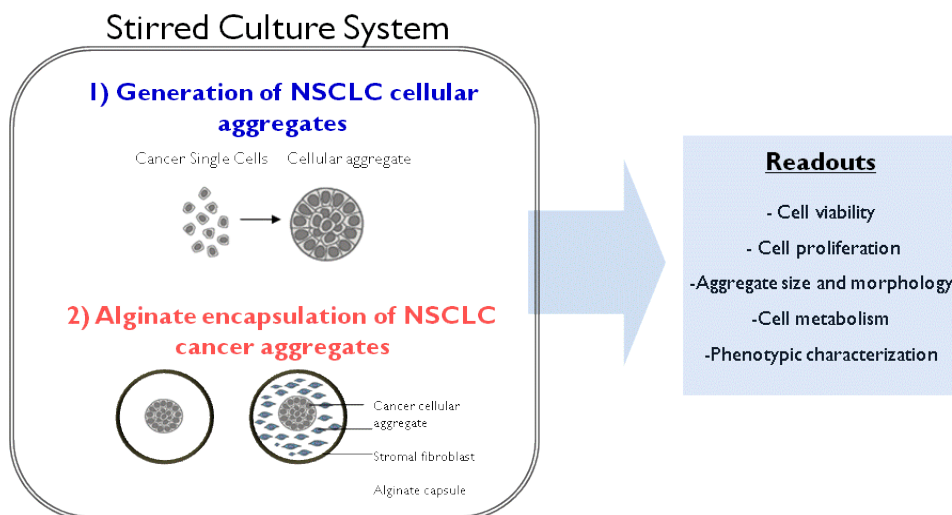


Figure 1.23 – Aim of the thesis and strategies performed to accomplish the objectives.

Materials and Methods

2. Materials and Methods

2.1. Cell lines and cell culture conditions

H460 and H1650 NSCLC cell lines were selected for the development of lung cancer aggregates due to their different origin within the tumour and because they represent the major NSCLC subtypes, adenocarcinoma and large-cell lung carcinoma (**table 1.1**). Both cell lines come from a metastatic site with pleural effusion (**table 2.1**) (Gong *et al.*, 2011). Malignant pleural effusion occurs when a cancer leads to an atypical amount of fluid between the thin layers of tissue (pleura) lining the outside of the lung and the wall of the chest cavity. Lung cancer accounts for 50-65% of malignant pleural effusions and it is associated with a poor outcome (Antony *et al.*, 2001; Sugiura *et al.*, 1997). H1650 cell line was further used to study the cell-cell, cell-ECM and tumor-stroma interactions because it represents a subtype of NSCLC, the bronchioalveolar carcinoma, which is characterized by unique pathologic, radiographic and clinical features, such as bilateral lung involvement, non symptomatic development and higher incidence in non smokers compared to other lung malignancies (Shivanthan and Wijesiriwardena, 2011; Tan *et al.*, 2003). Another important issue related to this type of NSCLC is its increase in incidence, particularly in younger and nonsmoking women (Furák *et al.*, 2003; Hirsch *et al.*, 2005). This cell line was also used due to its metastatic potential (Gong *et al.*, 2011).

The NSCLC cell lines H1650 and H460 were obtained from American Type Culture Collection and the immortalized patient-derived normal fibroblast 14195 cell line (NFs 14195), derived by Heiko van der Kuip (RBMF, Stuttgart) within the scope of the PREDECT project and immortalized by Moshe Oren (Weizmann Institute, Israel).

Table 2.1: Cell lines used to generate NSCLC cellular aggregates

| Name (Reference ATCC) | Type | Source |
|-----------------------------|----------------------------|------------------------------|
| H1650 (CRL-5883) | Bronchioalveolar carcinoma | Metastatic, pleural effusion |

| | | |
|-------------------|----------------------|------------------------------|
| H460 (HTB-177) | Large-cell carcinoma | Metastatic, pleural effusion |
|-------------------|----------------------|------------------------------|

Adapted from (Gong *et al.*, 2011)

H460 cell line was cultured in RPMI medium 1640 (1x) + GlutaMAX™-I (from Alfacene), supplemented with 10% (v/v) heat-inactivated fetal bovine serum (FBS), U.S. origin from Gibco®, 1% (v/v) of penicillin and streptomycin (P/S, Invitrogen) and 1 µg/mL of puromycin (Invivogen). HI650 and NFs 14195 cell lines were cultured in RPMI medium 1640 (1x) + GlutaMAX™-I (from Alfacene), supplemented with 10% (v/v) of heat-inactivated fetal bovine serum (FBS), U.S. origin from Gibco® and 1% (v/v) of penicillin and streptomycin. GlutaMAX™-I is a supplement already incorporated in the medium that contains a stabilized form of glutamine, the dipeptide L-alanyl-L-glutamine, which prevents the rapid degradation of glutamine and ammonia buildup in both adherent and suspension cultures (Christie & Butler, 1994). All cell lines were incubated at 37°C in humidified atmosphere of 5% CO₂.

All cell lines were routinely cultured in adherent and static conditions until establishment of the 3D culture. Cells were sub-cultured twice a week at 1.5x10⁴cell/cm² (HI650 and H460 cell lines) and 1x10⁴cell/cm² (NFs 14195 cell line) in standard tissue culture flasks (150cm² T-Flasks from BD Biosciences). For each sub-culture, cells were rinsed with Dulbecco's phosphate-buffered saline (DPBS), washed for 2 minutes with DPBS and trypsinized using 0.05% trypsin- Ethylenediaminetetraacetic acid (EDTA; Invitrogen), for 2-4 minutes. Viable cells were counted using trypan blue exclusion test as described on section 2.4.1.

2.2. Generation of NSCLC aggregates and culture conditions

HI650 and H460 cells were dissociated from the 2D static cultures by trypsinization using 0.05% trypsin-EDTA (Invitrogen) and inoculated as single cells at a density of 2x10⁵ cell/mL into silanized 125mL spinner-flasks, with straight blade paddle impeller (from Corning® Life Sciences, **figure 2.1**). This type of impeller improves stirring and minimizes shear stress derived from the hydrodynamic forces. To prevent cell attachment to the walls, spinner flasks were pre-coated with 2-3 ml of dimethyldichlorosilane (Merck 8.03452, Germany). The spinner flasks were placed on a magnetic stirrer. Inoculation was performed in 75mL of the correspondent medium of each cell line. During aggregation phase, cells were cultured in a batch operation mode, without medium exchange. Cultures were initiated with a stirring rate of 40 rpm in order to promote cell interactions. After 4 hours of cell culture,

50 mL of fresh corresponding medium were added to yield a final volume of 125 mL. For each cell line, stirring rate was adjusted throughout time until 60 rpm, according to the cell-cell aggregation profile (**figure 2.1**) to promote cell-cell adhesions and cell aggregation, to prevent cellular clumps and control size and shape of aggregates. Cells were allowed to aggregate and cell culture was maintained for 3 days and cell cultures were monitored every day, analyzing cell viability, concentration, metabolic activity, aggregate size, concentration and morphology during time.

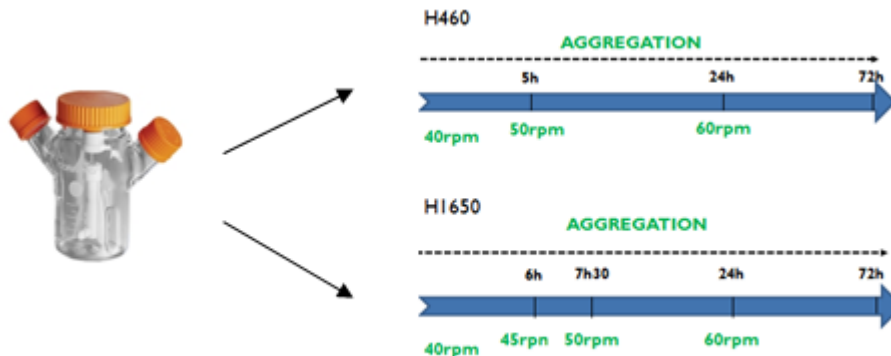


Figure 2.1 - Stirring profile for H460 and HI650 cellular aggregations using spinner-flasks with straight paddle impeller (Corning® Life Sciences). Stirring rate was adjusted for each cell line to promote cell aggregation, to prevent cellular clumps and to control size and shape of aggregates.

2.3. Development of a 3D NSCLC cellular model

2.3.1. Fibroblasts membrane staining protocol

Fibroblasts used in the co-cultures with HI650 aggregates were incubated with PKH dye (PKH26 Red Fluorescent Cell Linker Kit, Sigma-Aldrich) for membrane labelling in order to do an *in vitro* cell monitoring through fluorescence microscopy during co-culture. PKH26 is a fluorescent dye with long aliphatic tails that incorporates into lipid regions of the cell membrane, labelling cells with a red colour for long periods of time and without affecting cell viability. Briefly, cells were trypsinized and counted with the trypan blue exclusion method (described in section **2.4.1**). Cells were centrifuged at 300g for 5 minutes and then washed with serum-free medium and centrifuged as before. The pellet of cells was carefully resuspended in diluent provided by the kit. This cellular suspension was then incubated for 5 minutes with a 2x Dye Solution in diluent C, prepared immediately before use. After this, an equal volume of serum was added to the cellular suspension in order to stop the reaction. This cellular solution was diluted 1:2 in supplemented cell culture medium and centrifuged as described previously. Cells were washed 3 times with phosphate-buffered saline (PBS) and

then resuspended in supplemented cell culture medium before 3D culture with cancer cellular aggregates.

2.3.2. Encapsulation of NSCLC cellular aggregates

Polymer - Alginate: Ultra Pure MVG alginate (UP-MVG NovaMatrix, Pronova Biomedical, Oslo, Norway) was mixed with GRGDSP peptide-coupled MVG alginate (NOVATACH, NovaMatrix) in a 1:4 proportion. The final alginate solution was prepared at a concentration of 1.1% (w/v) in 0.9% (w/v) NaCl solution, which are formulations previously optimized in the group (Rebelo *et al.*, 2014; Serra *et al.*, 2011; Tostões *et al.*, 2011, 2012).

Microcapsules formation: H1650 cellular aggregates were encapsulated with 1.1 % (w/v) of alginate prepared as described in the previous paragraph. Encapsulation was performed in an electrostatically driven microencapsulation unit VarVI (Nisco) using an alginate-cell mixture prepared at a concentration of 6×10^6 cell/mL of alginate for mono-cultures and 12×10^6 cell/mL alginate for co-cultures. These encapsulation conditions yielded microcapsules with a diameter of approximately 500 μm . The crosslinking reaction of the microcapsules was done by precipitating the generated droplets directly from the nozzle into a 20 mM BaCl_2 solution, adjusted to 290-300 mOsm, using NaCl, buffered at pH 7.4 with 5 mM histidine (**figure 2.2**). Alginate microcapsules were washed three times with 0.9% (w/v) NaCl solution and once with RPMI 1640 – GlutaMAX™-I medium before being transferred to stirred culture systems.

Alginate microcapsules dissolution: Ba^{2+} -UP MVG alginate was dissolved by incubating the microcapsules with a chelating solution (50 mM EDTA in mQ water) for 5 minutes at room temperature (RT) using vortex.

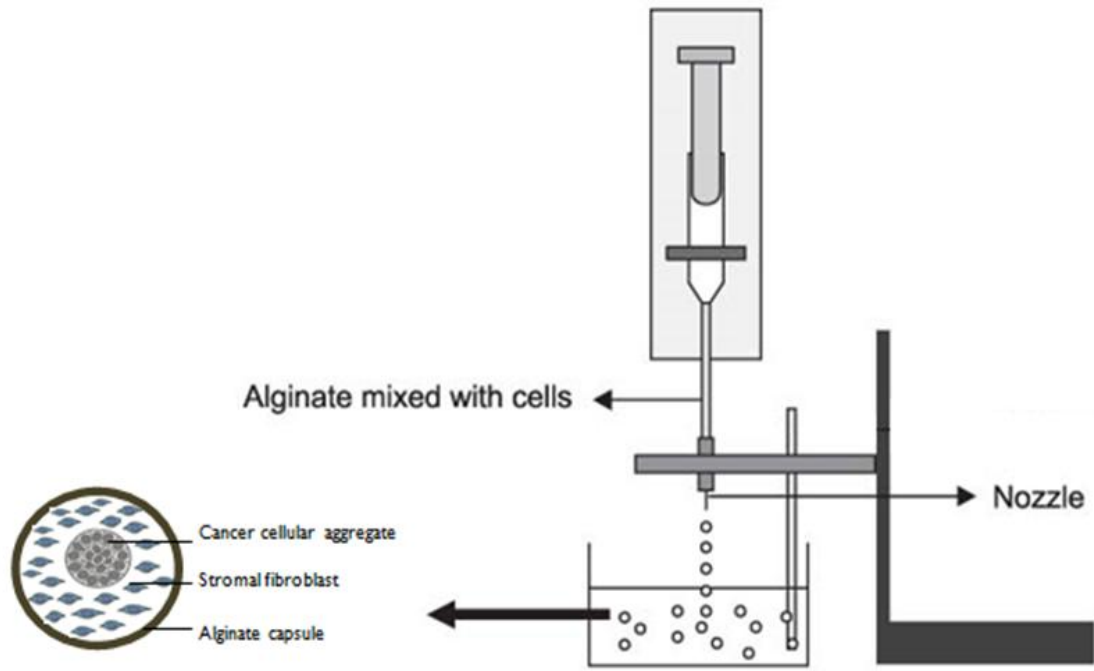


Figure 2.2 - Schematic illustration the cell encapsulation process with alginate. Capsules are formed when droplets of alginate-cells mixture contact with the BaCl_2 solution, entrapping the cancer aggregates inside with the single fibroblasts cells.

2.3.3. Mono- and co-culture of HI650 encapsulated aggregates

HI650 cells were induced to form cell aggregates during 3 days prior encapsulation by cultivating HI650 single cells in spinner flasks using the conditions previously described in section 2.2 (**figure 2.1**). Encapsulation of HI650 aggregates was performed at day 3 of aggregation phase, because HI650 aggregates were compact, dense and the shape was spherical and well defined. Agitation of the impeller of the spinner vessel used in aggregation phase was stopped to remove all the aggregates. Aggregates were filtered using a 70 μm strainer in order to remove single cells and non-representative aggregates, such as diploid and triploids. Aggregates were washed twice with PBS and centrifuged at 50 g for 3 minutes. HI650 aggregates (mono-culture) and HI650 aggregates mixed together with human lung NFs labelled with PKH26 14195 (co-culture) were embedded in the alginate polymeric solution as previously described in section 2.3.2 (**figure 2.2**). The fibroblasts were maintained in 2D cell culture until encapsulation process. Fibroblasts were mixed as single cells with HI650 aggregates in a 1:1 ratio for the co-culture condition. The initial cancer cell concentration for encapsulation was 2×10^5 cell/mL. The resulting capsules were transferred to 125 mL spinner vessels (Corning® Life Sciences, **figure 2.2**) equipped with paddle impellers and cultured in supplemented RPMI medium 1640 (1x) + GlutaMAX™ -1 at 60 rpm for additional 15 days. Culture medium was partially replaced at days 3, 5, 7, 10 and 12. This was done by stopping agitation (to let the aggregates deposit), removing 50% of the medium and feeding with 50% of fresh medium. Samples were collected from the spinner vessel at several time points (including before and after changing the cell culture medium) at days 0, 1, 2, 3, 5, 7, 10, 12 and 15 in order to monitor the cultures in terms of cell viability, metabolic activity, aggregate size, concentration and composition during time.

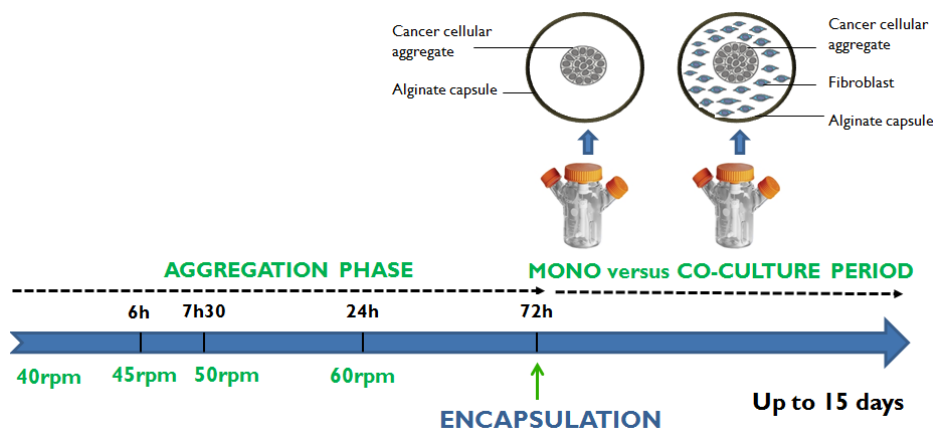


Figure 2.3 – Strategy performed to accomplish a 3D cellular model to evaluate the effect of tumour microenvironment on tumour progression.

2.4. Analytical methods to evaluate cell culture

2.4.1. Determination of cell concentration, cell viability, cell death and apoptosis

Trypan Blue exclusion method: During cell proliferation in adherent system and before inoculating cells in stirred suspension culture systems, cell viability and concentration was assessed using the trypan blue exclusion test. After trypsinization, cells were diluted in 0.1% (v/v) Trypan Blue dye (Gibco, Invitrogen Corporation, Paisley, 27 UK) in PBS using a 1:5 dilution. Non-viable cells, whose membrane is damaged, are stained by trypan blue and appear blue at the microscope whilst viable cells are not stained and appear white and bright. Cell concentration was evaluated using a Fuchs-Rosenthal hemacytometer and a microscope with phase contrast (DM IRB, Leica, Germany).

Crystal violet method: During cell culture in a stirred suspension culture system, nuclei were counted in order to obtain total cell number in culture. Total number of cells was counted using crystal violet method that stains nuclei in a deep purple color. Cells were centrifuged at 300g, for 5 minutes and then lysed using lysis solution (1% Triton X-100 in 0.1 M citric acid), overnight at 37°C. For encapsulated aggregates, alginate capsules were first dissolved with a solution of 50 mM EDTA in mQ water. Then, samples were centrifuged at 50g (in order not to damage the aggregates) for 5 minutes and the pellet of cells was lysed. In co-cultures of HI650 aggregates with immortalized NFs, cancer cells and fibroblasts were separated before lysis. After centrifuging the co-culture samples at 50g, for 5 minutes, the HI650 aggregates constituted the pellet as the fibroblasts remained in suspension in the supernatant because they are organized in single cells or small aggregates. The supernatant with fibroblasts is separated from the aggregates pellet and centrifuged at 300 g for 5 minutes. HI650 aggregates and fibroblasts pellets were washed twice with PBS to remove remaining dissolved alginate that could precipitate and interfere with cell counting. The pellets were then lysed, overnight at 37°C. At the moment of counting, nuclei were diluted in 0.1% crystal violet in lysis solution. Nuclei density was assessed using a Fuchs-Rosenthal hemacytometer and a microscope with phase contrast (DM IRB, Leica, Germany)

Cell membrane integrity assay: Aggregate viability was evaluated using the enzyme substrate fluorescein diacetate (FDA; Sigma-Aldrich, Steinheim, Germany) 1:500 in PBS and TO-PRO-3 iodide (Invitrogen) 1:500 in PBS dual staining. Aggregates were analyzed using a fluorescence microscope (Leica DM6000). FDA is a non-fluorescent cell permeant ester that stains viable cells, measuring enzymatic activity and cell membrane integrity at the same time. Enzymatic activity is required to activate FDA fluorescence through FDA hydrolysis by

intracellular esterases. Cell membrane integrity is necessary for retaining the fluorescein inside the cell, slowing the loss of fluorescence. On the other hand, TO-PRO®-3 is a carbocyanine monomer nucleic acid stain with far-red fluorescence. It indicates cell death because it crosses damaged cellular membranes and stains the nuclear double-stranded nucleic acids (dsDNA). Therefore, with FDA and TO-PRO-3 iodide dual staining, viable cells present green fluorescence and non-viable present far-red fluorescence.

Lactate dehydrogenase (LDH) activity: Lactate dehydrogenase (LDH) activity from the cell culture supernatant was determined as an indirect way to evaluate cell death. LDH is an intracellular enzyme only present in the cell culture supernatant upon cellular membrane damaged, which occurs during cell death. LDH (U/mL) activity from the culture supernatant was determined as described before (Serra *et al.*, 2011). Briefly, the rate of oxidation of NADH to NAD⁺ coupled with the reduction of pyruvate to lactate was monitored at 340 nm and U represents the μmol of NADH consumed in reaction (1) *per* minute. However, since the LDH is not a stable enzyme in the cell culture supernatant at 37°C after 24 hours, the cumulative value of LDH (LDH_{cum}) was estimated for each timepoint and time interval, respectively, using the following equation: $\text{LDH}_{\text{cum } i+1} = \text{LDH}_i + \text{LDH}_{i+1}$.



Apoptotic activity: The assessment of cell apoptotic activity can provide important complementary information about the 3D cell cultures. Apoptotic activity of encapsulated HI 650 aggregates and fibroblasts was performed with NucView™ 488, caspase-3 substrate, and MitoView™ 633, far-red fluorescent mitochondrial dye. This assay is based on caspase-3/7 activity and changes in the mitochondrial membrane potential using fluorescence microscopy. Caspase-3 substrate, which is non-fluorescent and non DNA dye, penetrates on cell membrane and it is cleaved by caspase-3/7 in cytoplasm, forming a high-affinity DNA dye. This DNA probe migrates to cell nucleus originating bright green stain. Therefore, NucView™ 488 dye has a dual function of detecting intracellular caspase 3/7 and at the same time stain cell nucleus. Consequently, apoptotic cells display a lower red fluorescence signal and higher green fluorescence when compared with non-apoptotic cells. MitoView™ 633 diffuses through cell membrane and accumulates in the mitochondria. This accumulation is dependent on the mitochondria function, which is impaired during apoptosis (Gross, McDonnell, & Korsmeyer, 1999; Joza *et al.*, 2001; Merad-Boudia, Nicole, Santiard-Baron, Saillé, & Ceballos-Picot, 1998). Therefore, apoptotic cells have lower MitoView™ 633 staining compared with healthy cells. Encapsulated HI650 aggregates from mono and co-

cultures were placed in a 24 well-plate and incubated for 2 hours in a humidified atmosphere at 37°C with 5% CO₂ with a 1:500 dilution of each dye (NucView™ 488 and MitoView™ 633). Encapsulated aggregates were washed 3 times with DPBS and then resuspended in 500µL of DPBS before being observed in fluorescence microscope (Leica DM6000, Germany).

2.4.2. Aggregate size determination

For aggregate size determination, aggregate suspensions were observed by phase contrast microscopy and aggregate size measured using ImageJ software. The average area was calculated by measuring the aggregate middle section area of a minimum of 100 aggregates. Aggregates with less than 20 µm diameter, generally duplets or triplets, were not considered because they represent a small percentage of the total cell number in culture (Serra et al., 2007).

2.4.3. Metabolite analysis

Glucose (Glc) and lactate (Lac) concentrations in the cell culture medium were analyzed using an YSI 7100MBS (YSI Incorporated, USA). The specific metabolic rates (qMet., µmol/(million cell.day⁻¹)) were calculated as described before (Serra et al., 2011) using the equation: $qMet. = \Delta Met / (\Delta Xv \cdot \Delta t)$, where ΔMet (µmol) is the variation in metabolite concentration during the time period Δt (day) and ΔXv (million cell) the average of total number of cells during the same time period. Cellular metabolic efficiency was calculated as the ratio between qLac/qGlc, representing the lactate/glucose yield ($Y_{Lac/Glc}$).

2.4.4. . Phenotypic characterization of the NSCLC cellular model

Immunofluorescence microscopy: Alginate capsules were collected from the mono and co-cultures in suspension culture and immediately fixed in 4% (w/v) paraformaldehyde (PFA) and 4% (w/v) sucrose solution in DPBS during 30 minutes. Then, the capsules were washed two times with DPBS and were dehydrated in DPBS solution with 30% of sucrose. For the cryosectioning, encapsulated aggregates were frozen at -80 C in Tissue Teck OCT™ (Sakura) and were sectioned in cryostat (Leica) in sections of 10 µm. Cryosections were washed twice with DPBS followed by permeabilization with 0.1% Tx-100 solution in DPBS for 10 minutes. After permeabilization, cryosections were washed 2 times with DPBS and blocked with 0.2% of FSG in DPBS for 30 minutes. Primary antibody was diluted in 0.2% FSG solution and incubated during 2 hours. After 2 washes with DPBS, cells were incubated

for 1 hour with secondary antibody in 0.2% FSG solution. The list of primary antibodies is presented in Table 2.2. Cryosections were finally washed twice with DPBS, mounted in ProLong mounting medium contain DAPI (Invitrogen) and visualized using a fluorescence microscope (Leica DM6000, Germany). Besides the antibodies, it was also used Alexa Fluor® 488 Phalloidin (Invitrogen), which is a bicyclic peptide that binds F-actin with high selectivity and presents green fluorescence because it is connected to Alexa Fluor® 488.

Table 2.2: List of antibodies and respective dilutions used for immunofluorescence microscopy

| Antibody | Marker | Supplier | Dilution used |
|-------------------------------------|------------------------------|-----------------------------|---------------|
| Anti-E-cadherin | Epithelial | BD Biosciences | 1:300 |
| Anti-ZO1 | Cell Polarity | Invitrogen | 1:100 |
| Anti-CK18 -FITC | Epithelial | Santa Cruz Biotechnology | 1:100 |
| Anti-vimentin | Mesenchymal | Sigma | 1:200 |
| Anti-Phalloidin- Alexa Fluor 488 | Cytoskeleton organization | Invitrogen | 1:100 |
| Collagen IV | ECM | Abcam | 1:100 |

2.4.5. Quantification of newly synthesized ECM components

Collagen concentration retained inside alginate capsules from mono- and co-cultures was assessed using SIRCOL Collagen colorimetric assay (Biocolor Ltd., U.K.). The Sircol Assay is a dye-binding method that enables analysis of acid and pepsin-soluble collagens, from type I to V. However, the dye reagent does not distinguish between collagen types, because it binds to tri-peptide sequence [(gly-X-Y)_n] (and many of these residues are converted post translationally into hydroxyproline residues) which are found in all mammalian collagen types. Briefly, cell culture samples were collected at days 5, 10 and 15 of mono- and co-culture. Alginate capsules were dissolved as described before and aggregates and fibroblasts were separated by centrifugation. Samples were kept at -80°C until collagen quantification.

Then, protein samples were transferred into low binding tubes and incubated overnight at 4°C with 1mL of pepsin (freshly dissolved), 100µL of Acid Neutralising Reagent and 200µL of cold Isolation and Concentration Reagent. Samples were then centrifuged at 12 000 rpm for 10minutes, supernatant was removed and 1mL of Sircol dye Reagent was added to each pellet. Samples were gently shaken for 30 minutes and centrifuged as before. 250 µL of Alkali Reagent was added to the samples, which were analyzed at 555nm. Collagen calibration curve was performed by serial dilutions of the collagen standard solution provided by the kit and further incubation with the alkali reagent.

2.5 Statistical analysis

The unpaired t-test was used for comparisons between two groups only. The one-way ANOVA, followed by the Tukey's pot-hoc, was used for comparisons between more than two groups. $p < 0.05$ was considered significant. Data are shown as mean \pm standard deviation of the means.

Results and Discussion

3. Results and discussion

3.1. Aggregation of NSCLC cell lines in stirred culture systems

The aim of the work was to generate NSCLC cellular models that could better mimic the *in vivo* tumour microenvironment, recapitulating cell-cell and cell-ECM interactions representative of cellular heterogeneity of tumours. In a first approach, the production of cellular aggregates of the NSCLC cell lines H460 and H1650 was established in stirred culture systems. The aggregation process followed for the generation of these aggregates was based on the strategy proposed by Serra *et al* (2009), where human pluripotent embryocarcinoma NTera2/cloneD1 (NT2) cells were cultured as 3D aggregates using stirred culture systems.

H460 and H1650 NSCLC cell lines were inoculated as single cells in spinner-flasks (**figure 2.2**) at a cell concentration of 0.2×10^6 cell/mL (**figure 3.1.I**) as described in Materials and Methods, section 2.2 and the aggregation process followed for 3 days. Aggregation was monitored by phase contrast microscopy throughout time (**figure 3.1**).

H460 and H1650 single cells started to attach to each other few hours after inoculation (**figure 3.1**). At day 1, both cell cultures presented aggregates in suspension, with spherical shape in the case of H1650, whereas H460 still presented an irregular shape by that time. At the third day of cell culture, both H460 and H1650 cultures presented aggregates with a round, spherical and compact shape and very few single cells in suspension (**figure 3.1**).

Fluorescein diacetate (FDA) and TOPRO iodide dual staining was used to evaluate cell viability during culture time using fluorescence microscopy, with a protocol described in the Materials and Methods, section 2.4.1. During the three days of aggregation, aggregates were composed mainly by viable cells (green). A few non-viable cells were found (red), corresponding to single cells that did not incorporate the aggregates (**figure 3.1**).

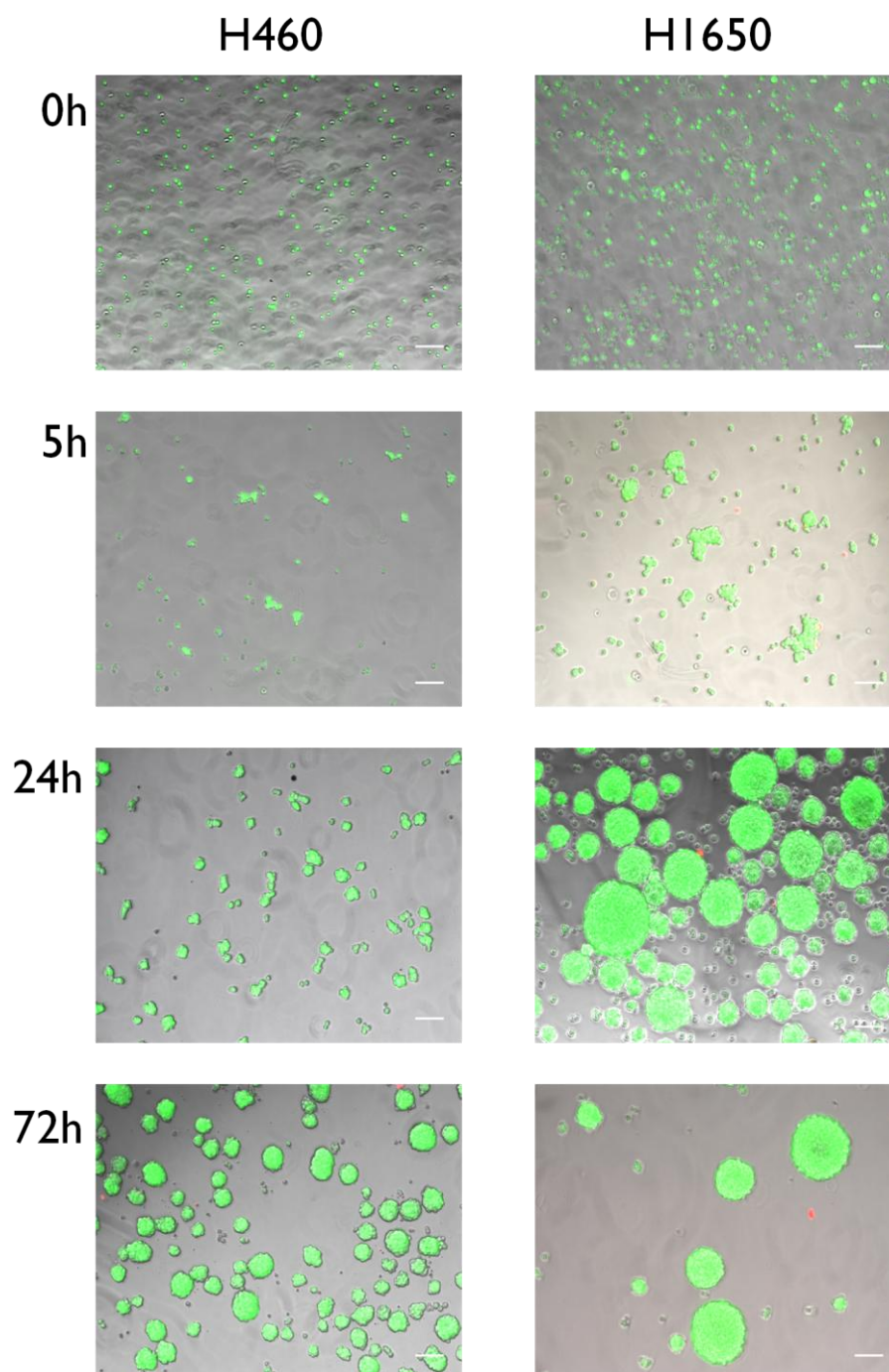


Figure 3.1 - Monitoring of aggregation of NSCLC cell lines in stirred culture systems. Images obtained by phase contrast microscopy and by fluorescence microscopy. H460 and HI650 cell cultures were monitored throughout time: 0, 5, 24 and 72 hours. Viable cells were stained with FDA (green) and non-viable cells were stained with TOPRO (red) as described in Materials and Methods, Section 2.4.1. Scale bars represent 100 μ m. Data are from one representative experiment of 4 (H460) and 5 (HI650) independent experiments.

Lactate Dehydrogenase (LDH) activity was also determined in order to evaluate cell death during aggregation (see Materials and Methods, section 2.4.1). Cumulative values of specific LDH release rates in the culture supernatant are shown in **figure 3.2**.

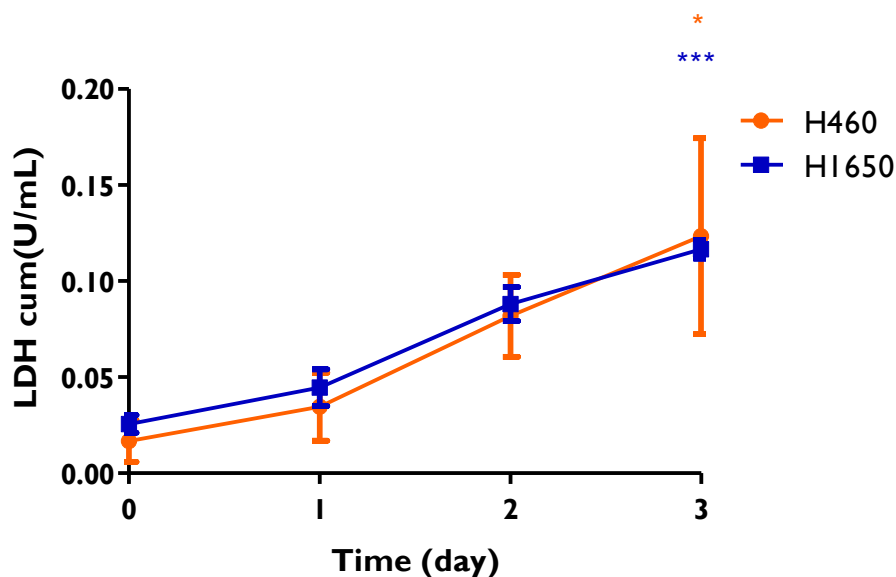


Figure 3.2 – Cell death expressed by cumulative values of LDH released during aggregation of NSCLC cell lines in stirred culture systems. Data are mean \pm SD from 2 (H460) and 3 (HI650) independent experiments. * $P < 0.01$ and *** $P < 0.05$ represent the significant differences between day 3 and day 0 of H460 LDH cumulative values by one-way ANOVA analysis with Tukey's post multiple comparison test.

Despite the progressive increase in cumulative LDH values for both cell lines, the values of LDH in the culture supernatant were low. These results are in agreement with the FDA/TOPRO assessment (**figure 3.1**), in which very few dead cells (in red) were detected.

Aggregate's size increased for both cultures overtime (**figure 3.1 and 3.3**): HI650 and H460 aggregates displayed a statistically significant higher mean area at day 3 in comparison with day 1 ($p < 0.001$). Moreover, HI650 aggregates were significantly bigger than H460 aggregates throughout time (**figure 3.3**) with average area of 7.36 ± 7.58 ($\times 10^3 \mu\text{m}^2$) and 3.94 ± 1.82 ($\times 10^3 \mu\text{m}^2$), respectively, at day 3 of cell culture. In addition, size distribution of HI650 aggregates was more heterogeneous than H460 cell line aggregates (**figure 3.3**) throughout the whole aggregation period.

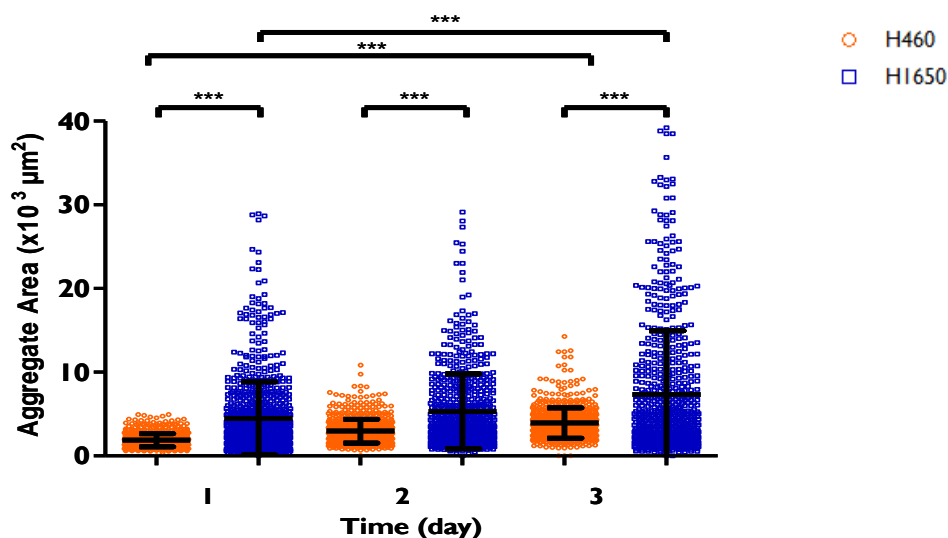


Figure 3.3 - Aggregate size profile along aggregation of NSCLC cell lines in stirred culture systems. Area of H460 and HI650 aggregates cell lines was measured as described in Materials and Methods, section 2.4.2. Data are mean \pm SD of the diameter of at least 100 aggregates from 5 independent experiments for each cell line. *** indicate significant difference with $P < 0.001$ by one-way ANOVA analysis with Tukey's post multiple comparison test.

There was an increase in aggregate size throughout time for both cell cultures. Cell concentration also increased throughout time for both cell lines. No statistically significant differences were observed between HI650 and H460 cell cultures (**figure 3.4 a**), as both cell lines displayed similar proliferation profiles. By comparing fold increase in cell concentration after 3 days of 3D cell culture (H460 and HI650 aggregates) and 2D cell culture routinely performed prior to aggregation, cells in 3D cell culture presented a lower fold increase. After 3 days of 2D cell culture, H460 cells had a fold increase of 12.1 ± 4.1 and HI650 cells a fold increase of 4.9 ± 2.4 . After 3 days of 3D cell culture, H460 had a fold increase of 2.2 ± 1.9 and HI650 cells a fold increase of 2.6 ± 2.9 . Lower proliferation rates in 3D cell culture comparing to 2D cell cultures were already observed for other types of cells by other authors, who noticed that when cells isolated from tissues are cultured into planar cell culture, they become progressively flatter, and divide abnormally (von der Mark *et al*, 1977; Petersen *et al.*, 1992). Baker *et al* (2012) reported that when cells grow in a monolayer, they can adhere and spread freely in the horizontal plane but lack support for spreading in the vertical dimension, which exists *in vivo*. The formation of normal epithelial structures requires adhesive and mechanical signals from neighbouring cells and basement

membrane in order to control proliferation (Baker & Chen, 2012a). Thus, the dimension in which cells are cultured is a crucial fate determinant and culturing cells in monolayer drives abnormal cell function and proliferation, whereas 3D culture mimics a more physiological state.

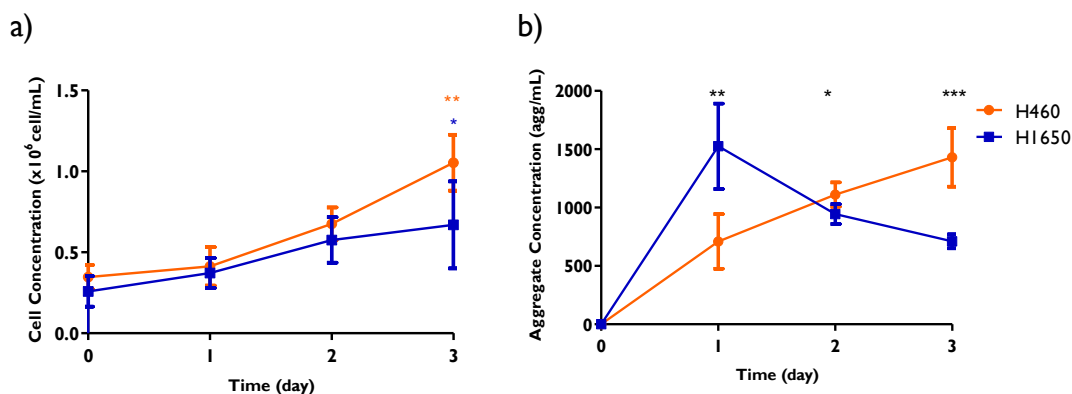


Figure 3.4 – Cell (a)) and aggregate (b)) concentration during aggregation of NSCLC cell lines in stirred culture systems. Presented data displays mean \pm SD from 3 (H460) and 2 (HI650) independent experiments. ** P<0.01 and *P<0.05 represent the significant differences between day 3 and day 0 of H460 and HI650 cell concentration. Black asterisks (* P<0.05, ** P<0.01 and *** P<0.001) represent significant differences between H460 and HI650 aggregate concentration in each timepoint. Statistical analysis was done by one-way ANOVA analysis with Tukey's post multiple comparison test.

Oppositely to the cell concentration profiles, in which both cell lines presented similar growth profiles, the analysis of aggregate concentration revealed a different trend (**figure 3.4 b**). The number of aggregates in culture formed by H460 cells grew continuously during the three days of aggregation phase. On the other hand, the concentration of HI650 aggregates in suspension decreased from day 1 onwards after an initial significant increase at the first day of aggregation. The number of aggregates in suspension was always statistically significantly different between H460 and HI650 cells throughout the aggregation phase, with different levels of significance at each day of culture as indicated with asterisks in figure 3.4 b).

In summary, H460 and HI650 cells formed homogeneous, spherical and compact aggregates with high viability (**figure 3.1**) and cell death was not significant during aggregation (**figure 3.2**). These results indicated that NSCLC aggregates were successfully produced using stirred culture systems. Moreover, the aggregation strategy resulted in suspension culture of H460 cells with high viability, that were not obtained by other authors

when culturing H460 in suspension, since they noticed a decrease in cell survival due to anoikis (Chunhacha, Pongrakhananon, Rojanasakul, & Chanvorachote, 2012; Lloyd & Hardin, 2011; Pongrakhananon, Nimmannit, Luanpitpong, Rojanasakul, & Chanvorachote, 2010; Rungtabnapa, Nimmannit, Halim, Rojanasakul, & Chanvorachote, 2011). Anoikis is a type of cell death that occurs when cells do not have cell-cell or cell-ECM attachment (Paoli, Giannoni, & Chiarugi, 2013; Wei, Yang, Zhang, & Yu, 2004). Anoikis constitutes an essential defense mechanism that prevents detached cells to adhere to new matrices in the wrong tissues and their abnormal growth in those sites, which can turn into a metastasis lesion (Y.-N. Kim, Koo, Sung, Yun, & Kim, 2012; Sakuma et al., 2010; Wei, Yang, Zhang, & Yu, 2002). A possible explanation for the successful formation of H460 aggregates in contrast with other works is the fact that those previous studies were performed in static 3D culture conditions, which provide significantly different culture conditions than the stirred tank system used in this thesis work. In the present work, the use of stirred culture systems promoted cell-cell interactions due to hydrodynamic forces (Moreira et al., 1995), may be responsible for the absence of anoikis. Furthermore, stirred culture systems allow efficient mass transport, with diffusion of oxygen, nutrients and pro-survival signals from one cell to another within the aggregates.

The increase on H460 aggregate's size and concentration, together with an increase in cell concentration (**figures 3.3 and 3.4 a**) suggested that the rise in H460 aggregate's size was mainly due to cell proliferation (**figure 3.4 a**). On the contrary, the increase on H1650 aggregate's size (**figure 3.3**) and the decrease on H1650 aggregate's concentration, together with the increase in cell concentration suggested that H1650 aggregate's size increase was mainly due to aggregate fusion. This phenomenon contributed to the production of larger aggregates than H460 aggregates (**figure 3.3**). These observations, together with the fact that H460 had a non-spherical shape at day 1 and a smaller size than H1650 aggregates throughout time whereas H1650 aggregates were already round and bigger at day 1 (**figure 3.1**) might be related to a EMT in H460 cells. It is described in the literature that these cells show low baseline expression of E-cadherin, an epithelial marker essential in cell adhesion, and high expression of vimentin, a mesenchymal marker related with higher motility and lower cell adhesion (Coldren et al., 2006; E. Y. Kim et al., 2014; Matsubara et al., 2010; Pallier et al., 2012). In consequence, these properties of H460 cells might explain a reduced adhesion to neighbouring tumour cells and a longer period necessary to establish the formation of round and compact aggregates when in comparison

with HI650 cells. Moreover, this may be further related with large-cell carcinoma pathological characteristic of fast spreading (Table I.1) (Popper, 2011; Sun *et al.*, 2012).

Glucose and lactate levels in the culture medium were monitored during aggregation, in order to evaluate cell metabolism (Birsoy *et al.*, 2014; H. Cruz *et al.*, 2000; Zielke *et al.*, 1980).

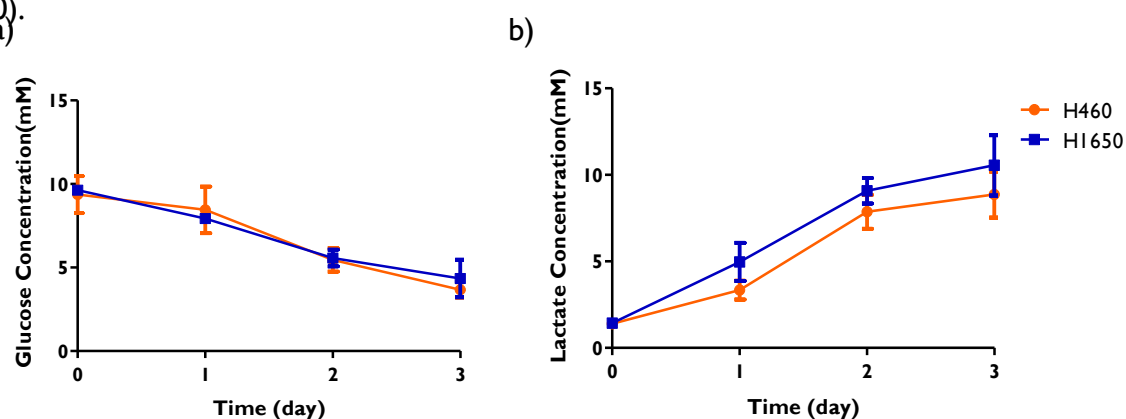


Figure 3.5 – Concentration of glucose (a) and lactate (b) in the cell culture medium during aggregation of NSCLC cell lines in stirred culture systems. Data are mean \pm SD from 4 (H460 cell line) and 5 (HI650 cell line) independent experiments.

For both H460 and HI650 cell cultures, there was a decrease in glucose and an increase in lactate concentration in the culture medium along time, with no statistically significant difference between the two cell lines (**figure 3.5**). These results indicated that cells were metabolic active. Furthermore, the glucose concentration profile revealed that there was no nutritional limitation regarding glucose supplementation since there was no depletion of this specific metabolite (**figure 3.5 a**). Moreover, the values of lactate measured in the cell culture medium did not reach toxic values. Lactate levels superior to 20mM were shown to be toxic for culture of chinese hamster ovary (CHO) cells *in vitro* (Castilho, Moraes, Augusto, & Butler, 2008). Nevertheless, cancer cells are reported to be adapted to high acid lactic concentrations (Carmona-Fontaine *et al.*, 2013; Goetze, Walenta, Ksiazkiewicz, Kunz-Schughart, & Mueller-Klieser, 2011; Sukhatme & Chan, 2012).

The determination of glucose and lactate concentration in the cell culture medium (**figure 3.5 a** and **b**) allowed to calculate the specific rates of glucose consumption (q_{Glc}) and lactate production (q_{Lac}), respectively (**figure 3.6 a** and **b**).

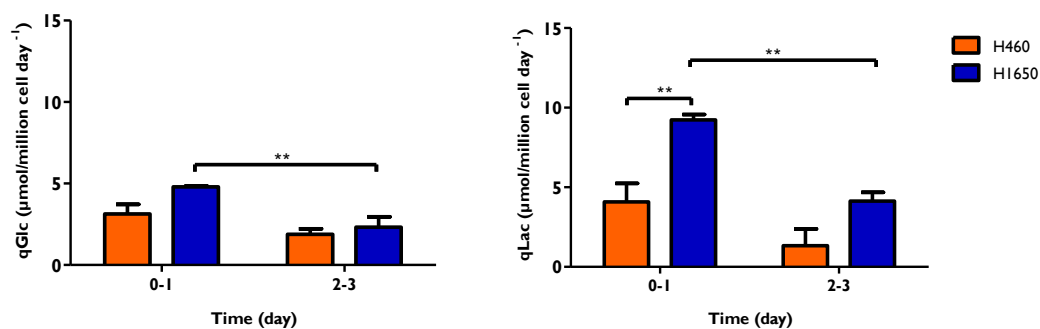


Figure 3.6 – Specific metabolic rates of glucose consumption (a) and lactate production (b) during aggregation of NSCLC cell lines in stirred culture systems, from day 0 to day 1 and from day 2 to day 3 of cell culture. Data are mean \pm SD from 3 independent experiments (H460 and HI650 cells). Asterisks indicate significant difference (* $P < 0.05$, ** $P < 0.01$ and *** $P < 0.001$) by one-way ANOVA analysis with Tukey’s post multiple comparison test.

For both H460 and HI650 cell lines, there was a tendency towards a decrease in qGlc (**figure 3.6 a**) and in qLac (**figure 3.6 b**) during aggregation. HI650 cells produced higher levels of lactate than H460 cells from day 0 to day 1 of aggregation (**figure 3.6 b**) without consuming statistically significant higher amounts of glucose than H460 cells on that time period (**figure 3.6 a**). This observation suggested that HI650 cells used glutamine (presented in the cell culture medium due to GlutaMAXTM-I (see Materials and Methods, section 2.1)) as an alternative energy and carbon source to glucose during the first hours of aggregation (Daye & Wellen, 2012). This could be seen as an adaptation response to a new environment and culture condition from 2D to 3D. Cancer cells are known to consume glutamine, besides glucose, in order to produce the necessary biomass (Daye & Wellen, 2012; Newsholme et al., 2003). Glutamine could have been uptaken by HI650 cells, producing glutamate, which could then be further metabolized to α -ketoglutarate that would enter in the TCA cycle (Maranga & Goochee, 2006). Ultimately, this sequence of events would result in the production of pyruvate, which in turn, could be converted to lactate (**figure 1.8**), increasing qLac by HI650 cells (**figure 3.6 b**). However, further detailed investigation need to be done to confirm this hypothesis, for instance, with metabolic flux analysis (MFA) using ¹³C labeled glucose and glutamine (Metallo, Walther, & Stephanopoulos, 2009; Walther, Metallo, Zhang, & Stephanopoulos, 2012). Furthermore, the ration between qGlc and qLac ($Y_{Lac/Glc}$) allowed defining the glycolytic metabolic efficiency throughout time (**figure 3.7**). . A highly efficient glucose metabolism, in which pyruvate produced in glycolysis is being incorporated in the TCA cycle with consequent energy production and less lactate

production, leads to $Y_{\text{Lac/Glc}}$ lower than 2 (Cruz *et al.*, 1999, 2000; Maranga and Goochee, 2006).

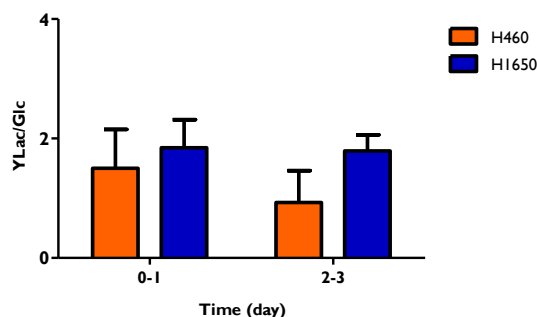


Figure 3.7 – Cellular Metabolic efficiency during aggregation of NSCLC cell lines in stirred culture systems. Data are mean \pm SD from 3 independent experiments (H460 and HI650 cells). Statistical analysis by one-way ANOVA analysis with Tukey’s post multiple comparison test.

H460 and HI650 aggregates had a similar metabolic efficiency profile which remained approximately constant during aggregation time, reaching values lower than 2 during the time period assessed (**figure 3.7**). A slight decrease on the mean ratio was observed for H460 cells between the first day of aggregation and the third day, however with no statistical significance. These results suggested an efficient metabolic profile, in contrast with Warburg effect commonly associated with cancer cells (Carmona-Fontaine *et al.*, 2013; Hsu & Sabatini, 2008). Comparing with 2D cell culture routinely performed prior aggregation, H460 and HI650 3D cell culture had higher metabolic efficiency ($Y_{\text{Lac/Glc}} < 2$) whereas Warburg effect was noticed in 2D cell culture ($Y_{\text{Lac/Glc}} = 2.03 \pm 0.146$). In accordance, H460 and HI650 cells have been reported to have high rate of glycolysis and reduced mitochondrial respiration, leading to the Warburg effect, when cultured in 2D conditions (Amoêdo *et al.*, 2011; Hao *et al.*, 2010; Zhang, C. *et al.*, 2011). The molecular signals from cell-cell and cell-ECM interactions presented *in vivo*, involved in control of cell proliferation (Ref das que tinhas atrás), may have led to lower proliferation rates in 3D cell compared to monolayer cultures, and consequently an increase in $Y_{\text{Lac/Glc}}$ (Baker and Chen, 2012; von der Mark *et al* 1977; Petersen *et al.*, 1992). The differences observed between 2D and 3D H460 and HI650 metabolic efficiency for the first three days of culture might also be related with a possible early adjustment period of the cells to the new culture conditions. For a more powerful analysis, monitoring of glucose consumption and lactate production rates must be followed for longer culture periods, as it will be discussed later in this thesis.

The adjustments on stirring parameters effectively controlled aggregate size and shape, avoided aggregate clumping and allowed an efficient transport of nutrients and oxygen to the aggregates since these were composed mainly by viable cells and there were no necrotic centres, as assessed by FDA/TOPRO fluorescent viability assay (**figure 3.1**). The different stirring profiles between cell lines (see Materials and Methods, section 2.5) may be due to the differences in NSCLC subtype, since H1650 was derived from adenocarcinoma and H460 from a large-cell carcinoma (Table 2.1). Large cell carcinoma is characterized by a fast spreading and lower expression of cell-cell adhesion proteins, such as E-cadherin, β -catenin, integrins, zonula occludens 1 (ZO-1) (Popper, 2011; Sun *et al.*, 2012; Coldren *et al.*, 2006; Kim, E. Y. *et al.*, 2014; Matsubara *et al.*, 2010; Pallier *et al.*, 2012). These cell-cell adhesion proteins are responsible for maintaining tight junctions, adherent junctions, desmosomes, gap junctions, and other cell-cell interactions which help to form epithelial tissue (Miyoshi & Takai, 2008; X. Zhong & Rescorla, 2012). These adhesion sites between adjacent epithelial cells are essential for cell function and homeostasis of the epithelial tissue (J. Partanen, 2012). However, molecular characterization with immunodetection and Western blot (WB) analysis should be carried out to confirm the correlation of different stirring profiles with different expression of cell-cell adhesion proteins, such as E-cadherin, β -catenin, integrins and ZO-1.

In conclusion, this agitation-based approach using spinner vessels is an efficient strategy for the generation of 3D NSCLC cellular aggregates resembling the cell-cell interactions and the 3D cellular organization. H460 and H1650 cellular aggregates were successfully produced with round and compact shape, high cell viability and proliferation ability, low levels of cell death and metabolic functionality. This stirring strategy is reproducible, since it produced homogenous aggregates in several independent experiments. On top of that, it is a highly robust system as due to its simplicity and efficiency, can be adapted according to each cell line requirements. Moreover, this approach can provide a significant input for the generation of knowledge on NSCLC cellular aggregates using stirred culture systems as currently there is a lack of published data on this topic.

3.2. Culture of encapsulated NSCLC aggregates in stirred culture systems

Co-cultures of tumour cell aggregates together with immortalized, non-transformed normal lung fibroblast (NFs) was the second step of the strategy to develop a 3D NSCLC cellular model that could better mimic NSCLC microenvironment. The H1650 cell line was

selected. as the strategy implemented in the previous section was successful in the establishment of reproducible spherical, compact and homogeneous HI650 cell aggregates. Moreover, HI650 cells represents a subtype of NSCLC, the bronchioalveolar carcinoma, with high levels of incidence (Shivanthan and Wijesiriwardena, 2011; Tan *et al.*, 2003) with a metastatic potential (Gong *et al.*, 2011), thus being a feasible cell model to study the effect of co-culture with fibroblasts on culture progression. Tumour microenvironment is composed by a wide array of cell types, including fibroblasts, immune cells and vascular cells but this thesis focused on the establishment of a cell model suitable for assessment of tumour-fibroblast cross-talk.. An alginate microencapsulation strategy was pursued in order to provide mechanical support and to confine the co-cultures within a restricted environment, with the different cell types organized spatially in an “*in vivo*-like” configuration, in which cancer aggregates and stromal cells could interact and proliferate. This spatial organization resembled the cellular heterogeneity within a tumour tissue, mimicking the heterogeneous distribution of cancer and stromal cells in the tumour.

HI650 cells were induced to form cellular aggregates prior encapsulation by culturing HI650 single cells using the previously described conditions (see Materials and methods, section 2.5). Encapsulation was performed at day 3 of HI650 aggregation, when HI650 aggregates already had a spherical and compact shape (**figure 3.1 IV**). Mono- and co-cultures of HI650 aggregates with NFs were performed in parallel as described in Materials and Methods, section 2.5. HI650 aggregates encapsulated with and without single cells of NFs were cultured in spinner flasks (**figure 2.2**), using the culture parameters described in the previous section with a constant stirring speed of 60 rpm, up to 15 days. Alginate capsules contained at least one HI650 aggregate in both mono-culture and co-culture conditions (**figure 3.8**). In co-culture condition, NFs surrounded HI650 aggregates and they were encapsulated in a HI650/NFs cell ratio of 1/1 (**figure 3.8 b**).

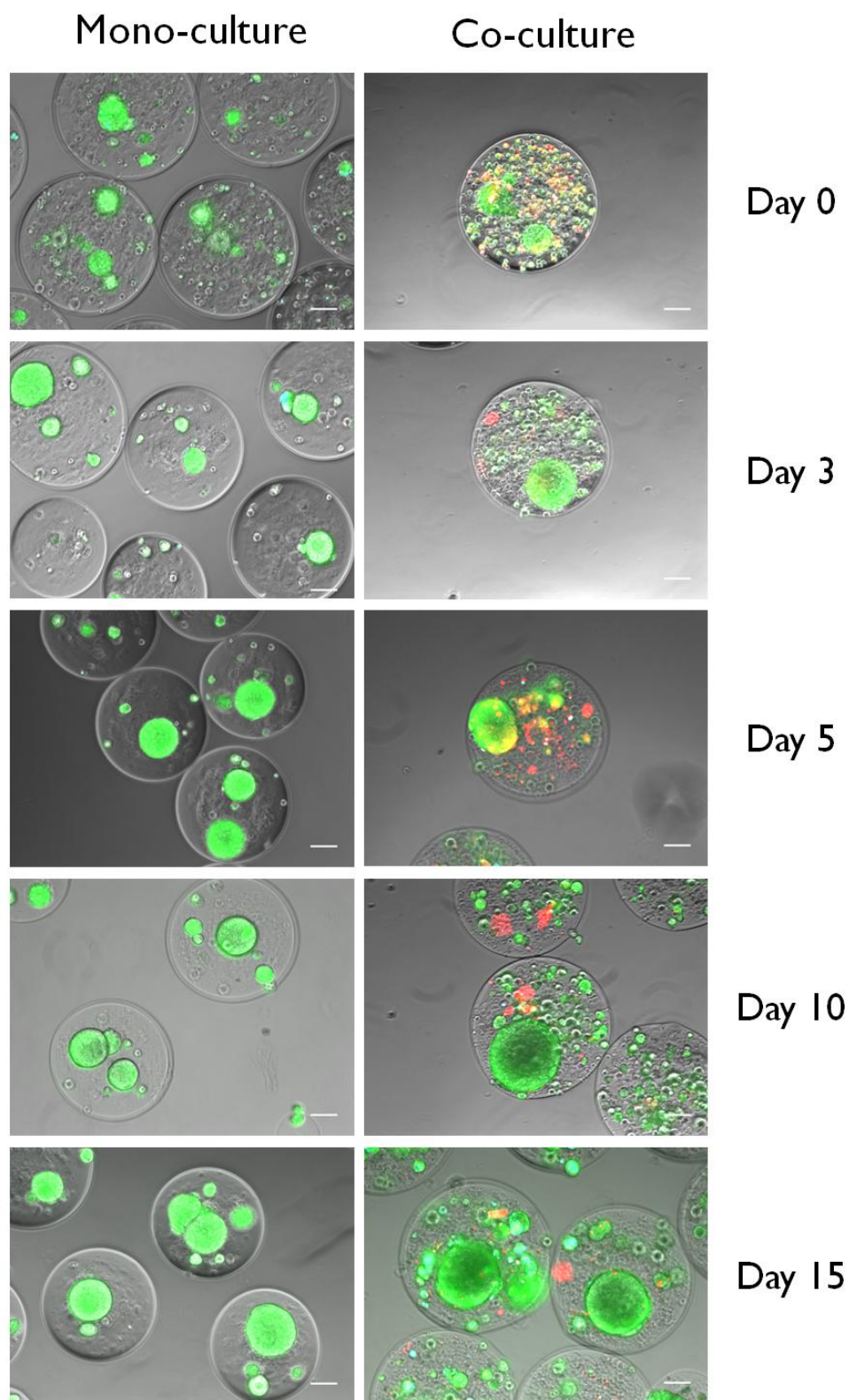


Figure 3.8 - Monitoring of mono and co-cultures of HI1650 aggregates encapsulated with NFs in stirred culture systems. Images obtained by phase contrast microscopy and fluorescence microscopy. Morphology and cell viability of aggregates were monitored during time (days 0, 3, 5, 10 and 15). Viable cells were stained with FDA (green) and non-viable cells were stained with TOPRO (blue). Immortalized fibroblasts were stained with PKH26, a cell membrane labeling (red). Scale bars

represent 100µm. Data are from one representative experiment of 2 independent experiments for both conditions.

Both in mono- and co-cultures, aggregates were composed mainly by viable cells (FDA, green), with just few non-viable cells (TOPRO, blue) detected (**figure 3.8**). Moreover, no necrotic centres were observed in aggregates in both conditions (**figure 3.8**), which suggested that the stirring conditions contributed for an efficient nutrient and oxygen distribution within the vessel and that alginate capsules allowed an efficient mass transport, enabling the diffusion of nutrients and oxygen to the centre of aggregates. In contrast, higher levels of cell death were observed on the fibroblast component throughout time (**figures 3.8**). There was an increase in LDH cumulative values throughout time for both cultures, which reflected an increase in cell death during cell culture (**figure 3.9**).

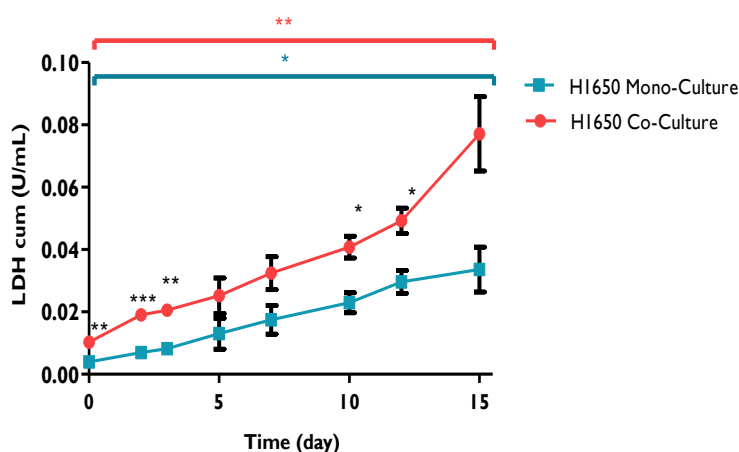


Figure 3.9 – Cell death expressed by cumulative values of LDH released during mono- and co-cultures of HI 650 aggregates encapsulated with NFs in stirred culture systems. Data are mean \pm SD from 2 independent experiments for each condition. * * P<0.01 and * P<0.05 represent significant differences from day 3 to day 0. Black asterisks represent significant differences between mono- and co-cultures. (* P<0.05, ** P<0.01 and *** P<0.001) by one-way ANOVA analysis with Tukey's post multiple comparison test.

NFs contributed to higher values of cumulative LDH in co-culture condition, indicative of higher cell death (**figure 3.8**). The alginate capsules used in this work contained RGD adhesion motifs to enhance fibroblast adhesion to the polymeric matrix and consequently to promote their viability and the establishment of their typical morphology (Horowitz et al., 2007). However the concentration of adhesions motifs might have been

insufficient in order to induce those effects to a full extent. Moreover, another possible explanation can be attributed to the ratio of tumour cells/fibroblasts. An increase of fibroblast concentration within the capsules might provide the required signalling cues derived from cell-cell and cell-ECM interactions, assisting them on positive feedback loops and promoting cell survival (Ref). One of advantages of model proposed in this work relies on its versatility and the possible explanations for fibroblast cell death observed in **figure 3.8** can be easily assessed on future experiments by adjusting specific parameters on the experimental set-up, namely the GRGDSP peptide-coupled MVG alginate proportion relative to UP-MVG alginate and NFs initial concentration.

Caspase-3 is an effector protease that can activate degradation enzymes, leading to apoptosis and, in consequence, to cell death (Singhal, Vachani, & Antin-ozerkis, 2005). Therefore, cell apoptosis was assessed by evaluation of caspase-3 activity, as described in Materials and Methods, section 2.4.5, in mono- and co-culture at days 5 and 15 by fluorescence microscopy (**figure 3.10**).

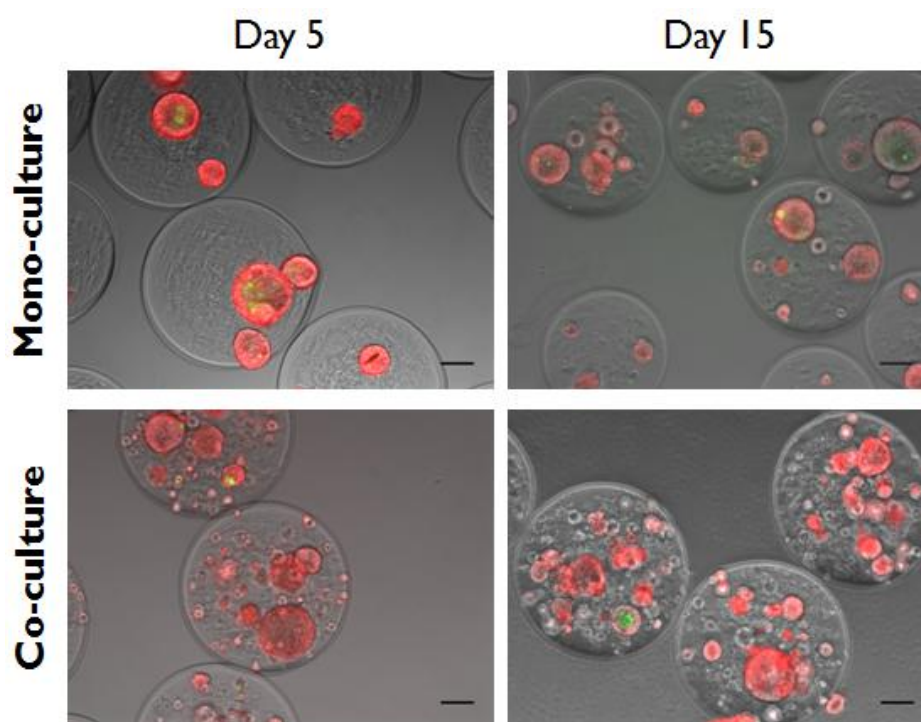


Figure 3.10 - Evaluation of apoptotic activity during mono- and co-cultures of HI650 aggregates encapsulated with NFs in stirred culture systems at days 5 and 15 of culture by fluorescence microscopy. Detection of caspase-3 activity (green) with NucView™ 488, caspase-3 substrate, and mitochondrial activity (red) with MitoView™ 633, far-red fluorescent mitochondrial dye. Scale bars represent 100 μm . Data is from one representative experiment for both conditions.

Mitochondrial activity (in red) was detected in all aggregates (**figure 3.10**), indicating cell viability. Although some apoptotic cells could be observed for mono- and co-cultures at days 5 and 15, there were not an accumulation of apoptotic cells in specific regions of aggregates, such as apoptotic centres. This suggested that this microencapsulation strategy combined with this agitation-based approach allowed a good diffusion of nutrients and oxygen to the whole aggregate, promoting high cell viability (**figure 3.8**) with no apoptotic centres (**figure 3.10**) and, therefore, a long-term cell culture. Although there were some cell death detected throughout time for both conditions (**figures 3.8 and 3.9**), this was not due to apoptosis.

However, these results are just preliminary and additional research will be carried out to further understand the cell death mechanisms by using, for example, spheroids cryosections and immunofluorescence assays with apoptotic markers, such as M30 (caspase-cleaved fragment of CK18), induced myeloid leukemia cell differentiation protein (MCL1), BCL-2 and pro-apoptotic Bcl-2 family member protein BIM, in order to provide further characterization.

The effect of co-culture on aggregate area was also analyzed. Despite oscillations in aggregate's area, especially in co-culture, there was not a significant tendency throughout time (**figure 3.11**). H1650 aggregates were larger and had a more heterogeneous area's distribution in co-culture condition at days 5 and 10 (**figure 3.11**) than in mono-culture. At day 5, aggregates in mono-culture had an average area of $5.1 \pm 5 (\times 10^3 \mu\text{m}^2)$ and in co-culture an average area of $11.5 \pm 9.6 (\times 10^3 \mu\text{m}^2)$. At day 10, mono-culture aggregates presented a mean area of $4.3 \pm 5.9 (\times 10^3 \mu\text{m}^2)$ and co-culture aggregates an average area of $12.2 \pm 14.1 (\times 10^3 \mu\text{m}^2)$. In future experiments, a higher number of aggregates must be measured on further experiments in order to investigate if NFs have any clear effect on aggregate's area.

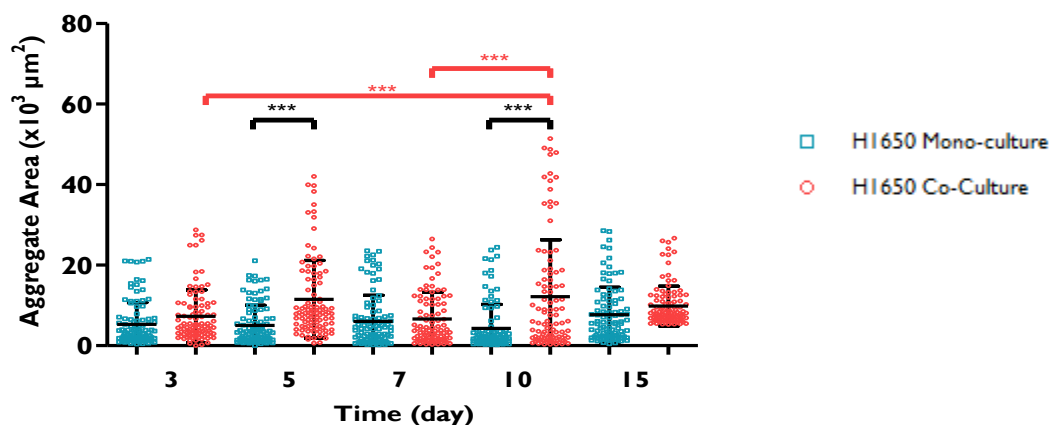


Figure 3.11 - Aggregate area profile of H1650 encapsulated aggregates in mono- and co-culture with NFs using stirred suspension culture systems; data represents mean \pm SD of the area of at least 100 aggregates from 2 independent experiments for each condition. Area of aggregates was measured as described in Materials and Methods, section 2.7. *** indicates significant difference between mono- and co-culture at days 5 and 10 with $P < 0.001$ by one-way ANOVA analysis with Tukey's post multiple comparison test. *** indicates significant difference between day 3 and day 10 and between day 7 and day 10 for co-culture condition with $P < 0.001$ by one-way ANOVA analysis with Tukey's post multiple comparison test.

Regarding cell concentration, there was an increase for mono- and co-cultures, which presented similar growth profile (**figure 3.12 a**). These results suggested that in the co-culture conditions studied, fibroblasts did not affect the proliferation of cancer cells, which maintained their replication ability until the end of the cultures. In order to confirm this result, immunodetection, WB and RT-qPCR analysis of Ki67, a proliferation marker, should be performed. To complement these results, cellular incorporation of 5-bromo-2'-deoxyuridine (BrdU) or 5-ethynyl-2'-deoxyuridine (EdU), nucleoside analogues to thymidine that are incorporated into DNA during active DNA synthesis and can be detected by flow cytometry and/or immunodetection.

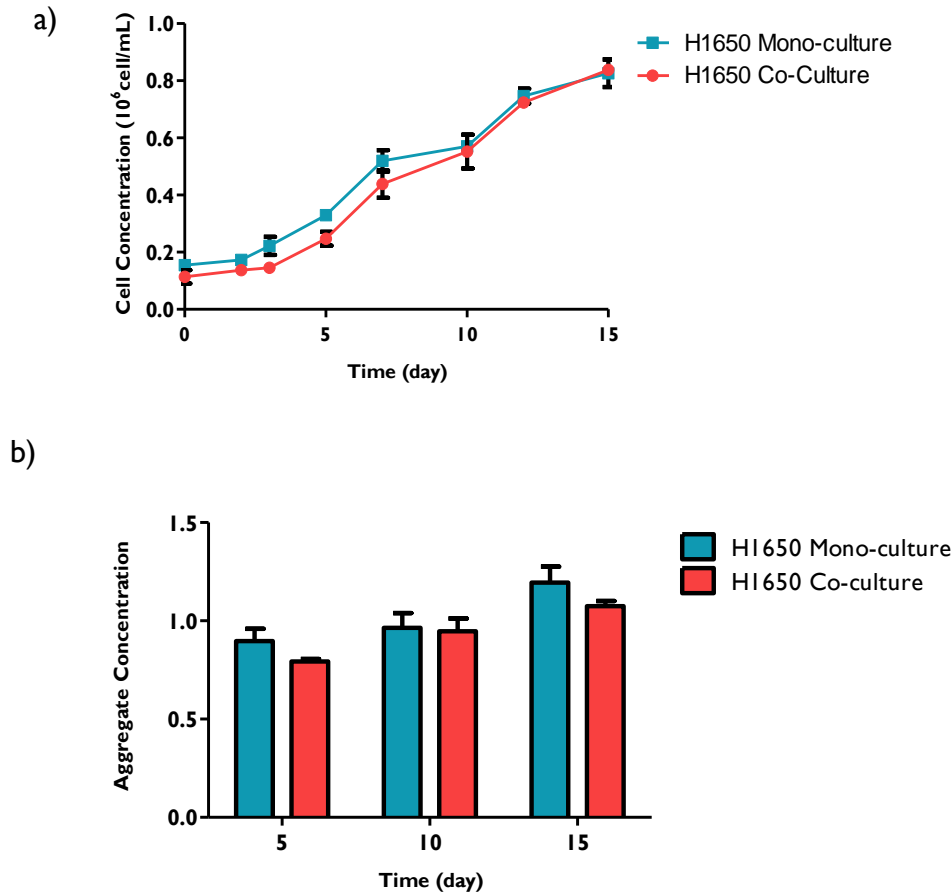


Figure 3.12 – Cell (a) and aggregate (b) concentration of HI650 encapsulated aggregates in mono- and co-culture with NFs using a stirred suspension culture system. Data are mean \pm SD from 2 independent experiments for each condition. Asterisks represent significant differences between mono- and co-cultures. (* $P < 0.05$, ** $P < 0.01$ and *** $P < 0.001$) by one-way ANOVA analysis with Tukey's post multiple comparison test.

Regarding aggregate concentration, it remained constant throughout time for both conditions, which suggest that there was no fusion of aggregates (**figure 3.12 b**) and that co-culture with NFs, in the conditions tested, did not induce any significant change on this specific parameter of HI650 cells. Once again, future experiments should contemplate the possibility of analyzing a higher number of aggregates, in order to confirm the presence or absence of any specific trend on the effect of fibroblasts on HI650 aggregates, as well as different approaches to improve fibroblast viability.

In summary, HI650 aggregates presented high viability and remained compact and spherical during the whole culture time in mono- and co-culture conditions (**figure 3.8**). Moreover, the size of generated aggregates was not sufficient to create oxygen and nutrients limitations and, consequently, apoptotic centres inside the aggregates (**figure 3.10**). Colon

cancer aggregates previously generated in spinner vessels in our group presented clear apoptotic cores which were related to their higher dimension and consequently to limitations on the diffusion of nutrients and oxygen (Alexandra & Silva, 2013).

3.3. Metabolic characterization of encapsulated NSCLC aggregates in mono- and co-culture

There was a decrease in glucose concentration and an increase in lactate concentration on cell culture medium along culture time for both mono- and co-cultures (**figure 3.12**), indicating that cells were metabolic active. The increase in glucose concentration and the decrease in lactate concentration at days 3, 5, 7, 10 and 12 (highlighted by arrows) corresponded to 50% medium exchange in order to mimic the metabolite supply and clearance obtained with blood circulation, responsible for supplying glucose and oxygen to the cells and removing waste metabolites from the cells (see Materials and Methods, section 2.3.3). Cells were not glucose deprived during the whole cell culture time. This enabled the maintenance of long-term cell cultures, with the high cell viability (**figure 3.8**) and cell proliferation (**figure 3.11 a**) until the last days of culture. At day 15, lactate concentration reached 17.4 ± 0.23 mM (**figure 3.12 b**), which were probably still not toxic for H1650 cells. In fact, H1650 cells have been previously reported to be adapted to high levels of lactate (Carmona-Fontaine et al., 2013; Y Zhao, Butler, & Tan, 2013). In addition, lactate might be used as energy source by tumour cells. Pérttega-Gomes et al (2014) reported a higher membranous expression of the lactate transporter monocarboxylate transporter I (MCT1), in cancer cells co-cultured with CAFs, suggesting transport of lactate into tumour cells from the acidic extracellular environment, which could mean that lactate might be used as a fuel by oxidative cancer cells (Pérttega-Gomes et al., 2014). These results also highlight the relevance of the metabolic interplay and crosstalk between tumour cells and fibroblasts. In this thesis, a preliminary metabolic profiling was performed by tracking glucose and lactate in the culture supernatants (**figures 3.14 a** and **b**, respectively) and calculating glucose consumption (**figure 3.14 c**) and lactate production (**figure 3.14 d**) rates, both mono- and co-cultures of H1650 and H1650/NFs, respectively.

a)

b)

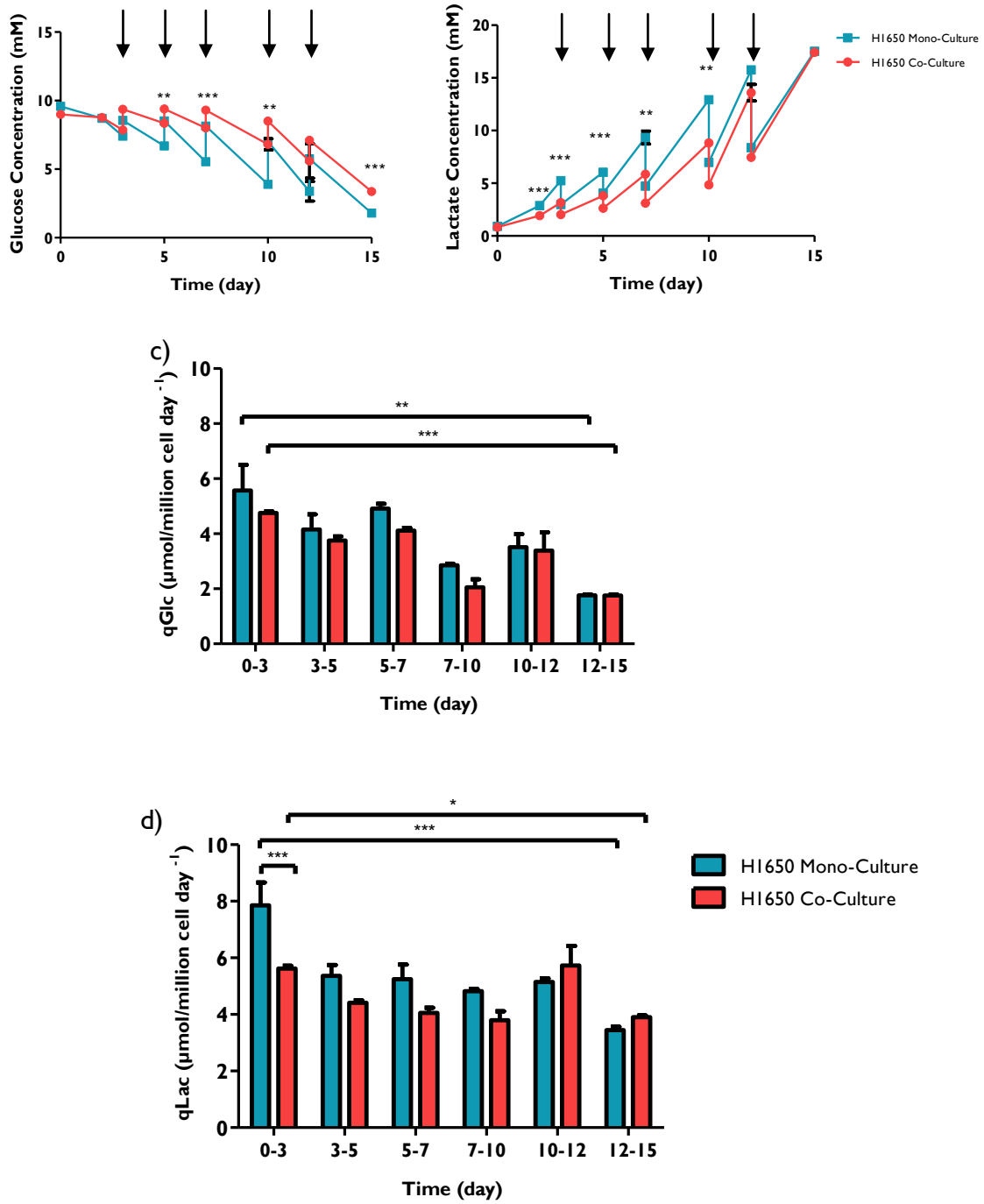


Figure 3.13 – Concentration of glucose (a) and lactate (b) in the cell culture medium of HI650 encapsulated aggregates in mono- and co-culture with NFs using a stirred suspension culture system. Arrows represent 50% of medium exchange. Specific metabolic rate of HI650 encapsulated aggregates in mono- and co-culture with NFs using a stirred suspension culture system for glucose consumption (c) and lactate production (d). Data represents mean \pm SD from 2 independent experiments for each condition. Asterisks indicate significant difference (* $P < 0.05$, ** $P < 0.01$ and *** $P < 0.001$) by one-way ANOVA analysis with Tukey's post multiple comparison test.

Mono-cultures of HI650 cells presented lower glucose concentration and higher lactate concentration on culture supernatant than co-cultures HI650 aggregates (**figure 3.13 a) and b)**). Nonetheless, specific consumption and production rates were not significantly different between both cell cultures. It can be hypothesized that the observed differences in metabolite concentration might be due to lactate consumption by cancer cells associated with upregulation of MCT1 (Amoedo, Rodrigues, & Rumjanek, 2014; Pértega-Gomes et al., 2014). However, this possibility still needs to be further addressed in future studies, through a complete metabolic flux analysis with labeled metabolites, that would allow distinguishing the contribution of each cell type and, for example, immunodetection and gene expression of MCT1 protein.

There was an overall decrease in qGlc and qLac for both mono- and co-culture throughout time (**figure 3.13 c) and d)**). This could be indicative of a less proliferative character of the cells, which might be achieving a plateau phase after the second week of culture. Regarding lactate production (**figure 3.13 b)**), there were higher levels in mono-culture on the first three days of cell culture, which can be related with lactate consumption by cancer cells in presence of NFs as an alternative energy source to glucose (Al, 2010). After these first days of culture, there were no statistically significant differences between the mono- and co-cultures in lactate production rates. This result can be due to cell death on fibroblasts component throughout time, which could decrease the possible effect of NFs on the metabolic activity of cancer cells. However, the effect of NFs on glucose consumption and lactate production has to be further investigated in order to understand if the NFs had an additive or synergistic effect in qGlc and qLac when co-cultured with cancer-cells (due to metabolic tumour-stroma crosstalk).

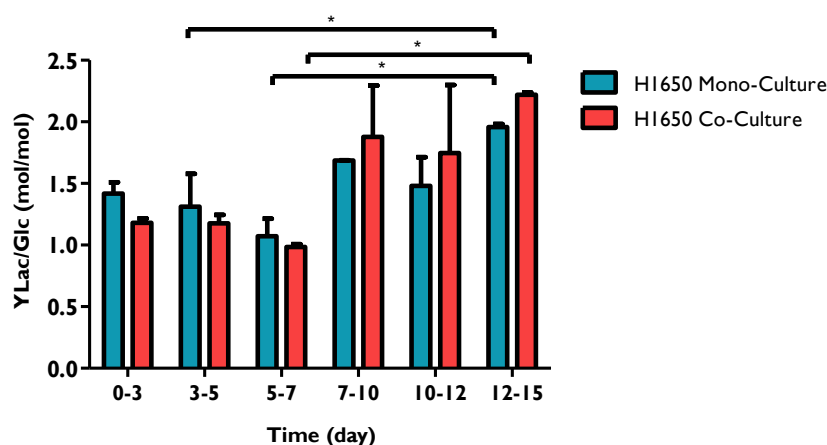


Figure 3.14 – Yield of lactate/glucose of HI650 encapsulated aggregates in mono- and co-culture with NFs in stirred culture systems. Data represents mean \pm SD from 2 independent experiments for each condition. Asterisks indicate significant difference (* $P < 0.05$) by one-way ANOVA analysis with Tukey's post multiple comparison test.

The values of $Y_{Lac/Glc}$ varied between 1 and 2 in mono-cultures and 1 and 2.3 in co-cultures (**figure 3.14**) throughout time. This suggested that there was a decrease in metabolic efficiency during time, especially during the last days of cell culture (day 12-15) (**figure 3.14**). In the beginning of cell culture $Y_{Lac/Glc}$ was inferior to 2, which indicated that consumed glucose was entering the TCA cycle. However, HI650 cells in 2D are reported to have high glycolytic metabolism and lower energy production via oxidative phosphorylation, the Warburg effect (Amoedo et al., 2014; Amoêdo et al., 2011; Hao, Chang, Tsao, & Xu, 2010). However, in 3D cell culture, cells are reported to have lower cell metabolism due to lower proliferation rates comparing to 2D cell culture (Amoêdo et al., 2011; Hao et al., 2010).

3.4. ECM deposition and phenotypic characterization mono- and co-cultures

Fibroblasts are known to be essential for tumour environment structure and to influence ECM composition in the tumour stroma with, for instance, an increase in collagen production (Airola & Fusenig, 2001; Joyce & Pollard, 2009; H Peter Rodemann & Rennekampff, 2011). This collagen production capacity is also reported in cancer cells (Airola & Fusenig, 2001). Therefore, collagen that was entrapped by alginate capsules was quantified in order to characterize the ECM component of the developed cell model (**figure 3.15**).

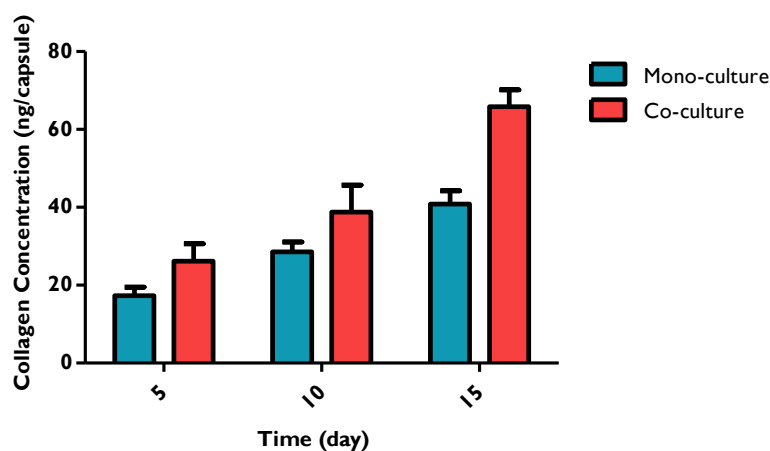


Figure 3.15 – Collagen concentration of HI650 encapsulated aggregates in mono- and co-culture with NFs in stirred culture systems throughout time. Data represents mean \pm SD from 1 experiment for each condition.

There was an increase in collagen concentration in both culture conditions throughout time, with a tendency towards higher values in co-culture, especially at day 15, which may indicate that fibroblasts promoted collagen deposition (**figure 3.15**). These results suggested that the developed 3D cellular model successfully reproduced the collagen accumulation characteristic of a reactive stroma (Airola & Fusenig, 2001). Cancer cells use the collagen fibres produced by the fibroblasts, so they can migrate through the stroma and reach the blood circulation, leading to metastasis (Joyce & Pollard, 2009). In addition, the presence of lactate in the extracellular space upregulates type I collagen production (Goetze *et al.*, 2011), which can be related with collagen accumulation detected throughout time (**figure 3.15**). Another important observation from collagen quantification is the increasing protein detected even in mono-cultures, showing that HI650 present the ability to secrete the ECM component when cultured in 3D conditions and encapsulated within a polymeric

matrix. Thus, the developed cellular model was able to recapitulate certain elements of tumour microenvironment, namely regarding ECM components (Drury & Mooney, 2003; Siegel & Massagué, 2003). Further experiments should be performed to evaluate the influence of fibroblasts on collagen production, specifically through immunofluorescence detection of collagen within the capsules.

The 3D NSCLC cell model generated in this thesis work was phenotypically characterized at day 15 by immunofluorescence microscopy using markers are related to hallmark features of cancer cells such as epithelial to mesenchymal transition and tumour microenvironment (**figure 1.9**) (Hanahan & Weinberg, 2011). Molecular markers of epithelial character (cytokeratin 18 – CK18), mesenchymal character (vimentin), polarity (ZO-1 and F-actin) and ECM components (collagen IV) were used for characterization of the HI650 aggregates throughout the culture period in both mono- and co-cultures .and results are presented in **figure 3.16**..

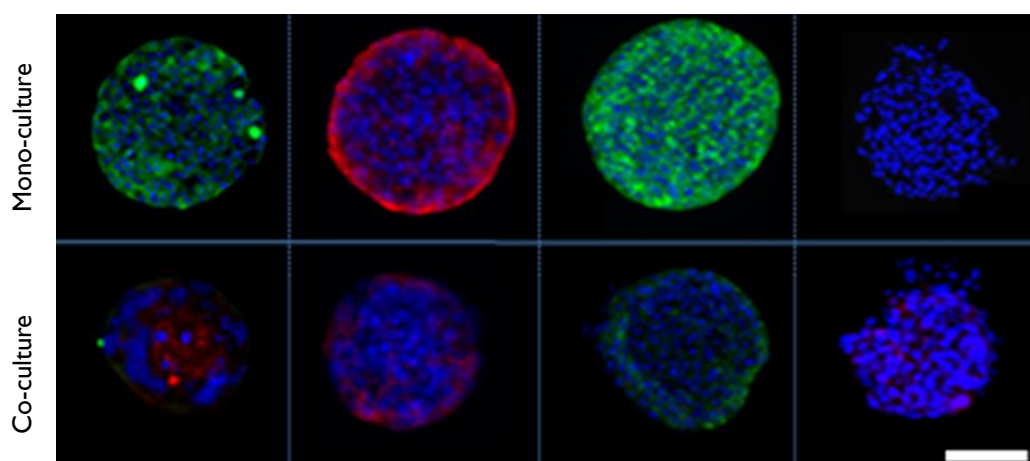


Figure 3.16 - Immunocharacterization of HI650 encapsulated aggregates in mono- and co-culture with NFs in stirred culture systems at day 15 of culture. Epithelial (CK 18, in red), mesenchymal (vimentin, in red), polarity (ZO-1, in red), cytoskeletal organization (F-actin in green, using the fluorescent molecular probe phalloidin) and ECM (Col IV, in red) markers were evaluated. Nuclei were counterstained with DAPI (blue). Scale bars represent 100 μm . Data presented is from one representative experiment for each condition.

At day 15, mono-cultures presented a clear epithelial phenotype with strong CK18 and apical ZO-1 immunolocalization, the later indicative of polarity (**figure 3.16**). However, co-cultures presented a diffuse labeling and there was reduced detection of CK18, indicating loss epithelial phenotype. Moreover, F-actin delineating cell junctions was less detected in

HI 650 aggregates cultured with fibroblasts (**figure 3.16**), suggesting the loss of epithelial cell adhesion.

In addition, Col IV (in red) was faintly expressed centrally within the aggregates (**figure 3.16**). These results were in accordance with quantification of collagen deposition (**figure 3.15**), indicating higher accumulation of ECM components within the co-cultures, which is essential to recapitulate the *in vivo* tumour microenvironment. Moreover, the mesenchymal marker vimentin was faintly detected in co-culture aggregates in contrast with mono-culture aggregates, which had no vimentin expression (**figure 3.16**).

Immunocharacterization of our cultures suggested that in co-culture of HI650 encapsulated aggregates with NFs, epithelial cancer cells initiate the loss of their epithelial phenotype and polarity, towards acquisition of a mesenchymal phenotype. At day 15 of culture, this process is still at an early stage and requires further validation at a longer culture period. At this period, tumour cells presented a mixed epithelial/mesenchymal phenotype. Thus, the presence of stromal cells might be promoting the EMT process. Acquisition of EMT phenotype by HI650 cells is essential to promote invasion, metastasis and drug resistance (Christiansen & Rajasekaran, 2006; J. M. Lee et al., 2006; Xiao & He, 2010).

Further molecular characterization, with other markers such as epithelial marker E-cadherin, through immunohistochemistry, WB and gene expression by reverse transcription-qPCR, should be performed to confirm the epithelial/mesenchymal phenotype observed in **figure 3.16**. Furthermore, samples from earlier time points would help to understand the evolution of epithelial/mesenchymal phenotype throughout time. In addition, longer culture periods could be advantageous to observe the phenotypic shift in more detail.

The work presented in this thesis comprised the development of a novel 3D NSCLC cellular model in which recapitulation of tumour microenvironment can be established. The strategy herein presented was based on co-culture of 3D NSCLC aggregates with fibroblasts within hydrogel capsules in stirred culture systems and represent a novelty in the field of *in vitro* models for NSCLC drug discovery. The novelty in our strategy relied on the combination of three key parameters that contributed for the establishment of a long-term co-culture NSCLC model: 3D cultures, stirred culture systems and cell encapsulation.

Firstly, the formation of H1650 aggregates was successfully established and tumour cells presented high levels of viability throughout the culture period (**figure 3.1**). Cell-cell interactions in 3D aggregates contributed for these viability levels as monolayer cultures lack some of these features to retain cell viability (Breslin & O'Driscoll, 2013; Justice et al., 2009; Zhang et al., 2006). In 2D cell culture, cells spread horizontally and lack the vertical dimension and the adhesive and mechanical signals from neighboring cells existing *in vivo*. These characteristics are essential for cell fate determination (Baker & Chen, 2012b). Thus 3D cellular organization is similar to physiological conditions (Baker & Chen, 2012a; Benien & Swami, 2014; Pampaloni et al., 2007) . Secondly, the hydrodynamic forces of stirred culture systems promote good diffusion of oxygen and nutrients and removal of waste metabolites, which enables high cell viability and long-term cell cultures. This culture system allows simple manipulation without affecting cell culture. This way, the alterations on cell culture characteristics, such as cell proliferation, viability and metabolism, are exclusively due to alterations in culture variables and not due to operation of the culture system. Thirdly, encapsulation strategy allowed obtaining capsules with adequate characteristics for aggregate culture. Capsules had an adequate permeability, stability and elasticity to enable a bi-directional diffusion of nutrients, oxygen, waste metabolites and soluble factors with possible paracrine function as well the retention inside the capsule of other soluble factors with autocrine action. Moreover, the capsule's dimension with approximately 500 μm of diameter and the spherical shape offer an optimal surface to volume ratio. This is appropriate to ensure a good mass diffusion to the centre of the capsule and to to accommodate NSCLC aggregates with similar size to the ones generated after 3 days of 3D NSCLC cell culture (**figure 3.3**). ECM is an essential characteristic of *in vivo* tissue microenvironment. The presence of ECM is indispensable for an adequate cell culture, since it gives the mechanical and adhesive support needed for cell survival, proliferation, differentiation and function. The use of ECM components in *in vitro* cell culture allows confining cells in the same spatial environment, promoting cell-cell and cell-ECM interactions that cells need to grow and organize in a tissue-like structure (Faucheux, Tzoneva, Nagel, & Groth, 2006; Sieh et al., 2012). This spatial confinement can include different types of cells, enabling co-cultures and the recreation of the microenvironment. This allows studying the cell-cell interactions, such as tumour-stroma crosstalk. Different materials are currently used in cell culture, such as collagen, matrigel, laminin and alginate (El-sherbiny & Yacoub, 2013; Glicklis et al., 2000; Godugu et al., 2013; Xu, Farach-Carson, & Jia, 2014). The use of inert materials to mimic

ECM characteristics are advantageous to study the tumor microenvironment as it does not influence the cellular factors secretion, while other ECM-mimicking materials, such as matrigel, have biologic origin and a non-defined composition, which can guide morphological changes and cellular organization (Ivascu & Kubbies, 2006; Sodunke et al., 2007). Alginate is already used to create hydrogels for cell encapsulation (Lan & Starly, 2011; O. SMIDSRÖD, 1974; Rebelo et al., 2014; Wikström et al., 2008). Alginate is an inert material and, consequently, do not interfere with factors secretion by cells (Lukashev & Werb, 1998). In addition, the gelification of alginate capsules was performed using Ba^{2+} , which was reported to give better long-term mechanical stability than Ca^{2+} ions, since Ca^{2+} -alginate gels are more sensitive to chelators, such as the lactate that is produced by cells (O. SMIDSRÖD, 1974). Moreover, lung tumour cells secrete surfactants that could affect the stability of the calcium-crosslinked hydrogels (Meyboom, 1997). Ba^{2+} did not present any toxicity to the cells as a crosslinking agent (Wikström et al., 2008; Zimmermann et al., 2007). Another advantageous of using alginate to encapsulate different cell types and create co-cultures is the possibility to separate the different cellular components, which enables to distinguish cell parameters, such as cell proliferation, viability, metabolism, molecular characterization, between the different types of cell. Moreover, the choice of alginate as the polymeric component and Ba^{2+} as the crosslinking agent to design the matrices proposed in this work was appropriate, since the developed capsules demonstrated stability and permeability for a long-term culture period. Additionally, the use of alginate enables to vary its components (such as polymer molecular weight, strength, thickness, chemical structure) in order to change permeability, stiffness and mechanical strength and, thus, resembling specific ECM characteristics. The combination of 3D NSCLC cellular co-culture with stirred culture systems and alginate microencapsulation constitutes a novel strategy for the development of a robust and scalable 3D NSCLC cell model appropriate for pre-clinical research. Encapsulation of H1650 cells, which were prior aggregated, with NFs allowed to co-culture different types of cells in stirred culture systems. This strategy resembled the tumour microenvironment, including cell-cell and cell-ECM interactions and tumour-stroma crosstalk and it was not performed before by other authors. Encapsulation of single cancer cells and fibroblasts resulted in hybrid aggregates (Dolznic et al., 2011; Hsiao et al., 2009). In these studies, spheroids were formed by encapsulation of single cell suspensions from two different cell types (e.g. cancer cells and fibroblasts) and fibroblasts migrated to the core or stood dispersed in the spheroid, mixed with cancer cells in a non-organized way (Lan & Starly, 2011). These results increase the

importance of the strategy of aggregating cancer cells prior to its alginate encapsulation with NFs in stirred culture systems. Alginate microencapsulation successfully allowed co-culturing fibroblasts with cancer aggregates within the capsule, which was not accomplished by other authors when encapsulating single cell fibroblasts, since the authors noticed that cells formed a clump few hours after encapsulation in alginate and died (Shimi, Hopwood, Newman, & Cuschieri, 1991; Zhang et al., 2006). Moreover, this cellular model is very versatile and can be used to encapsulate other types of cells, including immortalized and primary cell lines and different types of cellular aggregates (de Vos & Marchetti, 2002; Rebelo et al., 2014; Tostões et al., 2011; Wikström et al., 2008). Consequently, the developed cellular model allow mimicking the microenvironment of other solid tumours, for instance, breast and colon cancer (already accomplish in the group, data not published) and other tissues, such as liver and brain (Alessandri et al., 2013; Ivascu & Kubbies, 2007; Rebelo et al., 2014; Sodunke et al., 2007; Tostões et al., 2011; Zhang et al., 2005). Moreover, the generation of H460 aggregates had not been yet accomplished in suspension systems, increasing the novelty of aggregation using stirred culture systems. Previous studies aiming the development of H460 aggregates were done in static 3D cell culture and reported high cell death due to anoikis (Chunhacha et al., 2012; Lloyd & Hardin, 2011; Pongrakhananon et al., 2010; Rungtabnapa et al., 2011). In fact, the novelty of the developed 3D cellular model also relies in the fact that there is lack of literature on encapsulated NSCLC aggregates cultured in stirred systems, since NSCLC aggregates are usually generated in hanging drop or liquid overlay techniques (Amann et al., 2014; Chanvorachote et al., 2009; Ghosh, Lian, Kron, & Palecek, 2012; Ivascu & Kubbies, 2006; Rungtabnapa et al., 2011; Wei et al., 2002) or even embedded or on top of scaffolds (Choi et al., 2010; Godugu et al., 2013; Penzberg, 2005). These approaches do not include the alginate encapsulation strategy herein described nor the efficient mass transfer caused by stirring parameter of the cell culture system. Therefore, recapitulation of the tumour microenvironment created within the alginate capsule when co-culturing H1650 aggregates with NFs provides novelty and increased biological relevance to the cellular model herein described. Manipulation overtime was simple and did not disturb the cell culture, which constitutes another advantage of this 3D cellular model comparing, for instance, with hanging-drop or forced floating techniques, in which aggregates are separated in different wells or compartments (Amann et al., 2014; Kelm et al., 2003; Morizane et al., 2011; Tung et al., 2011). In contrast, the combined strategy herein developed allows tracking the same culture along time. Large numbers of homogeneous spheroids can be generated (**figures 3.1**

and 3.8) with the combined strategy developed in this work and it is suitable for drug testing because it allows standardized, rapid, and large-scale production of 3D NSCLC cellular models mimicking tumour microenvironment. It is also important to notice that the high cell viability (**figures 3.8 and 3.11**) and low cell apoptosis (**figure 3.17**) throughout the whole cell culture time demonstrated that this 3D cellular model is suitable for assessing disease progression and to test pharmaceutical compounds in different stages of disease. The strategy developed by combination of 3D cell culture, alginate microencapsulation and stirred systems lead to long-term cell cultures with high cell viability and proliferation. Thus, this cellular model would allow correlating the alterations of those parameters, cell apoptosis and aggregate's size with drug response, since modifications on those criteria are not related to the strategy itself.

The dynamic strategy proposed using stirred culture systems for aggregation of NSCLC cell lines resulted in application of a hydrodynamic force that promoted cell-cell interactions, which prevented anoikis, and efficient mass transport. In consequence, these culture conditions allowed diffusion of pro-survival signals from one cell to another and of oxygen and nutrients, resulting in NSCLC aggregates with high viability in suspension. Moreover, during the whole cell culture time, aggregates did not lose the compact and spherical shape and did not clump (**figures 3.1 and 3.8**) comparing to non-encapsulated aggregates in suspension cultures that formed large clumps with irregular shape (Serra *et al.*, 2011). These results showed that the stirring profiles efficiently controlled size and shape of aggregates. Culturing H1650 encapsulated aggregates with NFs in stirred culture systems also resulted in high cell viability and long-term cell culture, since there was high cell viability (**figure 3.8**), low cell death (**figure 3.9**) and no apoptotic centres (**figure 3.10**), demonstrating a good mass transport. The 3D cellular organization obtained with this novel strategy allowed cell proliferation (**figures 3.4 a) and 3.12 a)**) and metabolism characteristic of cancer cells, including the production of lactate (**figures 3.5 b) and 3.6 b)**). In the first days of 3D cell culture, cancer cells had higher metabolic efficiencies comparing with 2D cell culture (**figures 3.7 and 3.14**), characterized by the Warburg effect (Hsu & Sabatini, 2008; Otto Warburg, Franz Wind, 1926). The differences in initial days of 3D cell culture in cellular metabolic efficiency could be to an adaptation phase from 2D to 3D culture conditions and to alginate encapsulation. However, the Warburg effect was observed later on cell culture (from day 12 to day 15 in encapsulated H1650 with NFs in stirred culture systems) (**figure 3.14**). These results indicated that the developed cellular

model did not affect the metabolism characteristic of cancer cells. Longer culture periods would allow studying this phenomenon in greater detail. Moreover, as alginate allows separating the different cellular components from the co-culture, MFA studies with labeled glutamine and glucose could be performed to further analyze the metabolic pathways evolved in tumour-stroma crosstalk. Moreover, this 3D NSCLC cellular model mimics some of ECM characteristics. The use of an alginate hydrogel simulates the architecture, chemistry and signaling of *in vivo* environment comparing with 2D cultures (Ghidoni et al., 2008). Alginate capsules fulfilled the requisites of permeability, stability and elasticity, allowing bi-directional diffusion of nutrients, oxygen and soluble factors, which supported an efficient and long-term cell culture with high cell viability (**figures 3.8 and 3.12 a**). Inert alginate provides an aqueous mild and favorable environment for cell encapsulation; however, its natural structure does not provide adhesion points to the encapsulated cells which can result in a loss of cell viability along the culture period. The addition of RGD peptides mimicked the adhesion points of ECM existing *in vivo* (Faucheux et al., 2006; Sieh et al., 2012). The inclusion of these adhesion sequences on the matrix is particularly relevant for the encapsulation of fibroblasts, known for their elongated shape and anchorage-dependent character (Faucheux et al., 2006). The inert properties of alginate (O. SMIDSROD, 1974) and collagen deposition throughout time (**figure 3.15**) allowed to notice accumulation of newly-synthesized ECM components, in accordance with Col IV immunodetection at day 15 for H1650 encapsulated aggregates with NFs cultured in stirred culture systems (**figure 3.16**). Cells constantly remodel local ECM by degrading or synthesizing new ECM elements, such as collagen (Even-Ram & Yamada, 2005). A reactive stroma is characterized by collagen deposition (Airola & Fusenig, 2001). These collagen fibers promote tumour metastasis (Joyce & Pollard, 2009). This suggested an important role of fibroblasts in remodeling ECM composition, probably due to tumor-stroma crosstalk and the physiological relevance of this 3D cellular model to mimic the tumour microenvironment, including ECM and tumour-stroma interactions. The reduced expression of CK18, the diffuse labeling of ZO-1, , and faint detection F-actin and vimentin in H1650 encapsulated aggregates with NFs in stirred culture systems after 15days of cell culture suggested partial loss of polarity and epithelial phenotype and early steps on the acquisition of a mesenchymal phenotype (**figure 3.17**). Thus, fibroblasts could have enhanced the EMT process of cancer cells, as a result of tumour-stroma crosstalk along cell culture time. EMT has been related to higher motility, invasiveness and TKI resistance by EGFR mutated cancer cells, such as H1650 cells, during

NSCLC cancer treatment (G. Chen, Kronenberger, Teugels, Umelo, & De Grève, 2012; Choi et al., 2010; Ladanyi & Pao, 2008; Pallier et al., 2012). Therefore, this 3D NSCLC cellular model has the advantage to allow the study of EMT evolution throughout time and further application in drug screening.

Further studies are still required to conclude about the effect of HI650 encapsulated aggregates co-cultured with NFs in cell behaviour. Higher RGD-couple alginate: alginate ratio and higher NFs cellular concentration should be tested in order to evaluate the possible causes of NFs cell death detected throughout culture (**figures 3.8 and 3.9**). In next experiments, measurements of aggregate's area should consider more than 100 aggregates in order to see a tendency in aggregates size (**figure 3.12**). The evaluation of apoptotic activity needs further fluorescence assays using cryosections or entire aggregates and antibodies against apoptotic markers, such as M30, MCL1, BCL-2 and BIM. This would allow confirming that cell apoptosis was not detected in specific regions within the aggregate (as apoptotic centres) and that fibroblasts cell death was not due to apoptosis, since they presented mitochondrial activity throughout cell culture (**figure 3.10**). Moreover, MFA studies with labeled glucose and glutamine would enable to identify the metabolic pathways used preferentially by each cell type. Thus, it would enable to take further conclusions about the glycolytic metabolism characteristic of cancer cells, known as Warburg effect (Carmona-Fontaine et al., 2013; Daye & Wellen, 2012) and metabolic tumour-stroma crosstalk. MCT1 expression analysis by WB and RT-qPCR in HI650 encapsulated aggregates with NFs cultured in stirred systems and its immunodetection in cryosections or entire aggregates through confocal microscopy would give further support to the MFA results about the possible lactate consumption by cancer cells (Al, 2010; Fiaschi et al., 2012; Pértega-Gomes et al., 2014). Longer culture periods would also be suitable to characterize metabolic differences throughout time. The effect of NFs on HI650 encapsulated aggregates epithelial/mesenchymal phenotype should be confirmed by additional assays with immunodetection on cryosections or in entire aggregates in order to confirm a decrease in detection of epithelial and polarity markers, such as CK 18, ZO-1 and F-actin and, in contrast, an increase of detection of mesenchymal markers, such as vimentin, in HI650 aggregates. E-cadherin should also be assessed by immunofluorescence, since it is one of the mainly proteins involved in cell-cell adhesions (Bhatt, Rizvi, Batta, Kataria, & Jamora, 2013; Böhm, Totzeck, & Wieland, 1994). This would allow confirming that NFs contributed to a loss in epithelial phenotype and gain of mesenchymal characteristics, accelerating the EMT

phenomenon. The molecular expression of these epithelial and mesenchymal markers by WB and RT-qPCR would give further information about the effect of NFs in cancer cells phenotype. In addition, analyzing these parameters in different time points of cell culture would allow to take further conclusions about phenotypic alterations in HI650 encapsulated aggregates with NFs during co-culture in stirred culture systems. Moreover, the effect of NFs in remodeling the ECM by collagen accumulation needs further assays on collagen quantification, as well as molecular characterization of different collagen types (including Col IV). Furthermore, application of this 3D cellular strategy in computer-controlled bioreactors would allow a more accurate control on cell culture variables, enabling studying the effect of specific parameters, such as oxygen, pH, temperature, on cell culture readouts.

Conclusion

4. Conclusion

This thesis work successfully accomplished the aim that was proposed. Combination of 3D cell culture, stirred culture systems and alginate encapsulation generated a robust and scalable 3D NSCLC cellular model that recapitulated the tumour microenvironment with potential use for pre-clinical research and pharmacological applications. Alginate encapsulation of H1650 aggregates with NFs in stirred systems resembled the 3D spatial organization characteristic of *in vivo* tumour tissues, including cell-ECM and tumour-stroma interactions. The culture strategy herein described is a valuable tool to obtain highly reproducible homogeneous long-term cell cultures, while enabling a non-destructive sampling. This 3D cellular model can be used to culture other types of cells with cancer aggregates in order to study the tumour heterogeneity and, in consequence, the influence of different types of cells, such as endothelial and immune cells in cancer cell behaviour. Additionally, this 3D cellular model can be applied in drug screening test in pharmacological studies, with the possibility of high throughput with phenotypic characterization. The pharmacological potential of this strategy would allow a better understanding of tumour biology and decreasing the time and costs associated with drug discovery

In conclusion, 3D cell culture using alginate encapsulation combined with a stirred system successfully generated for the first time a 3D NSCLC cellular model that recapitulates the tumour microenvironment suitable for pre-clinical research.

Perspectives

5. Perspectives

Detection of caspase 3 activity, ECM, CAFs, epithelial, mesenchymal and apoptotic markers, by qRT-PCR, Western blot and immunofluorescence microscopy, will be used to evaluate the effect of tumour microenvironment in cancer cell behavior.

Metabolic flux analysis tools with labeled glucose and glutamine will be performed to better characterize the cell metabolism and evaluate the tumour-stroma metabolic crosstalk.

Encapsulation of cancer aggregates with CAFs would allow assessing the effect of reactive stroma comparing to normal stroma cells (NFs) on cancer cell characteristics.

The 3D cell culture strategy developed could be further improved by using controlled stirred tank bioreactors. It is expected that by controlling parameters such as mixing, pH, temperature, oxygen (for example, hypoxia versus normoxia) and nutrient supply (perfusion mode), a better understand of the role of tumour microenvironment in tumour progression will be obtained.

Test different pharmaceutical compounds, such as docetaxel, a microtubule-stabilizing taxane used in the clinical treatment of different types of cancer, will enable to validate this cellular model as a promising tool in pre-clinical research.

References

7. References

- Airola, K., & Fusenig, N. E. (2001). Differential stromal regulation of MMP-1 expression in benign and malignant keratinocytes. *The Journal of Investigative Dermatology*, 116(1), 85–92. doi:10.1046/j.1523-1747.2001.00223.x
- Akhtar, N., & Streuli, C. H. (2013). An integrin-ILK-microtubule network orients cell polarity and lumen formation in glandular epithelium. *Nature Cell Biology*, 15(1), 17–27. doi:10.1038/ncb2646
- Al, M.-O. et. (2010). 2010_Oxidative stress in cancer associated fibroblasts_reverse Warburg effect.pdf.crdownload. *Cell Cycle*, 9(16), 3256–3276.
- Alcaraz, J., Nelson, C. M., & Bissell, M. J. (2004). Biomechanical approaches for studying integration of tissue structure and function in mammary epithelia. *Journal of Mammary Gland Biology and Neoplasia*, 9(4), 361–74. doi:10.1007/s10911-004-1406-8
- Alessandri, K., Sarangi, B. R., Gurchenkov, V. V., Sinha, B., Kießling, T. R., Fetler, L., ... Nassoy, P. (2013). Cellular capsules as a tool for multicellular spheroid production and for investigating the mechanics of tumor progression in vitro. *Proceedings of the National Academy of Sciences of the United States of America*, 110(37), 14843–8. doi:10.1073/pnas.1309482110
- Alevizakos, M., Kaltsas, S., & Syrigos, K. N. (2013). The VEGF pathway in lung cancer. *Cancer Chemotherapy and Pharmacology*, 72(6), 1169–81. doi:10.1007/s00280-013-2298-3
- Alexandra, I., & Silva, M. (2013). Evaluation of Chemotherapeutic Potential of Natural Extracts Using 3D Models of Colon Cancer.
- Alves, P. (1996). Two-Dimensional Versus Three-Dimensional Culture Systems: Effects on Growth and Productivity of BHK Cells, 52, 429–432.
- Amann, A., Zwierzina, M., Gamerith, G., Bitsche, M., Huber, J. M., Vogel, G. F., ... Zwierzina, H. (2014). Development of an innovative 3D cell culture system to study tumour--stroma interactions in non-small cell lung cancer cells. *PLoS One*, 9(3), e92511. doi:10.1371/journal.pone.0092511
- Amoêdo, N. D., Rodrigues, M. F., Pezzuto, P., Galina, A., da Costa, R. M., de Almeida, F. C. L., ... Rumjanek, F. D. (2011). Energy metabolism in H460 lung cancer cells: effects of histone deacetylase inhibitors. *PLoS One*, 6(7), e22264. doi:10.1371/journal.pone.0022264
- Amoedo, N. D., Rodrigues, M. F., & Rumjanek, F. D. (2014). Mitochondria: are mitochondria accessory to metastasis? *The International Journal of Biochemistry & Cell Biology*, 51, 53–7. doi:10.1016/j.biocel.2014.03.009
- Antony, V. B., Loddenkemper, R., Astoul, P., Boutin, C., Goldstraw, P., Hott, J., ... Sahn, S. a. (2001). Management of malignant pleural effusions. *The European Respiratory Journal*, 18(2), 402–19. Retrieved from <http://www.ncbi.nlm.nih.gov/pubmed/11529302>
- Babakoohi, S., Fu, P., Yang, M., Linden, P. a, & Dowlati, A. (2013). Combined SCLC clinical and pathologic characteristics. *Clinical Lung Cancer*, 14(2), 113–9. doi:10.1016/j.clcc.2012.07.002
- Bailón-Moscoso, N., Romero-Benavides, J. C., & Ostrosky-Wegman, P. (2014). Development of anticancer drugs based on the hallmarks of tumor cells. *Tumour Biology : The Journal of the International Society for Oncodevelopmental Biology and Medicine*, 35(5), 3981–95. doi:10.1007/s13277-014-1649-y
- Baker, B. M., & Chen, C. S. (2012a). Deconstructing the third dimension: how 3D culture microenvironments alter cellular cues. *Journal of Cell Science*, 125(Pt 13), 3015–24. doi:10.1242/jcs.079509
- Baker, B. M., & Chen, C. S. (2012b). Deconstructing the third dimension: how 3D culture microenvironments alter cellular cues. *Journal of Cell Science*, 125(Pt 13), 3015–24. doi:10.1242/jcs.079509

References

- Bechyne, I., Szpak, K., Madeja, Z., & Czyż, J. (2012). Functional heterogeneity of non-small lung adenocarcinoma cell sub-populations. *Cell Biology International*, 36(1), 99–103. doi:10.1042/CBI20110151
- Beetschen, J. C. (2001). Amphibian gastrulation: history and evolution of a 125 year-old concept. *The International Journal of Developmental Biology*, 45(7), 771–95. Retrieved from <http://www.ncbi.nlm.nih.gov/pubmed/11732838>
- Benien, P., & Swami, A. (2014). 3D tumor models: history, advances and future perspectives. *Future Oncology (London, England)*, 10(7), 1311–27. doi:10.2217/fo.13.274
- Bhatt, T., Rizvi, A., Batta, S. P. R., Kataria, S., & Jamora, C. (2013). Signaling and mechanical roles of E-cadherin. *Cell Communication & Adhesion*, 20(6), 189–99. doi:10.3109/15419061.2013.854778
- Birsoy, K., Possemato, R., Lorbeer, F. K., Bayraktar, E. C., Thiru, P., Yucel, B., ... Sabatini, D. M. (2014). Metabolic determinants of cancer cell sensitivity to glucose limitation and biguanides. *Nature*, 508(7494), 108–12. doi:10.1038/nature13110
- Böhm, M., Totzeck, B., & Wieland, I. (1994). Differences of E-cadherin expression levels and patterns in human lung cancer. *Annals of Hematology*, 68(2), 81–3. Retrieved from <http://www.ncbi.nlm.nih.gov/pubmed/7511935>
- Bradley, J., Thorstad, W. L., Mutic, S., Miller, T. R., Dehdashti, F., Siegel, B. a, ... Bertrand, R. J. (2004). Impact of FDG-PET on radiation therapy volume delineation in non-small-cell lung cancer. *International Journal of Radiation Oncology, Biology, Physics*, 59(1), 78–86. doi:10.1016/j.ijrobp.2003.10.044
- Brenner, D. R., Boffetta, P., Duell, E. J., Bickeböller, H., Rosenberger, A., McCormack, V., ... Hung, R. J. (2012). Previous lung diseases and lung cancer risk: a pooled analysis from the International Lung Cancer Consortium. *American Journal of Epidemiology*, 176(7), 573–85. doi:10.1093/aje/kws151
- Breslin, S., & O'Driscoll, L. (2013). Three-dimensional cell culture: the missing link in drug discovery. *Drug Discovery Today*, 18(5-6), 240–9. doi:10.1016/j.drudis.2012.10.003
- Brito, C., Simão, D., Costa, I., Malpique, R., Pereira, C. I., Fernandes, P., ... Alves, P. M. (2012). 3D cultures of human neural progenitor cells: dopaminergic differentiation and genetic modification. *Methods (San Diego, Calif.)*, 56(3), 452–60. doi:10.1016/j.ymeth.2012.03.005
- Burey, P., Bhandari, B. R., Howes, T., & Gidley, M. J. (2008). Hydrocolloid gel particles: formation, characterization, and application. *Critical Reviews in Food Science and Nutrition*, 48(5), 361–77. doi:10.1080/10408390701347801
- Carmona-Fontaine, C., Bucci, V., Akkari, L., Deforet, M., Joyce, J. a, & Xavier, J. B. (2013). Emergence of spatial structure in the tumor microenvironment due to the Warburg effect. *Proceedings of the National Academy of Sciences of the United States of America*, 110(48), 19402–7. doi:10.1073/pnas.1311939110
- Carterson, A. J., Ho, K., Ott, C. M., Clarke, M. S., & Pierson, D. L. (2005). A549 Lung Epithelial Cells Grown as Three-Dimensional Aggregates : Alternative Tissue Culture Model for Pseudomonas aeruginosa Pathogenesis, 73(2), 1129–1140. doi:10.1128/IAI.73.2.1129
- Casey, R. C., Burleson, K. M., Skubitz, K. M., Pambuccian, S. E., Oegema, T. R., Ruff, L. E., & Skubitz, a P. (2001). Beta 1-integrins regulate the formation and adhesion of ovarian carcinoma multicellular spheroids. *The American Journal of Pathology*, 159(6), 2071–80. Retrieved from <http://www.pubmedcentral.nih.gov/articlerender.fcgi?artid=1850600&tool=pmcentrez&rendertype=abstract>
- Castilho, L., Moraes, A., Augusto, E., & Butler, M. (2008). *Cell metabolism and its control in culture. In Animal Cell Technology: From Biopharmaceuticals to Gene Therapy* (pp. 76–110). New York: Taylor & Francis Group. doi:10.4324/9780203895160

References

- Chang, H. Y., Chi, J.-T., Dudoit, S., Bondre, C., van de Rijn, M., Botstein, D., & Brown, P. O. (2002). Diversity, topographic differentiation, and positional memory in human fibroblasts. *Proceedings of the National Academy of Sciences of the United States of America*, *99*(20), 12877–82. doi:10.1073/pnas.162488599
- Chanvorachote, P., Nimmannit, U., Lu, Y., Talbott, S., Jiang, B.-H., & Rojanasakul, Y. (2009). Nitric oxide regulates lung carcinoma cell anoikis through inhibition of ubiquitin-proteasomal degradation of caveolin-1. *The Journal of Biological Chemistry*, *284*(41), 28476–84. doi:10.1074/jbc.M109.050864
- Chen, G., Kronenberger, P., Teugels, E., Umelo, I. A., & De Grève, J. (2012). Targeting the epidermal growth factor receptor in non-small cell lung cancer cells: the effect of combining RNA interference with tyrosine kinase inhibitors or cetuximab. *BMC Medicine*, *10*(1), 28. doi:10.1186/1741-7015-10-28
- Chen, H., Shen, A., Zhang, Y., Chen, Y., Lin, J., Lin, W., ... Peng, J. (2014). Pien Tze Huang inhibits hypoxia-induced epithelial-mesenchymal transition in human colon carcinoma cells through suppression of the HIF-1 pathway. *Experimental and Therapeutic Medicine*, *7*(5), 1237–1242. doi:10.3892/etm.2014.1549
- Chen, S.-Y. C., Hung, P. J., & Lee, P. J. (2011). Microfluidic array for three-dimensional perfusion culture of human mammary epithelial cells. *Biomedical Microdevices*, *13*(4), 753–8. doi:10.1007/s10544-011-9545-3
- Chen, Z., Zhang, D., Yue, F., Zheng, M., Kovacevic, Z., & Richardson, D. R. (2012). The iron chelators Dp44mT and DFO inhibit TGF- β -induced epithelial-mesenchymal transition via up-regulation of N-Myc downstream-regulated gene 1 (NDRG1). *The Journal of Biological Chemistry*, *287*(21), 17016–28. doi:10.1074/jbc.M112.350470
- Choi, Y. J., Rho, J. K., Jeon, B., Choi, S. J., Park, S. C., Lee, S. S., ... Lee, J. C. (2010). Combined inhibition of IGFR enhances the effects of gefitinib in H1650: a lung cancer cell line with EGFR mutation and primary resistance to EGFR-TK inhibitors. *Cancer Chemotherapy and Pharmacology*, *66*(2), 381–8. doi:10.1007/s00280-009-1174-7
- Christiansen, J. J., & Rajasekaran, A. K. (2006). Reassessing epithelial to mesenchymal transition as a prerequisite for carcinoma invasion and metastasis. *Cancer Research*, *66*(17), 8319–26. doi:10.1158/0008-5472.CAN-06-0410
- Christie, a, & Butler, M. (1994). Glutamine-based dipeptides are utilized in mammalian cell culture by extracellular hydrolysis catalyzed by a specific peptidase. *Journal of Biotechnology*, *37*(3), 277–90. Retrieved from <http://www.ncbi.nlm.nih.gov/pubmed/7765576>
- Chunhacha, P., Pongrakhananon, V., Rojanasakul, Y., & Chanvorachote, P. (2012). Caveolin-1 regulates Mcl-1 stability and anoikis in lung carcinoma cells. *American Journal of Physiology. Cell Physiology*, *302*(9), C1284–92. doi:10.1152/ajpcell.00318.2011
- Coldren, C. D., Helfrich, B. a, Witta, S. E., Sugita, M., Lapadat, R., Zeng, C., ... Bunn, P. a. (2006). Baseline gene expression predicts sensitivity to gefitinib in non-small cell lung cancer cell lines. *Molecular Cancer Research* : MCR, *4*(8), 521–8. doi:10.1158/1541-7786.MCR-06-0095
- Cruz, H., Freitas, C., Alves, P., Moreira, J., & Carrondo, M. (2000). Effects of ammonia and lactate on growth, metabolism, and productivity of BHK cells. *Enzyme and Microbial Technology*, *27*(1-2), 43–52. Retrieved from <http://www.ncbi.nlm.nih.gov/pubmed/10862901>
- Cruz, H. J., Ferreira, a S., Freitas, C. M., Moreira, J. L., & Carrondo, M. J. (1999). Metabolic responses to different glucose and glutamine levels in baby hamster kidney cell culture. *Applied Microbiology and Biotechnology*, *51*(5), 579–85. Retrieved from <http://www.ncbi.nlm.nih.gov/pubmed/10390815>
- Daye, D., & Wellen, K. E. (2012). Metabolic reprogramming in cancer: unraveling the role of glutamine in tumorigenesis. *Seminars in Cell & Developmental Biology*, *23*(4), 362–9. doi:10.1016/j.semcdb.2012.02.002
- De Vos, P., & Marchetti, P. (2002). Encapsulation of pancreatic islets for transplantation in diabetes: the untouchable islets. *Trends in Molecular Medicine*, *8*(8), 363–6. Retrieved from <http://www.ncbi.nlm.nih.gov/pubmed/12127717>

References

- Dearing, K. R., Sangal, A., & Weiss, G. J. (2014). Maintaining clarity: Review of maintenance therapy in non-small cell lung cancer. *World Journal of Clinical Oncology*, 5(2), 103–113. doi:10.5306/wjco.v5.i2.103
- Dolznic, H., Walzl, A., Kramer, N., Rosner, M., Garin-Chesa, P., & Hengstschläger, M. (2011). Organotypic spheroid cultures to study tumor–stroma interaction during cancer development. *Drug Discovery Today: Disease Models*, 8(2-3), 113–119. doi:10.1016/j.ddmod.2011.06.003
- Drury, J. L., & Mooney, D. J. (2003). Hydrogels for tissue engineering: scaffold design variables and applications. *Biomaterials*, 24(24), 4337–4351. doi:10.1016/S0142-9612(03)00340-5
- Eagle, H., Washington, C. L., Cohen, L., & Levy, M. (1966). SUBSTANCES OF LOW MOLECULAR WEIGHT : The Population-dependent Requirement by Cultured Mammalian Cells for Metabolites Which They Can Synthesize : II . The Population-dependent Requirement by Cultured Cells for Metabolites Which They Can Synthesize.
- El-sherbiny, I. M., & Yacoub, M. H. (2013). Review article Hydrogel scaffolds for tissue engineering : Progress and challenges.
- Faucheux, N., Tzoneva, R., Nagel, M.-D., & Groth, T. (2006). The dependence of fibrillar adhesions in human fibroblasts on substratum chemistry. *Biomaterials*, 27(2), 234–45. doi:10.1016/j.biomaterials.2005.05.076
- Fennema, E., Rivron, N., Rouwkema, J., van Blitterswijk, C., & de Boer, J. (2013). Spheroid culture as a tool for creating 3D complex tissues. *Trends in Biotechnology*, 31(2), 108–115. doi:10.1016/j.tibtech.2012.12.003
- Fiaschi, T., Marini, A., Giannoni, E., Taddei, M. L., Gandellini, P., De Donatis, A., ... Chiarugi, P. (2012). Reciprocal metabolic reprogramming through lactate shuttle coordinately influences tumor-stroma interplay. *Cancer Research*, 72(19), 5130–40. doi:10.1158/0008-5472.CAN-12-1949
- Finley, L. W. S., Zhang, J., Ye, J., Ward, P. S., & Thompson, C. B. (2013). SnapShot: cancer metabolism pathways. *Cell Metabolism*, 17(3), 466–466.e2. doi:10.1016/j.cmet.2013.02.016
- Friedrich, J., Seidel, C., Ebner, R., & Kunz-Schughart, L. a. (2009). Spheroid-based drug screen: considerations and practical approach. *Nature Protocols*, 4(3), 309–24. doi:10.1038/nprot.2008.226
- Furák, J., Troján, I., Szoóke, T., Tiszlavicz, L., Morvay, Z., Eller, J., & Balogh, Á. (2003). Bronchioloalveolar lung cancer: occurrence, surgical treatment and survival ☆. *European Journal of Cardio-Thoracic Surgery*, 23(5), 818–823. doi:10.1016/S1010-7940(03)00084-8
- Ghosh, G., Lian, X., Kron, S. J., & Palecek, S. P. (2012). Properties of resistant cells generated from lung cancer cell lines treated with EGFR inhibitors. *BMC Cancer*, 12(1), 95. doi:10.1186/1471-2407-12-95
- Glicklis, R., Shapiro, L., Agbaria, R., Merchuk, J. C., & Cohen, S. (2000). Three-Dimensional Porous Alginate Scaffolds, (M).
- Godugu, C., Patel, A. R., Desai, U., Andey, T., Sams, A., & Singh, M. (2013). AlgiMatrix™ based 3D cell culture system as an in-vitro tumor model for anticancer studies. *PloS One*, 8(1), e53708. doi:10.1371/journal.pone.0053708
- Goetze, K., Walenta, S., Ksiazkiewicz, M., Kunz-Schughart, L. a, & Mueller-Klieser, W. (2011). Lactate enhances motility of tumor cells and inhibits monocyte migration and cytokine release. *International Journal of Oncology*, 39(2), 453–63. doi:10.3892/ijo.2011.1055
- Gong, H. C., Wang, S., Mayer, G., Chen, G., Leesman, G., Singh, S., & Beer, D. G. (2011). Signatures of drug sensitivity in nonsmall cell lung cancer. *International Journal of Proteomics*, 2011, 215496. doi:10.1155/2011/215496

References

- Gout, S., & Huot, J. (2008). Role of cancer microenvironment in metastasis: focus on colon cancer. *Cancer Microenvironment: Official Journal of the International Cancer Microenvironment Society*, 1(1), 69–83. doi:10.1007/s12307-008-0007-2
- Green, J. A., & Yamada, K. M. (2007). Three-dimensional microenvironments modulate fibroblast signaling responses. *Advanced Drug Delivery Reviews*, 59(13), 1293–8. doi:10.1016/j.addr.2007.08.005
- Gross, A., McDonnell, J. M., & Korsmeyer, S. J. (1999). BCL-2 family members and the mitochondria in apoptosis. *Blood*, 93(11), 1899–1911.
- Grosso, J. F., & Jure-Kunkel, M. N. (2013). CTLA-4 blockade in tumor models: an overview of preclinical and translational research. *Cancer Immunity*, 13(January), 5. Retrieved from <http://www.pubmedcentral.nih.gov/articlerender.fcgi?artid=3559193&tool=pmcentrez&rendertype=abstract>
- Hait, W. N. (2010). Anticancer drug development: the grand challenges. *Nature Reviews. Drug Discovery*, 9(4), 253–4. doi:10.1038/nrd3144
- Hanahan, D., & Weinberg, R. a. (2011). Hallmarks of cancer: the next generation. *Cell*, 144(5), 646–74. doi:10.1016/j.cell.2011.02.013
- Hao, W., Chang, C.-P. B., Tsao, C.-C., & Xu, J. (2010). Oligomycin-induced bioenergetic adaptation in cancer cells with heterogeneous bioenergetic organization. *The Journal of Biological Chemistry*, 285(17), 12647–54. doi:10.1074/jbc.M109.084194
- Hashimoto, Y., Tazawa, H., Teraishi, F., Kojima, T., Watanabe, Y., Uno, F., ... Fujiwara, T. (2012). The hTERT promoter enhances the antitumor activity of an oncolytic adenovirus under a hypoxic microenvironment. *PLoS One*, 7(6), e39292. doi:10.1371/journal.pone.0039292
- Herbst, R. S., Heymach, J. V., & Lippman, S. M. (2008). Lung cancer. *The New England Journal of Medicine*, 359(13), 1367–80. doi:10.1056/NEJMra0802714
- Hirsch, F. R., Varella-Garcia, M., McCoy, J., West, H., Xavier, A. C., Gumerlock, P., ... Gandara, D. R. (2005). Increased epidermal growth factor receptor gene copy number detected by fluorescence in situ hybridization associates with increased sensitivity to gefitinib in patients with bronchioloalveolar carcinoma subtypes: a Southwest Oncology Group Study. *Journal of Clinical Oncology: Official Journal of the American Society of Clinical Oncology*, 23(28), 6838–45. doi:10.1200/JCO.2005.01.2823
- Holtfreter, J. (1944). A study of the mechanics of gastrulation. *Part II J. Exp. Zool.*, 95, 171–212.
- Hopper-Borge, W.-T. and. (2014). Drug Resistance Mechanisms in Non-Small Cell Lung Carcinoma. *J Can Res Updates*, 2(4), 265–282. doi:10.6000/1929-2279.2013.02.04.5.Drug
- Horn, L., & Carbone, D. P. (2014). Reducing lung cancer mortality: 2014 update. *Seminars in Oncology*, 41(1), 3–4. doi:10.1053/j.seminoncol.2013.12.004
- Horowitz, J. C., Rogers, D. S., Sharma, V., Vittal, R., White, E. S., Cui, Z., & Thannickal, V. J. (2007). Combinatorial activation of FAK and AKT by transforming growth factor- β 1 confers an anoikis-resistant phenotype to myofibroblasts. *Cellular Signalling*, 19(4), 761–71. doi:10.1016/j.cellsig.2006.10.001
- Hsiao, A. Y., Torisawa, Y. suke, Tung, Y. C., Sud, S., Taichman, R. S., Pienta, K. J., & Takayama, S. (2009). Microfluidic system for formation of PC-3 prostate cancer co-culture spheroids. *Biomaterials*, 30, 3020–3027. doi:10.1016/j.biomaterials.2009.02.047
- Hsu, P. P., & Sabatini, D. M. (2008). Cancer cell metabolism: Warburg and beyond. *Cell*, 134(5), 703–7. doi:10.1016/j.cell.2008.08.021

References

- Hughes, J. P., Rees, S., Kalindjian, S. B., & Philpott, K. L. (2011). Principles of early drug discovery. *British Journal of Pharmacology*, 162(6), 1239–49. doi:10.1111/j.1476-5381.2010.01127.x
- Huh, D., Hamilton, G. a, & Ingber, D. E. (2011). From 3D cell culture to organs-on-chips. *Trends in Cell Biology*, 21(12), 745–54. doi:10.1016/j.tcb.2011.09.005
- Hutmacher, D. W., & Singh, H. (2008). Computational fluid dynamics for improved bioreactor design and 3D culture. *Trends in Biotechnology*, 26(4), 166–72. doi:10.1016/j.tibtech.2007.11.012
- Hwang, Y.-S., Cho, J., Tay, F., Heng, J. Y. Y., Ho, R., Kazarian, S. G., ... Mantalaris, A. (2009). The use of murine embryonic stem cells, alginate encapsulation, and rotary microgravity bioreactor in bone tissue engineering. *Biomaterials*, 30(4), 499–507. doi:10.1016/j.biomaterials.2008.07.028
- Ivascu, A., & Kubbies, M. (2006). Rapid generation of single-tumor spheroids for high-throughput cell function and toxicity analysis. *Journal of Biomolecular Screening*, 11(8), 922–32. doi:10.1177/1087057106292763
- Ivascu, A., & Kubbies, M. (2007). Diversity of cell-mediated adhesions in breast cancer spheroids. *International Journal of Oncology*, 31(6), 1403–13. Retrieved from <http://www.ncbi.nlm.nih.gov/pubmed/17982667>
- Iwamoto, N., Distler, J. H. W., & Distler, O. (2011). Tyrosine kinase inhibitors in the treatment of systemic sclerosis: from animal models to clinical trials. *Current Rheumatology Reports*, 13(1), 21–7. doi:10.1007/s11926-010-0142-x
- Jang, S., Cho, H.-H., Cho, Y.-B., Park, J.-S., & Jeong, H.-S. (2010). Functional neural differentiation of human adipose tissue-derived stem cells using bFGF and forskolin. *BMC Cell Biology*, 11, 25. doi:10.1186/1471-2121-11-25
- Joyce, J. a, & Pollard, J. W. (2009). Microenvironmental regulation of metastasis. *Nature Reviews. Cancer*, 9(4), 239–52. doi:10.1038/nrc2618
- Joza, N., Susin, S. a, Daugas, E., Stanford, W. L., Cho, S. K., Li, C. Y., ... Penninger, J. M. (2001). Essential role of the mitochondrial apoptosis-inducing factor in programmed cell death. *Nature*, 410(6828), 549–54. doi:10.1038/35069004
- Junttila, M. R., & de Sauvage, F. J. (2013). Influence of tumour micro-environment heterogeneity on therapeutic response. *Nature*, 501(7467), 346–54. doi:10.1038/nature12626
- Justice, B. a, Badr, N. a, & Felder, R. a. (2009). 3D cell culture opens new dimensions in cell-based assays. *Drug Discovery Today*, 14(1-2), 102–7. doi:10.1016/j.drudis.2008.11.006
- Kalluri, R., & Zeisberg, M. (2006). Fibroblasts in cancer. *Nature Reviews. Cancer*, 6(5), 392–401. doi:10.1038/nrc1877
- Kato, Y., Ozawa, S., Miyamoto, C., Maehata, Y., Suzuki, A., Maeda, T., & Baba, Y. (2013). Acidic extracellular microenvironment and cancer. *Cancer Cell International*, 13(1), 89. doi:10.1186/1475-2867-13-89
- Kehoe, D. E., Jing, D., Lock, L. T., Tzanakakis, E. S., & Ph, D. (2010). Scalable Stirred-Suspension Bioreactor Culture, 16(2).
- Kelm, J. M., Timmins, N. E., Brown, C. J., Fussenegger, M., & Nielsen, L. K. (2003). Method for generation of homogeneous multicellular tumor spheroids applicable to a wide variety of cell types. *Biotechnology and Bioengineering*, 83(2), 173–80. doi:10.1002/bit.10655
- Kim, J. Bin. (2005). Three-dimensional tissue culture models in cancer biology. *Seminars in Cancer Biology*, 15(5), 365–77. doi:10.1016/j.semcan.2005.05.002
- Kim, E. Y., Kim, A., Kim, S. K., Kim, H. J., Chang, J., Ahn, C. M., & Chang, Y. S. (2014). Inhibition of mTORC1 induces loss of E-cadherin through AKT/GSK-3 β signaling-mediated upregulation of E-cadherin repressor

References

- complexes in non-small cell lung cancer cells. *Respiratory Research*, 15(1), 26. doi:10.1186/1465-9921-15-26
- Kim, Y.-N., Koo, K. H., Sung, J. Y., Yun, U.-J., & Kim, H. (2012). Anoikis resistance: an essential prerequisite for tumor metastasis. *International Journal of Cell Biology*, 2012, 306879. doi:10.1155/2012/306879
- Ladanyi, M., & Pao, W. (2008). Lung adenocarcinoma: guiding EGFR-targeted therapy and beyond. *Modern Pathology: An Official Journal of the United States and Canadian Academy of Pathology, Inc*, 21 Suppl 2, S16–22. doi:10.1038/modpathol.3801018
- Lammers, P. E., & Horn, L. (2013). Targeting angiogenesis in advanced non-small cell lung cancer. *Journal of the National Comprehensive Cancer Network: JNCCN*, 11(10), 1235–47. Retrieved from <http://www.ncbi.nlm.nih.gov/pubmed/24142825>
- Lan, S.-F., & Starly, B. (2011). Alginate based 3D hydrogels as an in vitro co-culture model platform for the toxicity screening of new chemical entities. *Toxicology and Applied Pharmacology*, 256(1), 62–72. doi:10.1016/j.taap.2011.07.013
- Landskron, G., De la Fuente, M., Thuwajit, P., Thuwajit, C., & Hermoso, M. a. (2014). Chronic Inflammation and Cytokines in the Tumor Microenvironment. *Journal of Immunology Research*, 2014, 1–19. doi:10.1155/2014/149185
- Lee, J. M., Dedhar, S., Kalluri, R., & Thompson, E. W. (2006). The epithelial-mesenchymal transition: new insights in signaling, development, and disease. *The Journal of Cell Biology*, 172(7), 973–81. doi:10.1083/jcb.200601018
- Lee, W., Jiang, Z., Liu, J., Haverty, P. M., Guan, Y., Stinson, J., ... Zhang, Z. (2010). The mutation spectrum revealed by paired genome sequences from a lung cancer patient. *Nature*, 465(7297), 473–7. doi:10.1038/nature09004
- Lilienblum, W., Dekant, W., Foth, H., Gebel, T., Hengstler, J. G., Kahl, R., ... Wollin, K.-M. (2008). Alternative methods to safety studies in experimental animals: role in the risk assessment of chemicals under the new European Chemicals Legislation (REACH). *Archives of Toxicology*, 82(4), 211–36. doi:10.1007/s00204-008-0279-9
- Lin, R.-Z., Lin, R.-Z., & Chang, H.-Y. (2008). Recent advances in three-dimensional multicellular spheroid culture for biomedical research. *Biotechnology Journal*, 3(9-10), 1172–84. doi:10.1002/biot.200700228
- Llinares, K., Escande, F., Aubert, S., Buisine, M.-P., de Bolos, C., Batra, S. K., ... Copin, M.-C. (2004). Diagnostic value of MUC4 immunostaining in distinguishing epithelial mesothelioma and lung adenocarcinoma. *Modern Pathology: An Official Journal of the United States and Canadian Academy of Pathology, Inc*, 17(2), 150–7. doi:10.1038/modpathol.3800027
- Lloyd, P. G., & Hardin, C. D. (2011). peroxide inhibits non-small cell lung cancer cell anoikis through the inhibition of caveolin-1 degradation”, 74078, 2010–2012. doi:10.1152/ajpcell.00483.2010.Caveolae
- Lukashev, M. E., & Werb, Z. (1998). ECM signalling: orchestrating cell behaviour and misbehaviour. *Trends in Cell Biology*, 8(11), 437–41. Retrieved from <http://www.ncbi.nlm.nih.gov/pubmed/9854310>
- Ma, P. C. (2012). Personalized targeted therapy in advanced non-small cell lung cancer. *Cleveland Clinic Journal of Medicine*, 79 Electro, eS56–60. doi:10.3949/ccjm.79.s2.12
- Malvezzi, M., Bertuccio, P., Levi, F., La Vecchia, C., & Negri, E. (2013). European cancer mortality predictions for the year 2013. *Annals of Oncology: Official Journal of the European Society for Medical Oncology / ESMO*, 24(3), 792–800. doi:10.1093/annonc/mdt010
- Manuel, R., & Gameiro, L. (2012). Rui Manuel Lucas Gameiro Domingues Process Engineering of Liver Cells for Drug Testing Applications Process Engineering of Liver Cells for Drug Testing Applications Copyright Rui Manuel Lucas Gameiro Domingues Tostões Faculdade de Ciências e Tecnologia – .

References

- Maranga, L., & Goochee, C. F. (2006). Metabolism of PER . C6 TM Cells Cultivated Under Fed-Batch Conditions at Low Glucose and Glutamine Levels. doi:10.1002/bit
- Martin, I., Wendt, D., & Heberer, M. (2004). The role of bioreactors in tissue engineering. *Trends in Biotechnology*, 22(2), 80–6. doi:10.1016/j.tibtech.2003.12.001
- Matsubara, D., Ishikawa, S., Sachiko, O., Aburatani, H., Fukayama, M., & Niki, T. (2010). Co-activation of epidermal growth factor receptor and c-MET defines a distinct subset of lung adenocarcinomas. *The American Journal of Pathology*, 177(5), 2191–204. doi:10.2353/ajpath.2010.100217
- Mazzoleni, G., Lorenzo, D., & Steimberg, N. (2009). Modelling tissues in 3D: the next future of pharmacotoxicology and food research? *Genes & Nutrition*, 4(1), 13–22. doi:10.1007/s12263-008-0107-0
- McMillin, D. W., Negri, J. M., & Mitsiades, C. S. (2013). The role of tumour-stromal interactions in modifying drug response: challenges and opportunities. *Nature Reviews. Drug Discovery*, 12(3), 217–28. doi:10.1038/nrd3870
- Mehta, H. J., Patel, V., & Sadikot, R. T. (2014). Curcumin and lung cancer-a review. *Targeted Oncology*. doi:10.1007/s11523-014-0321-1
- Merad-Boudia, M., Nicole, A., Santiard-Baron, D., Saillé, C., & Ceballos-Picot, I. (1998). Mitochondrial Impairment as an Early Event in the Process of Apoptosis Induced by Glutathione Depletion in Neuronal Cells: Relevance to Parkinson's Disease. *Biochemical Pharmacology*, 56(5), 645–655. doi:10.1016/S0006-2952(97)00647-3
- Mesquita, B. B. De, Chesson, A., Chytil, F., Grimble, R., Lotan, R., Norpoth, K., ... Thurnham, D. (1997). European Consensus Statement on Lung Cancer : Risk Factors and Prevention, 316–322.
- Metallo, C. M., Walther, J. L., & Stephanopoulos, G. (2009). Evaluation of 13C isotopic tracers for metabolic flux analysis in mammalian cells. *Journal of Biotechnology*, 144(3), 167–74. doi:10.1016/j.jbiotec.2009.07.010
- Meyboom, a. (1997). Reversible Calcium-dependent Interaction of Liposomes with Pulmonary Surfactant Protein A. ANALYSIS BY RESONANT MIRROR TECHNIQUE AND NEAR-IR LIGHT SCATTERING. *Journal of Biological Chemistry*, 272(23), 14600–14605. doi:10.1074/jbc.272.23.14600
- Meyvantsson, I., & Beebe, D. J. (2008). Cell culture models in microfluidic systems. *Annual Review of Analytical Chemistry (Palo Alto, Calif.)*, 1, 423–49. doi:10.1146/annurev.anchem.1.031207.113042
- Miller, Y. E. (2005). Pathogenesis of lung cancer: 100 year report. *American Journal of Respiratory Cell and Molecular Biology*, 33(3), 216–23. doi:10.1165/rcmb.2005-0158OE
- Minna, J. E. L. and J. D. (2012). Molecular Biology of Lung Cancer : Clinical Implications. *Clin Chest Med.*, 32(4), 703–740. doi:10.1016/j.ccm.2011.08.003.Molecular
- Miranda, J. P. (2010). Extending Hepatocyte Functionality for Drug-Testing Applications Using High-Viscosity Alginate – Encapsulated, 16(6). doi:10.1089/ten.tec.2009.0784
- Miyoshi, J., & Takai, Y. (2008). Structural and functional associations of apical junctions with cytoskeleton. *Biochimica et Biophysica Acta*, 1778(3), 670–91. doi:10.1016/j.bbame.2007.12.014
- Moreira, J. L., Alves, P. M., Aunins, J. G., & Carrondo, M. J. (1995). Hydrodynamic effects on BHK cells grown as suspended natural aggregates. *Biotechnology and Bioengineering*, 46(4), 351–60. doi:10.1002/bit.260460408
- Morizane, A., Doi, D., Kikuchi, T., Nishimura, K., & Takahashi, J. (2011). Small-molecule inhibitors of bone morphogenic protein and activin/nodal signals promote highly efficient neural induction from human pluripotent stem cells. *Journal of Neuroscience Research*, 89(2), 117–26. doi:10.1002/jnr.22547

References

- Mueller, M. M., & Fusenig, N. E. (2004). Friends or foes - bipolar effects of the tumour stroma in cancer. *Nature Reviews. Cancer*, 4(11), 839–49. doi:10.1038/nrc1477
- Mundel, T. M., Kieran, M. W., & Kalluri, R. (2006). Identification of Fibroblast Heterogeneity in the Tumor Microenvironment, (December), 1640–1646.
- Myrdal, G., Gustafsson, G., Lambe, M., Hörte, L. G., & Ståhle, E. (2001). Outcome after lung cancer surgery. Factors predicting early mortality and major morbidity. *European Journal of Cardio-Thoracic Surgery: Official Journal of the European Association for Cardio-Thoracic Surgery*, 20(4), 694–9. Retrieved from <http://www.ncbi.nlm.nih.gov/pubmed/11574210>
- N. Bhowmick, E. N. and H. M. (2011). Stromal fibroblasts in cancer initiation and progression, 432(7015), 332–337. doi:10.1038/nature03096.Stromal
- Newsholme, P., Lima, M. M. R., Procopio, J., Pithon-Curi, T. C., Doi, S. Q., Bazotte, R. B., & Curi, R. (2003). Glutamine and glutamate as vital metabolites. *Brazilian Journal of Medical and Biological Research = Revista Brasileira de Pesquisas Médicas E Biológicas / Sociedade Brasileira de Biofísica ... [et Al.]*, 36(2), 153–63. Retrieved from <http://www.ncbi.nlm.nih.gov/pubmed/12563517>
- O. SMIDSRÖD. (1974). Molecular Basis for some Physical Properties of Alginates in the Gel State. *J Chem Soc Faraday Trans*, 57, 263–274.
- Otto Warburg, Franz Wind, E. N. (1926). THE METABOLISM OF TUMORS IN THE BODY. *The Journal of General Physiology*, 8(6), 519–530.
- Pallier, K., Cessot, A., Côté, J.-F., Just, P.-A., Cazes, A., Fabre, E., ... Blons, H. (2012). TWIST1 a new determinant of epithelial to mesenchymal transition in EGFR mutated lung adenocarcinoma. *PLoS One*, 7(1), e29954. doi:10.1371/journal.pone.0029954
- Pampaloni, F., Reynaud, E. G., & Stelzer, E. H. K. (2007). The third dimension bridges the gap between cell culture and live tissue. *Nature Reviews. Molecular Cell Biology*, 8(10), 839–45. doi:10.1038/nrm2236
- Paoli, P., Giannoni, E., & Chiarugi, P. (2013). Anoikis molecular pathways and its role in cancer progression. *Biochimica et Biophysica Acta*, 1833(12), 3481–98. doi:10.1016/j.bbamcr.2013.06.026
- Partanen, J. (2012). *Epithelial Integrity as a Tumor Suppressor Mechanism – The Interplay Between Lkb1 and c-Myc in Breast Cancer Development*. University of Helsinki Finland.
- Partanen, J. I., Nieminen, A. I., & Klefstrom, J. (2009). 3D view to tumor suppression: Lkb1, polarity and the arrest of oncogenic c-Myc. *Cell Cycle Georgetown Tex*, 8, 716–724. Retrieved from <http://www.ncbi.nlm.nih.gov/pubmed/19221484>
- Peng, Q., Zhao, L., Hou, Y., Sun, Y., Wang, L., Luo, H., ... Liu, M. (2013). Biological characteristics and genetic heterogeneity between carcinoma-associated fibroblasts and their paired normal fibroblasts in human breast cancer. *PLoS One*, 8(4), e60321. doi:10.1371/journal.pone.0060321
- Penzberg, D.-. (2005). STUDIES OF FIBRONECTIN-CANCER CELLS INTERACTIONS UNDER STATIC AND DYNAMIC CONDITIONS . DIFFERENT ADHESIVE BEHAVIOR OF HIGH METASTATIC AND LOW METASTATIC SUBCLONE OF NCI-H460 * Maneva-Radicheva L I ., Zlateva N ., I Kostadinova A . I , Dimoudis N . 2 , [I , 2005(MAY), 315–328.
- Pértega-Gomes, N., Vizcaíno, J. R., Attig, J., Jurmeister, S., Lopes, C., & Baltazar, F. (2014). A lactate shuttle system between tumour and stromal cells is associated with poor prognosis in prostate cancer. *BMC Cancer*, 14, 352. doi:10.1186/1471-2407-14-352
- Petersen, O. W., Rønnov-Jessen, L., Howlett, a R., & Bissell, M. J. (1992). Interaction with basement membrane serves to rapidly distinguish growth and differentiation pattern of normal and malignant human breast epithelial cells. *Proceedings of the National Academy of Sciences of the United States of America*, 89(19), 9064–

8. Retrieved from
<http://www.pubmedcentral.nih.gov/articlerender.fcgi?artid=50065&tool=pmcentrez&rendertype=abstract>
- Pongrakhananon, V., Nimmannit, U., Luanpitpong, S., Rojanasakul, Y., & Chanvorachote, P. (2010). Curcumin sensitizes non-small cell lung cancer cell anoikis through reactive oxygen species-mediated Bcl-2 downregulation. *Apoptosis: An International Journal on Programmed Cell Death*, 15(5), 574–85. doi:10.1007/s10495-010-0461-4
- Popper, H. H. (2011). Large cell carcinoma of the lung – a vanishing entity? *Memo - Magazine of European Medical Oncology*, 4(1), 4–9. doi:10.1007/s12254-011-0245-8
- Raaschou-Nielsen, O., Andersen, Z. J., Beelen, R., Samoli, E., Stafoggia, M., Weinmayr, G., ... Hoek, G. (2013). Air pollution and lung cancer incidence in 17 European cohorts: prospective analyses from the European Study of Cohorts for Air Pollution Effects (ESCAPE). *The Lancet Oncology*, 14(9), 813–22. doi:10.1016/S1470-2045(13)70279-1
- Rathi N. Pillai and Taofeek K. Owonikoko. (2014). Small cell lung cancer: therapies and targets. *Seminars in Oncology*, 41(1), 133–42. doi:10.1053/j.seminoncol.2013.12.015
- Read, W. L., Page, N. C., Tierney, R. M., Piccirillo, J. F., & Govindan, R. (2004). The epidemiology of bronchioloalveolar carcinoma over the past two decades: analysis of the SEER database. *Lung Cancer (Amsterdam, Netherlands)*, 45(2), 137–42. doi:10.1016/j.lungcan.2004.01.019
- Rebelo, S. P., Costa, R., Estrada, M., Shevchenko, V., Brito, C., & Alves, P. M. (2014). HepaRG microencapsulated spheroids in DMSO-free culture: novel culturing approaches for enhanced xenobiotic and biosynthetic metabolism. *Archives of Toxicology*. doi:10.1007/s00204-014-1320-9
- Roato, I. (2014). Bone metastases: When and how lung cancer interacts with bone. *World Journal of Clinical Oncology*, 5(2), 149–155. doi:10.5306/wjco.v5.i2.149
- Rodemann, H. P., & Bamberg, M. (1995). Cellular basis of radiation-induced fibrosis. *Radiotherapy and Oncology: Journal of the European Society for Therapeutic Radiology and Oncology*, 35(2), 83–90. Retrieved from <http://www.ncbi.nlm.nih.gov/pubmed/7569029>
- Rodemann, H. P., & Rennekampff, H. (2011). Tumor-Associated Fibroblasts and their Matrix, 23–37. doi:10.1007/978-94-007-0659-0
- Rodrigues, C. a. V., Diogo, M. M., da Silva, C. L., & Cabral, J. M. S. (2011). Design and operation of bioreactor systems for the expansion of pluripotent stem cell-derived neural stem cells. *1st Portuguese Biomedical Engineering Meeting*, 1–3. doi:10.1109/ENBENG.2011.6026041
- Rowell, N. P., & Williams, C. J. (2001). Radical radiotherapy for stage I/II non-small cell lung cancer in patients not sufficiently fit for or declining surgery (medically inoperable): a systematic review. *Thorax*, 56(8), 628–38. Retrieved from <http://www.pubmedcentral.nih.gov/articlerender.fcgi?artid=1746110&tool=pmcentrez&rendertype=abstract>
- Rungtabnapa, P., Nimmannit, U., Halim, H., Rojanasakul, Y., & Chanvorachote, P. (2011). Hydrogen peroxide inhibits non-small cell lung cancer cell anoikis through the inhibition of caveolin-1 degradation, 235–245. doi:10.1152/ajpcell.00249.2010.
- Sakuma, Y., Takeuchi, T., Nakamura, Y., Yoshihara, M., Matsukuma, S., Nakayama, H., ... Miyagi, Y. (2010). Lung adenocarcinoma cells floating in lymphatic vessels resist anoikis by expressing phosphorylated Src, (December 2009), 574–585. doi:10.1002/path
- Santo, E., Mano, F., & Reis, R. L. (2013). Controlled Release Strategies for Bone, Cartilage, and Osteochondral Engineering — Part I: Recapitulation of Native Tissue Healing and Variables for the Design of Delivery Systems, 00(00). doi:10.1089/ten.teb.2012.0138

References

- Santo, V. E., Frias, A. M., Carida, M., Cancedda, R., Gomes, M. E., Mano, J. F., & Reis, R. L. (2009). Carrageenan-based hydrogels for the controlled delivery of PDGF-BB in bone tissue engineering applications. *Biomacromolecules*, 10(6), 1392–401. doi:10.1021/bm8014973
- Schmidt, J. J., Rowley, J., & Kong, H. J. (2008). Hydrogels used for cell-based drug delivery. *Journal of Biomedical Materials Research. Part A*, 87(4), 1113–22. doi:10.1002/jbm.a.32287
- Schneider, K., Schütz, V., John, G. T., & Heinzle, E. (2010). Optical device for parallel online measurement of dissolved oxygen and pH in shake flask cultures. *Bioprocess and Biosystems Engineering*, 33(5), 541–7. doi:10.1007/s00449-009-0367-0
- Sculier, J.-P., Meert, A.-P., & Berghmans, T. (2014). Updates in oncology. *European Respiratory Review: An Official Journal of the European Respiratory Society*, 23(131), 69–78. doi:10.1183/09059180.00009013
- Serra, M., Brito, C., Correia, C., & Alves, P. M. (2012). Process engineering of human pluripotent stem cells for clinical application. *Trends in Biotechnology*, 30(6), 350–9. doi:10.1016/j.tibtech.2012.03.003
- Serra, M., Brito, C., Leite, S. B., Gorjup, E., von Briesen, H., Carrondo, M. J. T., & Alves, P. M. (2009). Stirred bioreactors for the expansion of adult pancreatic stem cells. *Annals of Anatomy = Anatomischer Anzeiger: Official Organ of the Anatomische Gesellschaft*, 191(1), 104–15. doi:10.1016/j.aanat.2008.09.005
- Serra, M., Correia, C., Malpique, R., Brito, C., Jensen, J., Bjorquist, P., ... Alves, P. M. (2011). Microencapsulation technology: a powerful tool for integrating expansion and cryopreservation of human embryonic stem cells. *PloS One*, 6(8), e23212. doi:10.1371/journal.pone.0023212
- Serra, M., Leite, S. B., Brito, C., Carrondo, M. J. T., & Alves, P. M. (2007). Novel Culture Strategy for Human Stem Cell Proliferation and Neuronal Differentiation, 3566(September), 3557–3566. doi:10.1002/jnr
- Shackelford, R. E., Vora, M., Mayhall, K., & Cotelingam, J. (2014). ALK -rearrangements and testing methods in non-small cell lung cancer : a review ABSTRACT :, 5(January).
- Shimi, S. M., Hopwood, D., Newman, E. L., & Cuschieri, a. (1991). Microencapsulation of human cells: its effects on growth of normal and tumour cells in vitro. *British Journal of Cancer*, 63(5), 675–80. Retrieved from <http://www.pubmedcentral.nih.gov/articlerender.fcgi?artid=1972378&tool=pmcentrez&rendertype=abstract>
- Shivanthan, M. C., & Wijesiriwardena, B. (2011). Bronchoalveolar carcinoma on a background of chronic extrinsic allergic alveolitis in a spice miller – A case report. *Respiratory Medicine CME*, 4(3), 119–120. doi:10.1016/j.rmedc.2011.01.004
- Siegel, P. M., & Massagué, J. (2003). Cytostatic and apoptotic actions of TGF-beta in homeostasis and cancer. *Nature Reviews. Cancer*, 3(11), 807–21. doi:10.1038/nrc1208
- Sieh, S., Taubenberger, A. V., Rizzi, S. C., Sadowski, M., Lehman, M. L., Rockstroh, A., ... Hutmacher, D. W. (2012). Phenotypic characterization of prostate cancer LNCaP cells cultured within a bioengineered microenvironment. *PloS One*, 7(9), e40217. doi:10.1371/journal.pone.0040217
- Silzle, T., Randolph, G. J., Kreutz, M., & Kunz-Schughart, L. a. (2004). The fibroblast: sentinel cell and local immune modulator in tumor tissue. *International Journal of Cancer. Journal International Du Cancer*, 108(2), 173–80. doi:10.1002/ijc.11542
- Simian, M., Hirai, Y., Navre, M., Werb, Z., Lochter, a, & Bissell, M. J. (2001). The interplay of matrix metalloproteinases, morphogens and growth factors is necessary for branching of mammary epithelial cells. *Development (Cambridge, England)*, 128(16), 3117–31. Retrieved from <http://www.pubmedcentral.nih.gov/articlerender.fcgi?artid=2785713&tool=pmcentrez&rendertype=abstract>
- Singh, A. P., Chaturvedi, P., & Batra, S. K. (2007). Emerging roles of MUC4 in cancer: a novel target for diagnosis and therapy. *Cancer Research*, 67(2), 433–6. doi:10.1158/0008-5472.CAN-06-3114

References

- Singh, A. P., Chauhan, S. C., Bafna, S., Johansson, S. L., Smith, L. M., Moniaux, N., ... Batra, S. K. (2006). Aberrant expression of transmembrane mucins, MUC1 and MUC4, in human prostate carcinomas. *The Prostate*, 66(4), 421–9. doi:10.1002/pros.20372
- Singhal, S., Vachani, A., & Antin-ozerkis, D. (2005). Prognostic Implications of Cell Cycle , Apoptosis , and Angiogenesis Biomarkers in Non – Small Cell Lung Cancer : A Review Biomarkers in Non ^ Small Cell Lung Cancer : A Review, 3974–3986.
- Sodunke, T. R., Turner, K. K., Caldwell, S. a, McBride, K. W., Reginato, M. J., & Noh, H. M. (2007). Micropatterns of Matrigel for three-dimensional epithelial cultures. *Biomaterials*, 28(27), 4006–16. doi:10.1016/j.biomaterials.2007.05.021
- Su, M.-Y., Hsieh, S.-Y., Lee, Y.-R., Chang, M.-C., Yuan, T. T.-T., & Chang, J.-M. (2010). The relationship between energy status and AMP-activated protein kinase in human H460 lung cancer cells. *Cell Biochemistry and Function*, 28(7), 549–54. doi:10.1002/cbf.1685
- Sugiura, S., Ando, Y., Minami, H., Ando, M., Sakai, S., & Shimokata, K. (1997). Prognostic value of pleural effusion in patients with non-small cell lung cancer. *Clinical Cancer Research : An Official Journal of the American Association for Cancer Research*, 3(1), 47–50. Retrieved from <http://www.ncbi.nlm.nih.gov/pubmed/9815536>
- Sukhatme, V. P., & Chan, B. (2012). Glycolytic cancer cells lacking 6-phosphogluconate dehydrogenase metabolize glucose to induce senescence. *FEBS Letters*, 586(16), 2389–95. doi:10.1016/j.febslet.2012.05.052
- Sun, J.-M., Ahn, M.-J., Ahn, J. S., Um, S.-W., Kim, H., Kim, H. K., ... Park, K. (2012). Chemotherapy for pulmonary large cell neuroendocrine carcinoma: similar to that for small cell lung cancer or non-small cell lung cancer? *Lung Cancer (Amsterdam, Netherlands)*, 77(2), 365–70. doi:10.1016/j.lungcan.2012.04.009
- Sutherland, R. M., McCredie, J. a, & Inch, W. R. (1971). Growth of multicell spheroids in tissue culture as a model of nodular carcinomas. *Journal of the National Cancer Institute*, 46(1), 113–20. Retrieved from <http://www.ncbi.nlm.nih.gov/pubmed/5101993>
- Tan, M. A. L., Teichberg, S., Roberts, B., & Hajdu, S. I. (2003). Ultrastructural findings in metastatic bronchioloalveolar carcinoma. *Annals of Clinical and Laboratory Science*, 33(3), 289–94. Retrieved from <http://www.ncbi.nlm.nih.gov/pubmed/12956444>
- Timmerman, R., McGarry, R., Yiannoutsos, C., Papiez, L., Tudor, K., DeLuca, J., ... Fletcher, J. (2006). Excessive toxicity when treating central tumors in a phase II study of stereotactic body radiation therapy for medically inoperable early-stage lung cancer. *Journal of Clinical Oncology : Official Journal of the American Society of Clinical Oncology*, 24(30), 4833–9. doi:10.1200/JCO.2006.07.5937
- Tostões, R. M., Leite, S. B., Miranda, J. P., Sousa, M., Wang, D. I. C., Carrondo, M. J. T., & Alves, P. M. (2011). Perfusion of 3D encapsulated hepatocytes--a synergistic effect enhancing long-term functionality in bioreactors. *Biotechnology and Bioengineering*, 108(1), 41–9. doi:10.1002/bit.22920
- Tostões, R. M., Leite, S. B., Serra, M., Jensen, J., Björquist, P., Carrondo, M. J. T., ... Alves, P. M. (2012). Human liver cell spheroids in extended perfusion bioreactor culture for repeated-dose drug testing. *Hepatology (Baltimore, Md.)*, 55(4), 1227–36. doi:10.1002/hep.24760
- Travis, W. D. (2011). Classification of lung cancer. *Seminars in Roentgenology*, 46(3), 178–86. doi:10.1053/j.ro.2011.02.003
- Travis, W. D., Brambilla, E., Van Schil, P., Scagliotti, G. V, Huber, R. M., Sculier, J.-P., ... Nicholson, a G. (2011). Paradigm shifts in lung cancer as defined in the new IASLC/ATS/ERS lung adenocarcinoma classification. *The European Respiratory Journal*, 38(2), 239–43. doi:10.1183/09031936.00026711

References

- Tung, Y.-C., Hsiao, A. Y., Allen, S. G., Torisawa, Y., Ho, M., & Takayama, S. (2011). High-throughput 3D spheroid culture and drug testing using a 384 hanging drop array. *The Analyst*, *136*(3), 473–8. doi:10.1039/c0an00609b
- Vasekar, M., Liu, X., Zheng, H., & Belani, C. P. (2014). Targeted immunotherapy for non-small cell lung cancer. *World Journal of Clinical Oncology*, *5*(2), 39–47. doi:10.5306/wjco.v5.i2.39
- Velasco, D., Tumarkin, E., & Kumacheva, E. (2012). Microfluidic encapsulation of cells in polymer microgels. *Small (Weinheim an Der Bergstrasse, Germany)*, *8*(11), 1633–42. doi:10.1002/sml.201102464
- Vinci, M., Gowan, S., Boxall, F., Patterson, L., Zimmermann, M., Court, W., ... Eccles, S. a. (2012). Advances in establishment and analysis of three-dimensional tumor spheroid-based functional assays for target validation and drug evaluation. *BMC Biology*, *10*(1), 29. doi:10.1186/1741-7007-10-29
- Von der Mark, K., Gauss, V., von der Mark, H. and Müller, P. (1977). Relationship between cell shape and type of collagen synthesised as chondrocytes lose their cartilage phenotype in culture. *Nature*, *267*, 531–532.
- Walenta, S., Snyder, S., Haroon, Z. a, Braun, R. D., Amin, K., Brizel, D., ... Dewhurst, M. W. (2001). Tissue gradients of energy metabolites mirror oxygen tension gradients in a rat mammary carcinoma model. *International Journal of Radiation Oncology, Biology, Physics*, *51*(3), 840–8. Retrieved from <http://www.ncbi.nlm.nih.gov/pubmed/11699496>
- Walther, J. L., Metallo, C. M., Zhang, J., & Stephanopoulos, G. (2012). Optimization of ¹³C isotopic tracers for metabolic flux analysis in mammalian cells. *Metabolic Engineering*, *14*(2), 162–71. doi:10.1016/j.ymben.2011.12.004
- Wang, Y., & Wang, J. (2014). Mixed hydrogel bead-based tumor spheroid formation and anticancer drug testing. *The Analyst*, *139*(10), 2449–58. doi:10.1039/c4an00015c
- Warner, D. O. (2006). Review article: Age related alterations in respiratory function - anesthetic considerations, 1244–1257.
- Wei, L., Yang, Y., Zhang, X., & Yu, Q. (2002). Anchorage-independent phosphorylation of p130(Cas) protects lung adenocarcinoma cells from anoikis. *Journal of Cellular Biochemistry*, *87*(4), 439–49. doi:10.1002/jcb.10322
- Wei, L., Yang, Y., Zhang, X., & Yu, Q. (2004). Cleavage of p130Cas in anoikis. *Journal of Cellular Biochemistry*, *91*(2), 325–35. doi:10.1002/jcb.10760
- Wikström, J., Elomaa, M., Syväjärvi, H., Kuokkanen, J., Yliperttula, M., Honkakoski, P., & Urtti, A. (2008). Alginate-based microencapsulation of retinal pigment epithelial cell line for cell therapy. *Biomaterials*, *29*(7), 869–76. doi:10.1016/j.biomaterials.2007.10.056
- Xiao, D., & He, J. (2010). Epithelial mesenchymal transition and lung cancer. *Journal of Thoracic Disease*, *2*(3), 154–9. doi:10.3978/j.issn.2072-1439.2010.02.03.7
- Xu, X., Farach-Carson, M. C., & Jia, X. (2014). Three-dimensional in vitro tumor models for cancer research and drug evaluation. *Biotechnology Advances*, 1–13. doi:10.1016/j.biotechadv.2014.07.009
- Zhang, X., Wang, W., Xie, Y., Zhang, Y., Wang, X., Guo, X., & Ma, X. (2006). Proliferation, viability, and metabolism of human tumor and normal cells cultured in microcapsule. *Applied Biochemistry and Biotechnology*, *134*(1), 61–76. Retrieved from <http://www.ncbi.nlm.nih.gov/pubmed/16891667>
- Zhang, X., Wang, W., Yu, W., Xie, Y., Zhang, X., Zhang, Y., & Ma, X. (2005). Development of an in vitro multicellular tumor spheroid model using microencapsulation and its application in anticancer drug screening and testing. *Biotechnology Progress*, *21*(4), 1289–96. doi:10.1021/bp0500031
- Zhao, Y., Butler, E. B., & Tan, M. (2013). Targeting cellular metabolism to improve cancer therapeutics. *Cell Death & Disease*, *4*(3), e532. doi:10.1038/cddis.2013.60

References

- Zhao, Y., Yao, R., Ouyang, L., Ding, H., Zhang, T., Zhang, K., ... Sun, W. (2014). Three-dimensional printing of HeLa cells for cervical tumor model in vitro. *Biofabrication*, 6(3), 035001. doi:10.1088/1758-5082/6/3/035001
- Zhong, X., & Rescorla, F. J. (2012). Cell surface adhesion molecules and adhesion-initiated signaling: understanding of anoikis resistance mechanisms and therapeutic opportunities. *Cellular Signalling*, 24(2), 393–401. doi:10.1016/j.cellsig.2011.10.005
- Zhong, Y., Delgado, Y., Gomez, J., Lee, S. W., & Perez-soler, R. (2001). Loss of H-Cadherin Protein Expression in Human Non-Small Cell Lung Cancer Is Associated with Tumorigenicity Loss of H-Cadherin Protein Expression in Human Non-Small Cell Lung Cancer Is Associated with Tumorigenicity 1, 1683–1687.
- Zhuang, H., Zhao, X., Zhao, L., Chang, J. Y., & Wang, P. (2014). Progress of clinical research on targeted therapy combined with thoracic radiotherapy for non-small-cell lung cancer. *Drug Design, Development and Therapy*, 8, 667–675. doi:10.2147/DDDT.S61977
- Zielke, H. R., Sumbilla, C. M., Sevdalian, D. A., Hawkins, R. L., & Ozand, P. T. (1980). Lactate: A major product of glutamine metabolism by human diploid fibroblasts. *Journal of Cellular Physiology*, 104, 433–441. doi:10.1002/jcp.1041040316
- Zimmermann, H., Wählich, F., Baier, C., Westhoff, M., Reuss, R., Zimmermann, D., ... Zimmermann, U. (2007). Physical and biological properties of barium cross-linked alginate membranes. *Biomaterials*, 28(7), 1327–45. doi:10.1016/j.biomaterials.2006.11.032